A GPS-Based Head Up Display for Driving Under Low Visibility Conditions

MINNESOTA DEPARTMENT OF TRANSPORTATION

Research

Technical Report Documentation Page

1. Report No. MN/RC – 2003-03	2.	3. Recipients Accession No.	
4. Title and Subtitle A GPS-BASED HEAD UP DISPLAY SYSTEM FOR DRIVING UNDER LOW VISIBILITY CONDITIONS		5. Report Date January 2000	
		6.	
7. Author(s) Max Donath, Craig Shankwitz and Heonmin Lim		8. Performing Organization Report No.	
9. Performing Organization Name and Address Department of Mechanical Engineering University of Minnesota 111 Church Street S.E. Minneapolis, MN 55455		10. Project/Task/Work Unit No.	
		11. Contract (C) or Grant (G) No. (c) 74708 (wo) 60	
12. Sponsoring Organization Name and Address Minnesota Department of Transportation Office of Research Services 395 John Ireland Boulevard Mail Stop 330 St. Paul, Minnesota 55155		13. Type of Report and Period Covered Final Report 1998 - 1999	
		14. Sponsoring Agency Code	
15. Supplementary Notes			

16. Abstract (Limit: 200 words)

This paper describes the design, development, and the evaluation of a Head Up Display (HUD) system for drivers of ground based vehicles. The HUD, which projects visual information into the driver's forward-looking visual field, is a conceptually ideal driver assistive device for those who must drive under degraded visual conditions. Most researchers concur that the driver's forward-looking (i.e. preview) visual field is the most essential input for carrying out the two primary driving tasks: lane keeping and obstacle avoidance. The conformal augmented HUD was developed to provide an intuitive adjunct that provides a high fidelity reconstructed image of essential aspects of the visual field superimposed on the actual field of view.

The HUD was programmed to draw appropriate perspective projections of the road boundaries as seen from the driver's viewpoint as calculated from dynamic position measurements provided by Differential GPS (DGPS).
The mismatch error between the projected and the real road boundaries was measured and analyzed. Experiments were performed using 5 Hz DGPS. Results showed that the current system can draw the superimposed images with errors of less than 0.5 degrees of visual sight angle while the vehicle was driven at various speeds along the test track.

17. Document Analysis/Descriptors		18.Availability Statement	
Head Up Display Field of View	GPS Visibility	No restrictions. Document available from: National Technical Information Services, Springfield, Virginia 22161	
19. Security Class (this report) Unclassified	20. Security Class (this page) Unclassified	21. No. of Pages 171	22. Price

A GPS-BASED HEAD UP DISPLAY SYSTEM FOR DRIVING UNDER LOW VISIBILITY CONDITIONS

Final Report

Prepared by

Max Donath, Ph.D./Professor
Department of Mechanical Engineering
University of Minnesota

Craig Shankwitz, Ph.D.
Department of Mechanical Engineering
University of Minnesota

Heonmin Lim, MS
Department of Mechanical Engineering
University of Minnesota

January 2000

ACKNOWLEDGEMENTS

TABLE OF CONTENTS

LIST OF FIGURES

LIST OF TABLES

EXECUTIVE SUMMARY

This paper describes the design, development, and evaluation of a Head Up Display (HUD) system for drivers of ground based vehicles. The HUD, which projects visual information into the drivers' forward-looking visual field, is a conceptually ideal driver assistive device for those who must drive under degraded visual conditions such as heavy snowfall, blowing snow, fog, and during night time conditions. Most researchers concur that the driver's forward-looking (i.e. preview) visual field of view is the most essential input for carrying out the two primary driving tasks: lane keeping and obstacle avoidance. The conformal augmented HUD described here was developed to provide an intuitive adjunct that provides a high fidelity reconstructed image of essential aspects of the visual field superimposed on the actual field of view.

The HUD was developed using a Differential Global Positioning System (DGPS), a computer system which processes signals and generates graphical images, and an optical system which projects the computer image onto the driver's visual field of view. The computer system was programmed to draw appropriate perspective projections of the road boundaries as seen from the driver's viewpoint as calculated from dynamic position measurements provided by DGPS. A digital map was used to generate the projected road images for the experiment. The mismatch error between the projected and the real road boundaries was measured and analyzed. Experiments were performed using 5 Hz DGPS. Results showed that the current system can draw the superimposed images with errors

less than 0.5 degrees of visual sight angle while the vehicle was driven at various speeds along the test track. Based on the results described here, a new improved HUD system is under development.

Chapter 1   Background

1.1   A Northern State Perspective on Road Visibility

Driving in a northern climate during winter can be quite challenging. Heavy snowfall and

blowing snow can make it difficult to drive even on bright sunny days. Blowing snow

resulting from a combination of wind and dry powdery snow can be particularly

problematic for winter driving. Drivers depend on their forward-looking visual sensing

when they drive either on or off the road. Hills [1] (1980) estimated that more than 90%

of all input to the driver is visual information. Degradation of drivers' visual sight,

especially of their forward looking field of view, due to fog, darkness, or any other

substance or mechanism that occludes their field of view either partially or fully, makes it

difficult to identify obstacles and road boundaries. Difficulties in seeing the road induces

increased brain workload, stress, and fatigue. Drivers exposed to these difficult

conditions are likely to cause collisions with other vehicles or objects either in the driving

lane or as a result of unexpected departure from the driving lane. Coverage of the road by

snow or occlusion by blowing snow may result in a loss of visual perception of the road.

The lack of visual information or driver's visual perception may lead to a misjudgment or

improper driver reaction to certain driving situations. Many researchers indicate that loss

of vehicle control due to slippery road surface conditions may be such a secondary effect.

Whiteout conditions, often encountered by snowplows working on highways due to the

nature of their task, can be considered as an extreme case of the degraded visual condition and not only makes operating snowplows very difficult but also blinds drivers of other vehicles around the plow. This can lead to fatal car crashes. Under whiteout condition, there are no visual cues or they may be extremely limited. Two photos in Figure 1 show two examples of severe snow conditions in Minnesota reported in local newspapers. The first picture is a house in a rural area covered by snow. The small dark spot at the left-top corner of the picture appears to be either a car trying to return home or an abandoned vehicle. The field of view seen by the driver can be bright on a sunny day, that the contrast, differences between objects or colors in the visual scenery, may be extremely poor. It is well known that human vision is seriously affected when there is poor contrast in the visual field of view.
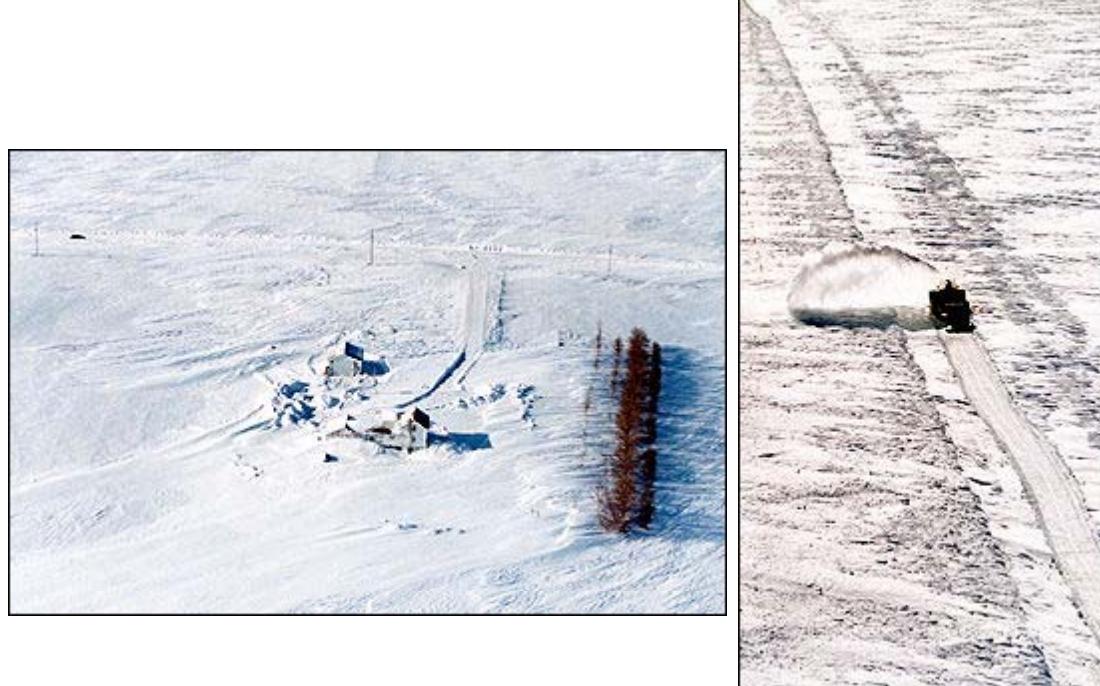
Figure 1. Severe weather condition in Minnesota.

A bright scene without significant contrast is similar to the Ganzfeld which will be discussed shortly. The driver of the snow-blower equipped truck in the second picture is probably having a difficult time determining where the road boundaries are. Both well-trained professional plow drivers and normal passenger car drivers feel uncomfortable driving under these conditions. The drivers' forward-looking vision simply does not provide enough information to facilitate control of the vehicle. Even a simple task, i.e. maintaining the vehicle on the road, can become very difficult. The flat surface profiles associated with the prairies typical of the midwest also makes it more difficult to find visual cues. An important consideration is that snowplow operators need to go out to plow the roads no matter how severe the driving conditions are. Snowplow drivers are exposed to even worse visual condition than normal winter driving. Their visual field is already blocked by the many instruments and other plow attachments around them. Controllers or warning devices that are often installed in the cab make the situation even worse, since they are usually positioned close to or in their forward looking visual field of view in order to solicit a faster response or to make it easy to monitor the instrument panels. Additionally, snow blown up from the front or side-blades blocks their visual field even more.

Operating or maneuvering aircraft in extreme low visibility conditions have been studied by Ganzfeld [2] (1988). A Ganzfeld (empty field) is a spatially extended, structureless visual field of homogeneous texture and uniform illumination that can be similar to winter driving on a road totally covered by snow. Even though snow-covered road scenes

may not be exactly the same as a Ganzfeld, research on Ganzefelds provides us significant information about how difficult it is to perform tasks, such as vehicle control, when the visual field is severely degraded. In a laboratory, a Ganzfeld can be produced in several ways. The most simple approach for inducing the experience is to place one-half of a Ping-Pong ball over each eye, blocking out images of objects but not the light. The human subject sees an empty but evenly white visual field and soon loses his/her visual perception. An experience similar to such an empty field can occur in real environments during high-altitude flight in thick fog or on a snowy day in a featureless rural road. Pilots exposed to such an empty visual field can lose control of their vehicle. Losing visual information longer than a certain amount of time can cause confusion. Scientists believe that one third of the human brain neurons are devoted to visual processing. Massive amounts of unstimulated visual neurons can lead to confusion.

Night time plowing can lead to even worse condition in consideration of the degradation of the forward-looking visual field. Reflected headlight beams make the drivers' forward-looking view extremely difficult. Snowflakes glare brightly when they are illuminated at night and make the average brightness level brighter than normal. The higher average brightness level causes the iris to adapt to the increased brightness and as a result, the eyes become insensitive to the darker objects behind the glaring snowflakes. These darker objects which are vital to driving include road boundaries, obstacles, other vehicles, and signs. The white spots associated with the snowflakes in the visual field can be thought as 'noisy' spots with the noise having stronger values than the signals. Movement of the white snowflakes either coming towards the driver or blowing laterally

can cause visual confusion as well. The effort by the driver to filter out the white noisy spots in the visual field can lead to fatigue with an increased potential for road departure or collision. Driving in thick fog during the night or day can result in a similar situation. Such effects are not exclusively related to driving in snow or fog. Heavy rainfall with a thin sheet of water on the ground can result in ground reflections from the headlights. Being able to distinguish real headlights from reflected light is another serious problem.

1.2   How Do We Drive?

Safe driving on a road means maintaining the forward motion of a vehicle without colliding with to obstacles, (usually referenced as 'collision avoidance') or departing from the driving lane, (called 'lane keeping'). Drivers continuously control vehicle speed, lateral position, and heading direction by adjusting the acceleration/ brake pedals and the steering wheel. When we focus on the low, or local, level tasks of driving, it can be readily demonstrated that drivers behave similarly to a typical feedback controller whose specifications are the desired speed, position, and orientation of vehicle and the actuator inputs are asserting forces to (or displacements of) the pedals and to the steering wheel. Forward-looking visual information is the most important sensory input for driving activities. The earliest paper addressing automotive driving was an article published by Gibson et al. [3] in 1938. In this paper, they developed the concept of the field of safe travel (as shown in Figure 2), and tried to understand drivers' behavior as resultant of responsive reactions needed to pass through the safe travel space. The field of safe travel is an area in which the driver feels safe to move in based on his or her visual perception.
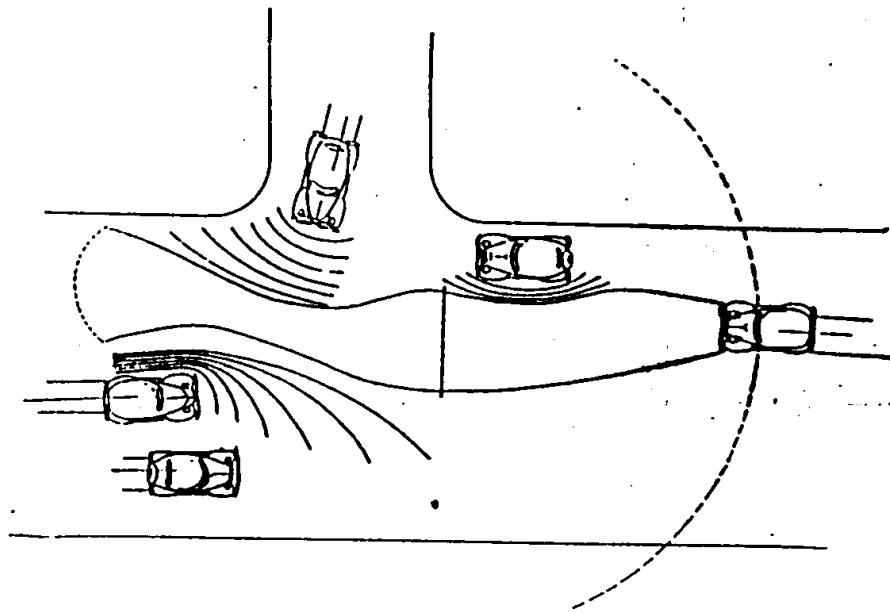
Figure 2. The field of safe travel and the minimum stopping zone of a driver in traffic.

Gibson felt that the safe travel field is affected by obstacles or vehicles on the road while drivers try to follow the perceived safe travel path. The following paragraphs are abstracted from Gibson's discussion. "The visual field of the driver is a rather special sort of field in several respects. It is selective in that the elements of the field which are pertinent to locomotion stand out, are attended to, while non-pertinent elements, such as 'scenery,' normally recede into the background. The most important part of the terrain included in this pertinent field is the road. Within the boundaries of the road lies an indefinitely bounded field called the "field of safe travel." It consists, at any given moment, of the field of possible paths that the car may take unimpeded. It can be imagined as a sort of tongue protruding forward along the road. Its boundaries are chiefly determined by objects or features of the terrain with a negative 'valence' in perception, in

6

other words obstacles. The field of safe travel itself has a positive 'valence,' more especially along its mid-line." The 'valence' is a term usually used in chemistry. This word was used here to introduce the concept of a potential field around the vehicle path similar to the potential field around an atom or a molecule. The potential fields around an atom affects the movement of the atom. Gibson considered a similar concept for the driver's control strategy. By *valence*, positive or negative, he refers to the significance of objects in the sense of an attraction or repulsion. The above Figure 2 is a representation of the field at a specific instant. The field of safe travel is a moving spatial field. While the car moves, the field moves along with the car through the space. Obstacles including other cars affect the safe travel field. Sound wave-like curves surrounding the other vehicles represent equal potential curves that bend, twist, and distort the safe travel field. He concluded that drivers recognize the valences of obstacles and construct a field of safe travel equivalent to a path of minimum potential energy, then drive through the perceived safe travel space. As he pointed out, the forward-looking visual field significantly affects the construction of the field of safe travel, while the degradation of the forward-looking visual field affects or decreases the ability to maintain vehicle control.

1.3   Problem Description and Objectives

Obviously, drivers need to be able to see some distance into the forward-looking visual field for the driving tasks: lane keeping and obstacle avoidance. Many researchers have concluded that drivers' ability to perceive the forward-looking (i.e. preview) visual field is the most essential input for the driving tasks. A degraded or occluded forward-looking

7

visual field results in decreased driving performance. Heavy snowfall or blowing snow in winter, fog, or nighttime driving typically contributes to degraded visual conditions. Providing an improved forward-looking field of view can directly increase driving performance and reduce crashes related to the degraded driving conditions. The goal of the research described in this report is to develop a Head Up Display (HUD) system which can improve the forward-looking visual field using the Differential Global Positioning System (DGPS), digital maps, computer graphics, and a superimposing optical system. The HUD is a driver assistive device which presents an virtual image superimposed on the drivers forward-looking field of view. To develop a HUD system that actually enhances the forward-looking field of view, the following needs to be analyzed and the implemented.

- Construction of the digital map
- Building and calibrating the optical system so that the virtual focus is in front of the vehicle.
- Processing DGPS position signal and estimating the vehicle orientation
- Projecting the road boundaries into the HUD optical system so that the drivers' eye perspective is maintained.
- Ensuring that the projected and real road boundaries match with minimal error.

Previous research on various topics related to driver performance and assistive display technology as they apply to pilots and drivers have been examined and are described in the following sections.

1.4 The Forward Looking Visual Field

The difficulties of driving in adverse weather conditions or at night time comes from either complete or partial loss of the forward-looking visual field. Hills [1] (1980) estimated that more than 90% of all input to the driver is visual information. The effects of the forward-looking visual field view has been studied by many researchers since the first appearance of automobiles.

Wohl [4] (1961) presented a theoretical analysis for a concept of forward reference (or looking ahead) distance. In his paper, he concluded that the forward reference distance is directly proportional to velocity (or desired velocity), which means that drivers need to see further ahead if they drive faster. On the contrary, if their forward-looking distance is limited or blocked, then their driving performance deteriorates.

Senders [5] (1967) studied the sampling rate of the drivers' visual field and presented a possible minimum sampling rate for the forward-looking visual field. Senders manipulated sampling rates for given velocities by periodically raising and lowering a visor attached to a helmet that his subjects wore while driving. He reported that sampling rates of approximately 0.5 sec looking forward for every 3 sec is sufficient to maintain adequate velocity control at 50 mph. Although he didn't mention lane keeping tasks, this may indicate that a driver is able to do without information farther than 3 sec away once he captures enough visual information. The 0.5 second time interval would be the time to

integrate the visual scene. A calculation of 3 seconds of the headway at 50 mph yields 219.8 ft (67.05 m) of look ahead distance at a speed of 50 mph.

Rockwell et al. [6] (1970) at Ohio State University reported that a comfortable velocity selection depended on the distance of available information in their report "Visual Requirements in Night Driving," prepared for the National Cooperative Highway Research Program. Drivers participated in the experiments selected a higher velocity when more forward-looking visual information was available. During night time driving, the forward-looking distance was controlled by limiting the location of the headlight illumination to a specific area at a specified distance. When headlights were set to illuminate a zone 250 ft away from the vehicle, drivers selected lower velocities than the selected speed when headlights were placed to illuminate an area 75 ft ahead. The performance for lateral control was best when the headlights were positioned so as to illuminate 75 ft ahead of the vehicle and deteriorated as the location of the headlamp illumination was moved closer or further away from the 75 ft position. From the report, it seems that drivers mostly depend on the visual information located around the 75 ft range. The following conclusions were reported:

- The velocity selection appears to be a function of the illuminated distance, i.e. the available visual information.
- The velocity maintenance, i.e. low variability in velocity, is a function of the width of the view angle of the available visual information.
- The maintenance of lateral control is a function of the illuminated distance.

10

The illuminating distance of headlights documented in the regulations on automobiles also suggests the required amount of forward-looking distance. For most passenger vehicles [7] (1996), the high beam headlights should illuminate up to 350 ft which covers the minimum forward-looking distance. For commercial vehicles [8] (1997), the headlights in the normal low beam position should help drivers see up to 250 ft ahead, and high beams illuminate 350 to 500 ft ahead. Although they are not directly related to each other, the forward-looking distance in time space can be considered as very similar to the forward-looking distance recommended in state drivers' manual. The Minnesota State DOT recommends a 2-seconds rule [7] (1997) for safety reasons when you are following a car ahead of you. It is recommended that 2-seconds of moving distance should be maintained from the front vehicle. The time of 2-seconds yields 89 ft for 30mph, and 147 ft for 50 mph. Somewhere between 75 ft to 150 ft ahead of the vehicle seems to be where drivers need to look at while driving.

Modjtahedzadeh and Hess [9] (1993) presented a model for automotive driver's steering control behavior based on preview and compensatory steering dynamics. In their model, the human driver model composed of three sub-sections; preview, low frequency compensation, and high frequency compensation. The high frequency compensation represents the driver's neuromuscular system that controls and actuates the actual steering wheel position, and is represented as the neuromuscular effect on the displacement of the steering wheel, δ_{SW}, as a result of the speed of the hand or the steering wheel. The low frequency compensation subsystem compensates for the large

error. Its input is the lateral position error and the output is the desired steering output.

The lateral position error is calculated in the preview subsystem, G_I in Figure 3. The

driver can extract information from the visual scene over and above that obtained from

the instantaneous feedback of lateral deviation error as shown in Figure 3. Foveal and

parafoveal vision work in parallel to provide information about the visual field. He

implemented the transfer function to describe the driver's preview as a combination of a

time advance factor $e^{-\tau_p s}$ and a first-order filter $1/(T_4 s + 1)$. "The preview simply refers to

the amount of time, τ_p, that the input is advanced in time before being used as an input to

the closed-loop system. Thus in the preview model, the driver is hypothesized to operate

upon a lateral position error defined as the difference between an advanced "desired

path," $Y_{DP}(t)$, and the instantaneous position of the vehicle, $Y_V(t)$.

The diagram shows a driver/vehicle control model block diagram. The top section is labeled with three regions: "Preview", "Low Frequency Compensation", and "High-Frequency Compensation (structural model)".

Signal flow: Y_R enters G_I, output Y_{DP}, then summing junction producing Y_e, into G_C, output U_1, into G_L, into summing junction, into summing junction, into G_{NM}, output δ_{sw}, into G_V, output Y_V. Feedback blocks G_{P2} (with U_M) and G_{P1}. The whole enclosed region is labeled "Driver Model".

$$G_I = \frac{e^{\tau_r s}}{T_4 s + 1} \qquad G_L = e^{-\tau_0 s} \qquad G_{P2} = \frac{K_2}{(s + \frac{1}{T_2})^{k-1}}$$

$$G_C = K_7 (T_3 s + 1) \qquad G_{NM} = \frac{\omega_n^2}{(s^2 + 2\zeta_n \omega_n s + \omega_n^2)} \qquad G_{P1} = \frac{K_1 s}{s + \frac{1}{T_1}}$$

Figure 3. Driver/vehicle control model, Modjtahedzadeh and Hess 1993

The use of a desired path will include the possibility of preview and input filtering to account for the fact that drivers often internally generate a desired path that is a smoothed version of the commanded path implied by the lane centerline."

In their experiment, Modjtahedzadeh and Hess showed that 0.75 s time advance, or preview, yielded the same response as a real human subject's response in the lane keeping task. For obstacle avoidance task, 0.85 s of preview yielded same results as human subjects. Both experiments were performed at the speed of 50 km/h (around 30 mph). At the speed of 50 km/h, the 0.75 s is equivalent to 10.41 m (34.1 ft) and 0.85 s is

13

equivalent to 11.80 m (38.7 ft). Their results would seem to indicate a possible minimum amount of the preview information needed for the driving task.

1.5 In-Vehicle Information Display Devices

Since the appearance of the first automobile, there have been continuing efforts to develop devices to assist drivers to reach their destinations safely and effectively. Road signs, symbols, maps, and virtually everything in the vehicle including seats, steering wheels, braking systems, and various indicators can be thought as a result of these efforts.

Recent developments in vehicle based Intelligent Transportation Systems (ITS) include navigation systems, Advanced Traveler Information Systems (ATIS), collision avoidance or warning systems, and advanced vehicle monitoring and control systems. These systems are designed to assist drivers with the driving tasks using emerging technologies. A number of ATIS systems are commercially available or under development in the United States, Europe, Japan, and Korea. The major objectives of ITS are improving safety, reducing travel time, and increasing mobility through the use of advanced technology. For instance, recent in-vehicle navigation systems [10, 11, 12, 13] (1999) perform dynamic routing to the desired destination using digital maps, coordinate data (latitude and longitude) from the Global Positioning System (GPS), and other road status information, and present the resultant guidance information to the driver. Due to recent development of more accurate high-end GPS devices and digital maps, it is now possible to present even more detail and high fidelity information to the driver.

While the vehicle is in motion, real time navigation information must be conveyed to the driver without distracting his/her visual attention from the roadway. How to effectively perform this task is one of the most important research problems with respect to the development of in-vehicle information display systems. Physical devices, choice of format and content of the information are major concerns. The information should be presented in an intuitive manner that has minimal adverse impact on driving mental workload.

The Head Up Display (HUD) which presents visual information in the drivers' forward-looking visual field using an image source and an optical subsystem is conceptually ideal for presenting navigation or guidance information to the driver. By presenting superimposed images in the drivers' field of view, HUDs can reduce the amount of time needed for a driver to capture the display information, while maintaining attention to important events in the outside world. HUDs, which were first used in fighter aircraft in the 1940's, have become a very effective means of displaying flight instrument data in the pilot's visual field and are now being introduced into the automotive world.

1.6 Head Up Display Systems in Aviation

HUDs in the aviation world have been improved greatly since their first appearance during World War II. They are now being used extensively in fighter aircraft, helicopters, and commercial airplanes [14] (1983).

Generally, HUDs are being used as instrument displays but they also can be used as a visual guidance device for better control of aircraft in critical situations, such as landing on a runway during adverse weather conditions. The pilot captures the current state of the aircraft with respect to the outer environment through the visual information displayed by the guidance system and is thus able to control the aircraft. Understanding the human operator's control performance and the relationship to the visually presented control input is one of the important issues in human-centered control systems.

Grunwald et al. [15] (1976) developed a model for vehicular control by visual field cues and performed several experiments for its validation in his paper published in 1976. They proposed a basic model for control-oriented visual field information (VFI) and formulated it based on an optimal control framework.
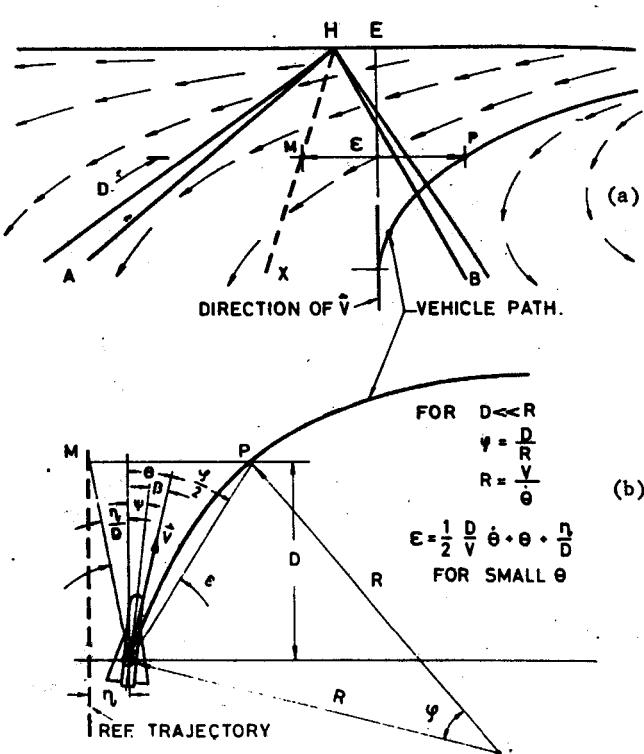
Figure 4. Visual field for curved motion.

In Figure 4, the top illustration (a) is the visual field seen by the pilot and the bottom one is a plan view of curved motion of an aircraft. What is identified as the "vehicle path" in Figure 4 is the predicted path if all instantaneous conditions were maintained. The desired path is to follow reference trajectory, XMH line. Point H is the focal point of the human eye's optical system to where all perspective projection converges. The point E is the focus of expansion from where all of the environmental scene diverges out, i.e. it is where the airplane is heading at that very moment. The arrows in illustration (a) of Figure 4 indicate the movement of the scene in that specific part of the visual field. When the vehicle moves along a straight path, the point E is the only point in the visual field which is apparently stationary, and all other textural points in the visual field appear to have

17

relative motion with velocity vectors as indicated by the arrows. For curved motion, the

focus of expansion, E, no longer exists. The vehicle's future path is given by the solid

curved line in illustration (b). Figure 4 shows a runway of infinite length with guidelines

HA and HB and center line HX. The control task involves keeping the aircraft laterally

on HX. The flight level and speed are maintained as constants. The nomenclature,

indicated in Figure 4 are

η Lateral deviation from HX

V   Velocity vector of the vehicle

θ Path angle between V and HX

ψ Yaw angle between HX and vehicle axis

β Slip angle between V and vehicle axis

The control error at distance D ahead of the aircraft is defined in Figure 4 as the visual

angle subtended between points P and M at distance D, where M is a point on HX and P a

point on the future vehicle path. Following the geometry of Figure 4, the error ε is given

by

$$\varepsilon = \frac{1}{2}\frac{D}{V^2}\ddot{\psi} + \frac{\dot{\psi}}{V} + \frac{\eta}{D}$$

The vehicle control task involves reducing ε to zero. Test pilots were asked to maintain ε

to a minimum with the displayed visual scenes using a simulator. Based on several

18

simulated experiments for a remotely piloted aircraft, Grunwald clearly showed that the

pictorial display of Figure 4 (a) showing only the solid lines could be used for aircraft

control tasks.

In his later paper [16] (1981), Grunwald expanded the VFI concept to the helicopter

maneuvering and developed a perspective tunnel display as shown in Figure 5. Each

rectangle, which forms a tunnel-like shape in the screen, defines the desired trajectory of

the aircraft in 3-D space. The line AA represents the instrument horizon, which is parallel

to the true horizon. The aircraft is slanted in the counter clockwise direction, angle ϕ.

Point C indicates the center of the image and represents the vehicle's forward

longitudinal axis. Point F represents the intersection of a tunnel square and the vehicle's

desired trajectory. Point S is the center of the nearest square. The length of FS projected

on the F_z axis indicates vertical deviation, and the projection on the F_y axis indicates the

lateral deviation when the F_z and F_y axes are defined as perpendicular and parallel to the

true horizon AA. The attitude with respect to the tunnel can be estimated from the

deviation of focal point F from the center of the image C. An impression of forward

motion is derived from the "passing by" of the tunnel segments.
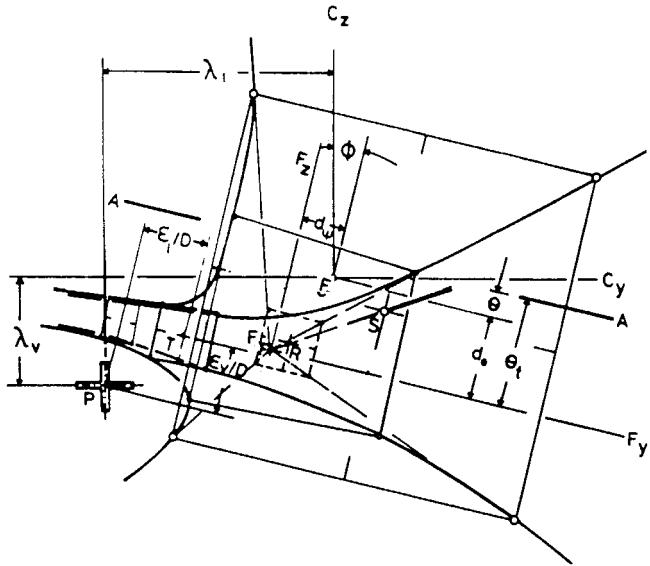
Figure 5. Perspective tunnel display format.

One of the most important features of the perspective tunnel display format is the

predictor symbol, a cross mark displayed at P. The predictor symbol was designed to give

the pilot additional rate information of position and attitude angles. The relative position

and its movement implicitly give the rate information. It was reported that peripheral

vision, which captures the pattern of visual velocity vectors in the visual field, is essential

to the perception of lateral rate and acceleration cues. The perceived rate information acts

as a damping factor in the human centered visual feedback control of aircraft. However,

due to the nature of the tunnel display that displays only small amount of visual field near

the tunnel, Grunwald found that the experimental visual feedback easily becomes

unstable. To increase the system damping factor, Grunwald intentionally added a

predictor symbol whose dynamics were derived by assuming that aircraft proceeds from

the present moment to the future with constant lateral and vertical accelerations. The

predictor symbol is drawn where the aircraft will be in a certain amount of future time. In

20

his experiments, he found that longer prediction time resulted in larger lateral deviation but less roll activity (i.e. smooth and stable), and vice versa. There was a range of optimal prediction time for both good lateral deviation and stable flight, which was 4 to 7 seconds of prediction time. The forward-looking visual information is essential to control of vehicles either flying in the air or moving on the ground. The result of that 4 to 7 seconds of forward-looking information yielded the best performance due to the high speed of the aircraft. On the contrary, pilots maneuvering performance could be decreased if their forward-looking visual field is degraded or limited.

Displays are also important to pilots of advanced rotorcrafts who are being asked to perform very difficult tasks in conditions when out-of-window visual cues are very poor or non-existent. Hover and low-speed maneuvering have long been recognized as one of the most intensive control tasks. To aid pilots in these situations, advanced control and display concepts [17] (1991) [18] (1990) have been developed and evaluated. Because rotorcrafts are highly maneuverable yet can be moved very slowly, giving 3-dimensional visual clues to pilots is very important in order to let them control the vehicles precisely. The display format shown Figure 6 has been fully developed and studied by Hess et al. The display format is very similar to the position-velocity-acceleration (PVA) representation used in the Pilot Night Vision System (PNVS) of the Army AH-64 Apache helicopter.
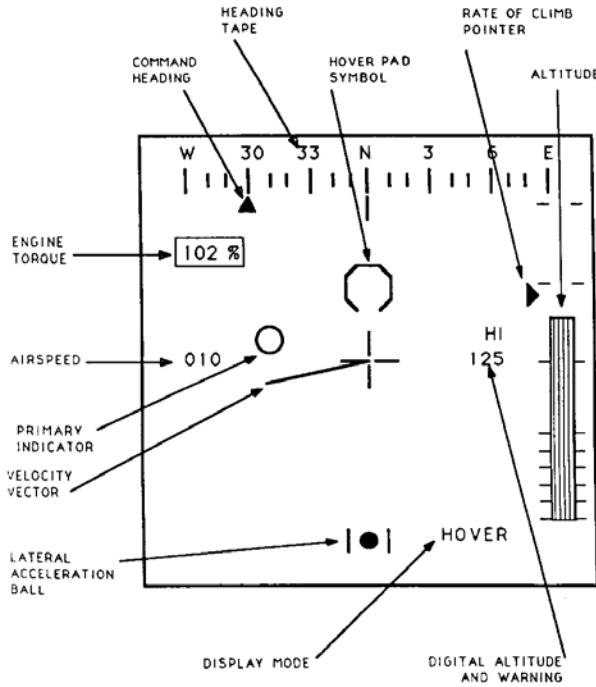
Figure 6. Position-velocity-acceleration display format.

This display format is superimposed on a forward-looking infrared (FLIR) image and presented to the pilot on a helmet-mounted (i.e. head mounted) display. The cross symbol indicates commanded target location. Horizontal line of the cross mark represents lateral axis and vertical line is longitudinal (vehicle's heading direction) axis. The hover-pad symbol that is just above the cross in Figure 6 indicates longitudinal and lateral vehicle position. In Figure 6, there is no lateral deviation. Velocity information is given by clock-needle-like velocity indicator. Its length is speed and its direction represents the moving direction. The primary indicator (small circle left of cross) represents the rotorcraft's inertial acceleration. The movement of a small solid ball on the bottom of the screen indicates lateral acceleration. Hess and Gorder [18] (1990) studied performances and handling qualities of the rotorcraft with respect to several display formats. Three different

22

display formats have been created and studied by them to find the best display format; status display, predictor display, and command display formats. In the status display, the primary indicator was used to provide true acceleration information. In the predictor display format, the primary indicator represents a prediction of the position of the tip of the vehicle velocity vector at programmed seconds later. In the command mode display, the primary indicator was used to provide flight direction information. In this mode, the primary indicator indicates the error between commanded and current angle of the vehicle, and the pilot was commanded to control the vehicle so that the error becomes zero. Simulation results performed by Hess and Gorder [18] (1990) show that the predictor and command displays offer excellent performance and handling qualities in both the pad tracking and capture tasks.

1.7 Automotive Head Up Display Systems

The first automotive HUD was introduced by General Motors in 1988 [19]. The system was developed by a General Motors team from Oldsmobile, CPC-Advanced Vehicle Engineering, Delco Electronics, and Hughes Aircraft Company. Even though the first trial was only for displaying a small fraction of the instrument panel information (vehicle speed) to the driver's field of view, it received significant public interest for various applications [20] (1995). The basic automotive HUD concept is illustrated in Figure 7. There are two ways in which the HUD can facilitate the driving task: First, with key driving data such as vehicle speed as part of the HUD image, the driver can keep his eyes looking toward the road ahead while accessing and responding to the information; in

addition, his eyes remain adapted to the ambient light level in his primary visual field.

Secondly, with the projected image focused to appear two or more meters forward of the

driver, the need to re-accommodate from the road scenery to the HUD image is reduced.
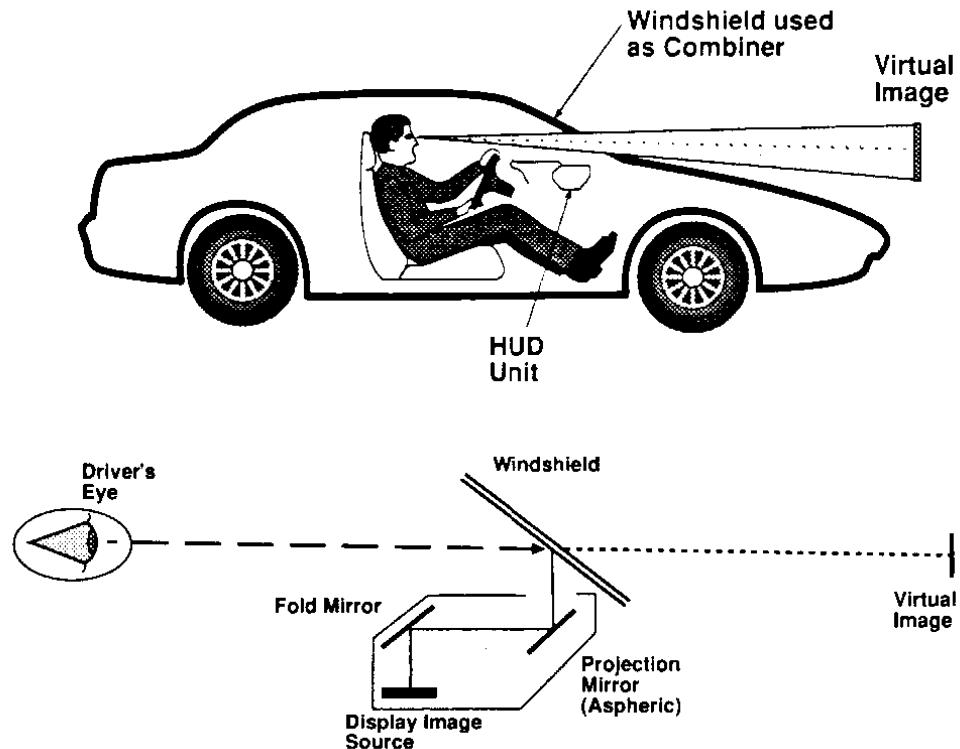
Figure 7. The first automotive head up display introduced by General Motors.

The HUD system was designed so that its visual field of view is 1.5 degrees high and 3

degrees wide, and appears at 2.4 meters forward of the driver's head (near the front

bumper). The eye motion box in which the driver doesn't feel sensitive to movement of

the image as his head or eye moves was designed to be 130 mm by 130 mm.

In October 1998, General Motors announced a night vision system for the prototype model year-2000 Cadillac DeVille. A HUD was adopted to display infrared image in the forward-looking visual field ahead of the windshield [21] (1998).

The first human factors research on automotive HUDs was performed by Sojouner [22] in 1990. His major interest was drivers' response for the conventional instrument speedometer as compared to a HUD projector. He found that the HUD speedometer produced generally superior performance on the experimental tasks; maintaining lane keeping, detection of the sudden appearance of obstacles in driving lane, reading speed indicator values, etc. The HUD type display enabled subjects to respond to the salient cues appearing in the forward-looking view significantly quicker than a normal instrument panel. Sojouner concluded that the factor that enabled subjects to detect and respond significantly more quickly for a salient visual cue was the nature of the HUD which didn't require that one redirect or accommodate one's gaze when shifting from the changing visual scene to the speedometer.

Steinfeld and Green [23] (1998) performed experiments to determine the response to navigation information on a simulated full-windshield HUD. The simulated full-windshield means that visual information was superimposed through out the full windshield. Their simulated HUD experiments were performed on a stationary driving-simulator composed of three random-access slide projectors whose operations were controlled by computer systems. By superimposing two images, a real roadway image and HUD-like image, they simulated a full-windshield HUD. Participants were asked to

decide left or right turns for the presented images and press piano-like keyboard switches to indicate their recognized results. The experimental results showed that there could be a significant amount of improvement in recognition times when 3-dimensional perspective projection was used in the HUDs. They reported that response times of HUDs were 20% shorter than instrument panel type displays. Even though their experiments were for a stationary simulator, their results showed that HUDs were much more beneficial than the normal instrument panel type of display.

1.8   Paper Overview

The rest of this paper is structured as follows:

- Chapter 2, Digital Road Map, describes the composition of the digital map used for the HUD development. A general explanation of the Minnesota Road Research Project (Mn/ROAD) test facilities, details of the coordinate system, and structure of the map data are described in this chapter.

- Chapter 3, Head Up Display System, describes the HUD system used for the experiment, component by component. The truck that was used as a test bed, the DGPS sensor and its data acquisition system, and the computer system including operating system, hardware, and software development tools are described in this chapter as well.

- Chapter 4, Computer Graphics, presents all of the mathematical calculations needed for the computer to draw the HUD screen. The block diagram of the software, coordinate frames, the perspective projection, and the database queries are described in this chapter.

- Chapter 5, Driving Simulator, presents a simple kinematics model simulator developed for software debugging and testing in the lab. A joystick interface to the simulator was implemented to simulate driving control.

- Chapter 6, Experimental Setup, discusses the yaw angle estimation, measured DGPS characteristics, definition of look-back distance, and mismatching error.

- Chapter 7, Experimental Results, presents calibration results of the HUD optical system, measured mismatch error between real road shape and the HUD projected images, and time to draw the HUD screens. Effects of different look-back distance on the mismatch error are discussed in the chapter.

- Chapter 8, Conclusions, discusses about the result of the experiments and further research.

Chapter 2   Digital Road Map

2.1   Mn/ROAD Research Facilities

The Mn/ROAD testing facilities of the Minnesota Department of Transportation

(Mn/DOT) were used for the HUD system development and experiments. The

Mn/ROAD testing facilities are located 40 miles northwest of Minneapolis and currently

support various transportation research efforts. The Mn/ROAD is the world's largest and

most comprehensive outdoor pavement laboratory, distinctive for its electronic sensor

network embedded within six miles of its test pavement. The sensor network and

extensive data collection system facilitates the study of the effect of heavy commercial

truck traffic and the effects of the annual freeze/thaw cycle on pavement materials and

road designs.

Figure 8 shows the overall shape of the centerline of the Low Volume Road (LVR). The

LVR is the main testing section for many experiments including our HUD experiments.

The LVR is kept closed from public access for safety reasons. The LVR is a two-way

road consisting of straight and curved sections. Each part of road has been constructed

based on mathematical parameters, and the parameters will be discussed in the following

section in detail. Two loops at the end of each side are of constant radii and the other

sections are straight lines whose azimuth direction is 52.6 degree to the West from North.

Units for each axis in Figure 8 are coordinate values of the Minnesota South State

Coordinate frame in meters.
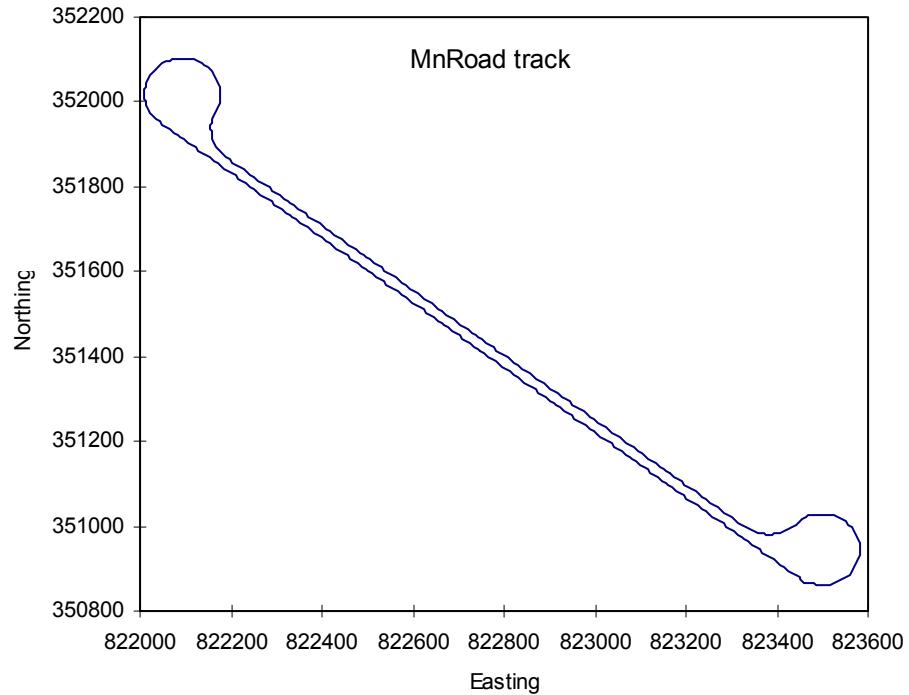
Figure 8. Low volume road of Mn/ROAD testing facilities.

The total perimeter of the LVR of Mn/ROAD is approximately 2.2 miles long. Driving

speed on the straight sections is limited to 40 mph for safety reasons.

2.2 Coordinate Frames for Digital Road Map

The Minnesota South State Coordinate system [24] (1999) has been used as the coordinate frame to express the digital map used for the HUD development and experiments. There are many possible coordinate systems that can be used to express a location on the surface of the earth, but following are the most commonly used coordinate frames;

- Longitudinal and latitudinal angle
- State coordinate frame
- County coordinate frame

Latitude and Longitude

Because the Earth is spherical in shape, it is convenient to determine a location on the surface of the Earth if the location values are expressed in terms of an angle from a reference point. Longitude and latitude are the most commonly used angles to express a location on the earth surface or in orbits around the earth. Latitude is a measurement on a globe or map of location north or south from the Equator. Longitude is a measurement of location east or west of the prime meridian at Greenwich, the specially designated imaginary north-south line that passes through both geographic poles and Greenwich,

31

England. Longitude is the amount of arc created by drawing first a line from the center of the Earth to the intersection of the Equator and the prime meridian and then another line from the center of the Earth to any point elsewhere on the Equator.

The combination of meridians of longitude and parallels of latitude establishes a framework or grid by means of which exact positions can be determined in reference to the prime meridian and the Equator. Typical latitude and longitude values near Mn/ROAD area are +45.1 degrees North, and -93.4 degrees West. Almost of all current GPS systems give latitude and longitude values as location data.

State Coordinate Frame

Even though the actual landscape on the Earth is a curved surface, we recognize and utilize land as if it is a flat surface. A Cartesian coordinate system whose axes are defined as three perpendicular vectors is usually used. In a Cartesian coordinate system, the location of a point is expressed in terms of a relative distance, expressed in either meters or feet, from a reference point along each axis. Each state has its own standard coordinate system to locate points within their state boundaries. All construction and measurements are done using distance dimensions (meters or feet). Therefore a curved surface on the Earth needs to be converted into a flat surface and this conversion is called a projection. There are many projection methods used as standards for various local areas all over the earth surface. Every projection involves some degree of distortion due to the fact that a surface of a sphere is constrained to be mapped onto a plane. The standard projection method for Minnesota is the Lambert Conformal Conic Projection [25, 26] (Figure 9),

which is a conic projection for making maps and charts in which a cone is, in effect, placed over the Earth with its apex aligned with one of the geographic poles. The cone is positioned so that it cuts into the Earth at one parallel and comes out again at a parallel closer to the Equator; both parallels are chosen as standards, or bounds, of the area to be charted. Points on the Earth are then projected onto the cone along lines radiating from the center of the Earth; the map or chart results when the cone is slit along a meridian and laid out flat.
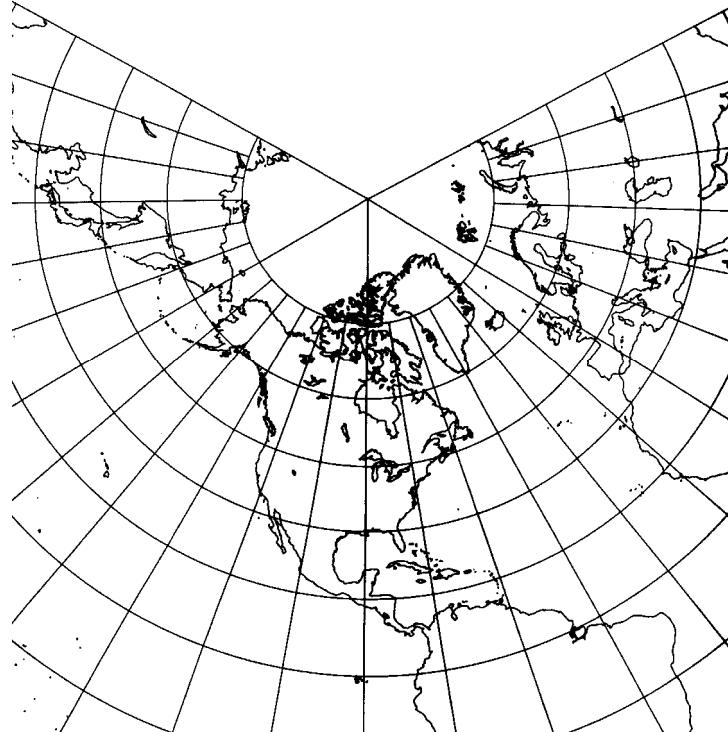
Figure 9. Lambert conformal conic projection [26].

The Lambert Conformal Conic Projection is extensively used in ellipsoidal form for large scale mapping of regions of predominantly east-west extent, including topographic

quadrangles (1:24,000 and 1:62,500 scale) for many of the U.S. State Plane Coordinate

System zones, maps in the International Map of the World (1:1,000,000 scale) series, and

the U.S. State Base Maps (1:500,000 scale). The following constants apply for all

Minnesota State plane zones:

- Projection = Lambert Conformal Conic

- False Northing = 100000.000 m

- False Easting = 800000.000 m

- Eccentricity = e = 0.08181919104283185

- Flattening = f = 0.003352810681183637

- Inverse Flattening = 1 / f = 298.2572221008827

The Minnesota State Coordinate System is divided into three sub-coordinate areas: South,

Central, and North Zones. The Minnesota South State Coordinate Frame was used to

build a digital map of the Mn/ROAD test track for HUD development and experiments.

The Mn/ROAD facilities are located in the North American Datum of 1983 (NAD83)

Minnesota South State Plane. The conversion equations to calculate the state coordinate

values from GPS receiver's longitudinal (λ) and latitudinal (ϕ) angle data are as follows

(the units of λ and ϕ angles are in radians in the following equations.):

$$Q = \frac{1}{2}\left[\ln\left(\frac{1.0 + \sin\phi}{1.0 - \sin\phi}\right) - E \cdot \ln\left(\frac{1.0 + E\sin\phi}{1.0 - E\sin\phi}\right)\right]$$

$$R = \frac{K}{\exp(Q\sin\phi_0)}$$

$$\gamma = (\lambda_0 + \lambda)\sin\phi_0$$

X and Y are calculated based on the above as:

$$X = E_0 + R\sin\gamma$$

$$Y = R_b + N_b - R\cos\gamma$$

where the required constants are

$$\phi_0 = 44.5014884140\,\text{deg}$$
$$\lambda_0 = 94.0\,\text{deg}$$
$$K = 11914387.7514$$
$$E = 0.081819191$$
$$E_0 = 800000.0$$
$$R_b = 6667126.8494$$
$$N_b = 100000.0$$

The resultant X and Y are the state coordinates in meter units. The Minnesota South State Coordinate Frame was also used to express the location of the test vehicle, and a moving coordinate frame attached to the vehicle, as explained in following chapters.

County Coordinate Frame

The County coordinate frame is also used for a more accurate geometrical expression. The Mn/ROAD facilities are located in Wright County. Their original construction data was expressed in the county coordinate frame. However, to express the coordinates of the LVR at Mn/ROAD, we needed to know each parametric point in terms of the Minnesota State Coordinate System. The locations of each parametric point using the Mn/ROAD construction data was calculated using the MnCon software supported by Mn/DOT. The MnCon is a freely available software package that can be downloaded from the following web-site,

http://rocky.dot.state.mn.us/

This page is maintained by the

Office of Land Management, Minnesota Department of Transportation

395 John Ireland Boulevard

St. Paul, MN 55155

MnCon is a Windows-based software application which performs conversions within the NAD83. It works using keyboard input or ASCII (text) files of specific formats. The software can convert between any two of the 73 different map projections including: latitude/longitude, Universal Transverse Mercator zone 15, the three Minnesota state plane zones and 68 Minnesota county coordinate system zones.

2.3 Digital Map

The digital map used for HUD development was made from the construction data of

Mn/ROAD. Only the LVR part was included in the digital road map. The digital map

contains a series of numeric location data of the centerline of the LVR. The construction

data is given by the number of shape parameters including starting points and ending

points of the straight paths, centers of circular sections, their starting and ending angles,

etc. al. (Figure 10) The following table shows these parameters.

Points	Wright County Coordinate (ft)	Minnesota South State Plane (m)
p1	546,500.480, 202,514.466	823,330.315, 350,997.461
p2	546,860.825, 202,536.871	823,440.135, 351,004.443
p3	547,328.341, 202,358.084	823,582.706, 350,950.150
p4	546,886.572, 202,122.761	823,448.159, 350,878.237
p5	542,279.243, 205,654.364	822,042.380, 351,952.673
p6	542,391.713, 206,142.100	822,076.452, 352,101.379
p7	542,685.823, 205,737.087	822,166.267, 351,978.060
p8	542,757.806, 205,383.295	822,188.358, 351,870.258
c1	546,667.779, 202,732.723	823,381.213, 351,064.055
c2	547,053.871, 202,341.018	823,499.057, 350,944.831
c5	542,446.542, 205,872.621	822,093.278, 352,019.267
c7	542,925.104, 205,601.553	822,239.256, 351,936.852

Table 1. Parameters for the Low Volume Road (LVR) of Mn/ROAD.

The LVR is composed of 2 circular paths, South-East and North-West, and 2 straight

paths, south and north path. The road points starts from the lower circular path and go in

the clock-wise direction. The locations for each point are defined as follows and their

locations are drawn in Figure 10.

- p1 is the starting point of the south-east circular path as well as the end point of the north straight path.

- c1 is the center of rotation of the first concave circular path. This circle ends at point p2.

- p2 is where the circular shape changes curvature to the lower big circle (an inflection point).

- c2 is the center of rotation for the big circular path.

- p3 is the middle of the south-east circular path.

- p4 is the end point of the circular road and the starting point of the south straight path.

- p5 is the end point of the south straight path and the starting point of the north-west circular path.

- p6 is the middle of the north-west circular path.

- p7 is the end point of the first part of the north-west circular path where the circular shape changes curvature (inflection point).

- p8 is the end point of the small circular path and the starting point of the north straight path.

Units for each axis of Figure 10 are meters in Minnesota State Coordinate frame. The X-axis, captioned as Easting, represents East (+) and West (-). The Y-axis, captioned as Northing, represents North (+) and South (-).
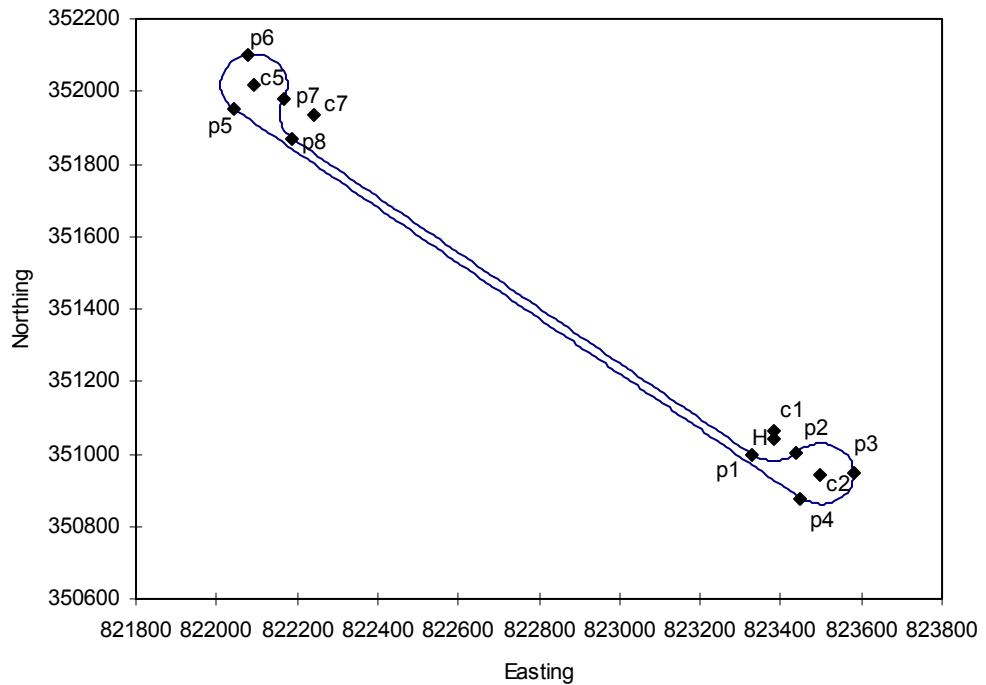
Figure 10. Geometric points of LVR of Mn/ROAD (units are meters).

Other data for special locations in the Mn/ROAD area are

- H-Mn/ROAD (main office of Mn/ROAD)

  Latitude: 45 15' 31.99906", Y:351,040.296 (1,151,704.705 ft)
  Longitude: -93 42' 7.61646", X:823,381.396 (2,701,377.131 ft)

- Differential GPS base station antenna

  Latitude: 45 15' 32", Y:351,019.858 (1,151,637.651 ft)
  Longitude: -93 47' 7", X:816,853.893 (2,679,961.481 ft)

- Front of the truck parking garage (GPS measured values)

  Latitude: 45.25965971 degree, 45 15' 34.774956"
  Longitude: -93.70139578 degree -93 42' 5.024808"

Road map generating software was developed to prepare digital map files from the parametric location data set. Each road point was generated at uniform 10 meters intervals. As a result of the software processing, a total of 422 points was generated and stored into a data file. Only a specific part of the stored map data was read and processed by the map query routines in the HUD software when the HUD was operational. The road points represent only the centerline of the Mn/ROAD. No other road structures and signs were included in the map data file. The database was programmed so that all 3-dimensional coordinate (including elevation) information is stored and processed, however, the elevations of the road points were assumed as constants for the entire area within Mn/ROAD for the experiments described in the paper.

A query area to extract only the required information from the entire road map was defined mathematically in consideration of the vehicle movement. Detailed equations and a working scheme of the query area will be discussed in the following chapters after the definition of the coordinate frames used for the HUD graphic display.

Chapter 3   Head Up Display System

The HUD system described in this paper is composed of the following sub-systems: the optical systems (including video image generator, image projector, and combiner), the computer system, the DGPS system, and the operating software, each of which will be described below.

3.1   Optical System

The optical part of the Delco manufactured DataVision^{TM} HUD system model 110, was used for the HUD development and experiments. This model was originally developed by Hughes Aircraft Company to apply their HUD technologies from advanced military jet fighters to the commercial market in an affordable package for a variety of applications as a part of a Mobile Data Terminal (MDT). The major purpose of the Delco HUD was to display crucial character-based information in the drivers' field of view to allow them to observe important messages without loosing eye contact with their forward-looking visual field. The HUDs were used for police vehicles in order to display computerized vehicle information about a suspect vehicle while following the car. Some of the latest luxury vehicle models also have options incorporating a HUD to display information from the instrumentation panel.

Typically, the HUDs are designed to be used as a character-based information (or numerical icon displaying) display unit. Major components of the HUDs are as follows (see Figure 11).

- Mobile Data Terminal

  This unit communicates with the central computer to access information needed.

- Electronic Unit

  This unit generates character based video images for the information accessed through the MDT unit.

- Projection Unit

  This unit receives video signal from the electronic unit and projects video images onto the combiner. The projection unit has an liquid crystal display (LCD) matrix and high-intensity light source similar to most video projectors except that it is small so that so that the device can fit near the drivers seat space.

- Combiner

  The combiner is a reflecting screen for the projected light from the projection unit. The combiner is the area where the driver looks through. In the combiner, the driver can see both the real outside road scene and the computer generated images.
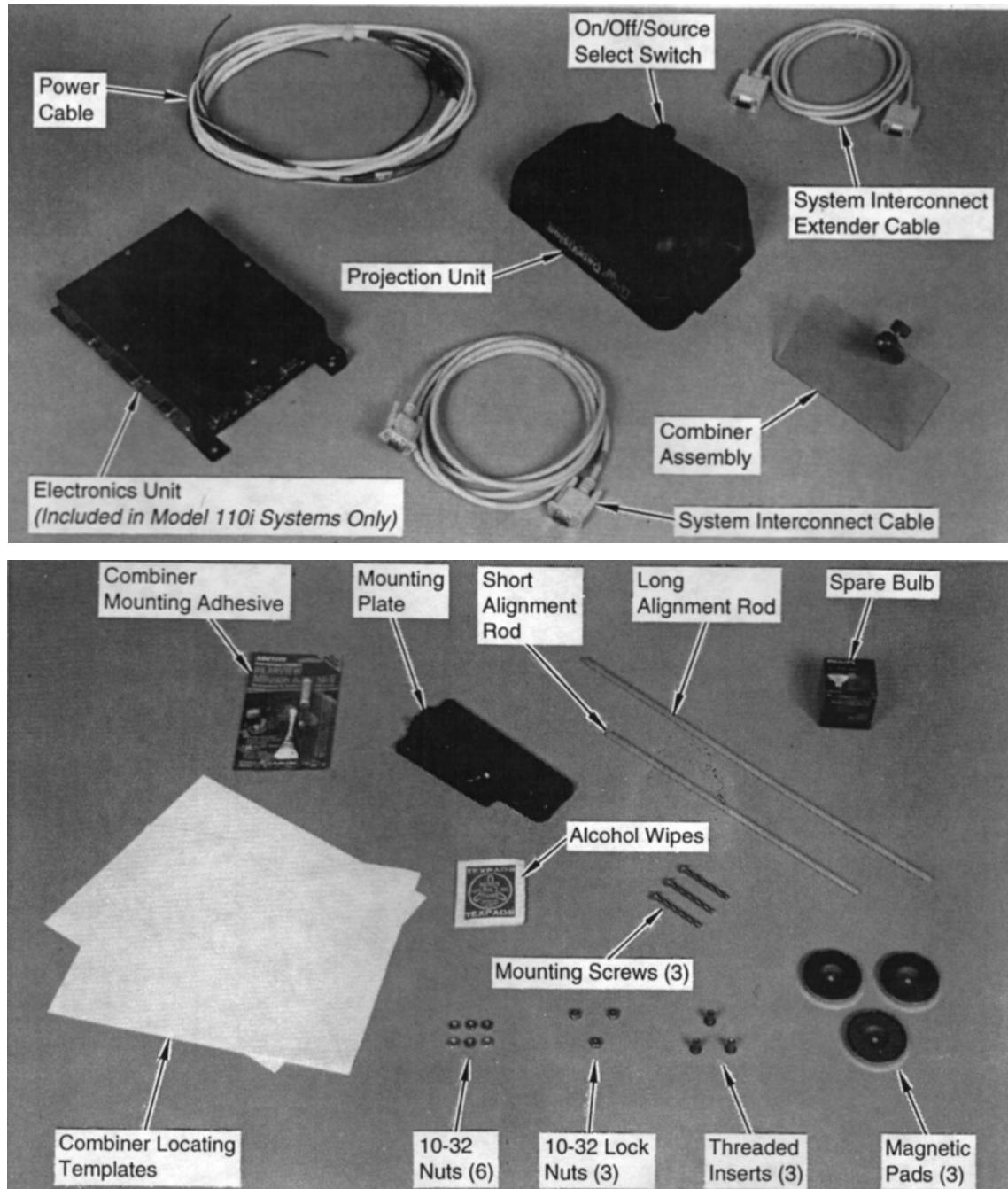
Figure 11. Delco manufactured the DataVision System.

Even though the Delco HUD was designed with their own character based computer

systems, the image projector has an additional NTSC video input feature and this feature

was used for the HUD development described in this paper. Video output from the

graphics processor was fed into a scan converter which converts VGA input into the

needed NTSC video signal. The unit projects the image on to a combiner, a partially

reflective, but essentially transparent optically correct plastic lens. The light reaching the

eyes is a combination of the light passing through the lens and light reflected from the

projector. The driver actually sees two images superimposed together. The image passing

through the combiner comes from the actual frontal field of view while the reflected

image is generated by the graphics processor. The combiner's optical characteristics

allow it to generate a virtual screen projected to float 30 - 40ft ahead of the unit. This

feature, which results in a virtual focus in front of the vehicle, ensures that the driver's

eyes do not have to focus back and forth between the real image and the virtual image,

thus reducing eye strain.
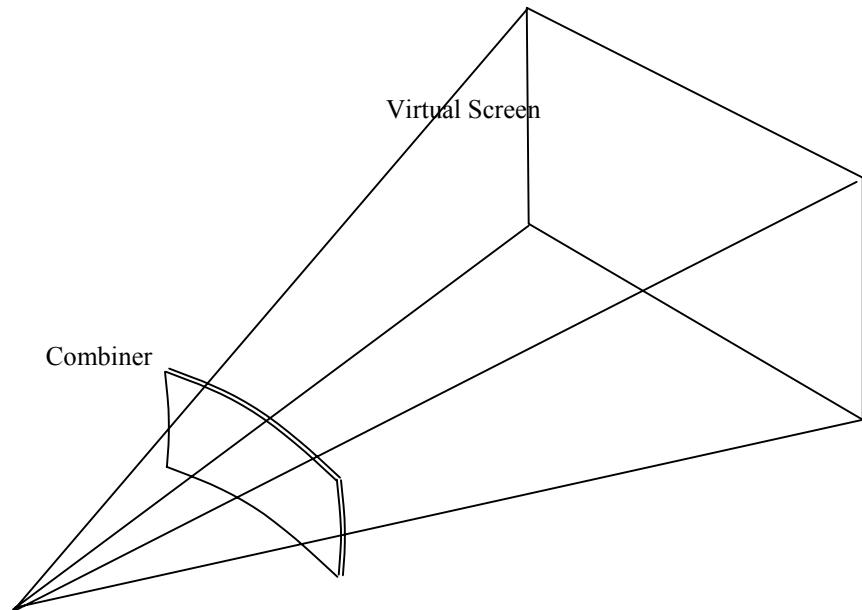
Figure 12. The virtual screen composed by the combiner.

The following table shows the measured essential characteristic of the optical system.

Parameters		Specifications
Visual Image Size		6.3 degree (horizontal) by 4.5 degree (vertical)
Virtual Screen	Distance	43.2 ft (13.15 m)
	Size	1445 mm (horizontal) by 1030 mm (vertical)

Table 2. Measured parameters of the HUD optical system.

The visual image size expressed as an angle was calculated using the measured distance to the virtual screen and its width and height. The 6.3 degree of sight angle is very narrow compared to the drivers' visual sight angle in normal driving situations. The width of the left half (driver's side) of the front windshield is 853.4 mm and the distance from the drivers eye position is 701.0 mm. Even in the case when the driver is looking only through the left half of the full windshield, the sight angle is 62.65 degrees which is far larger than that of the current HUD's optical system. Recently a larger combiner was designed by our group and is presently being tested but it will not be described here.

Figure 13, 14, and 15 show the layout of the projector and combiner in the truck in actual use.

Figure 13. Layout of the head up display (driver side view).

Figure 14. Layout of the head up display (passenger side view).
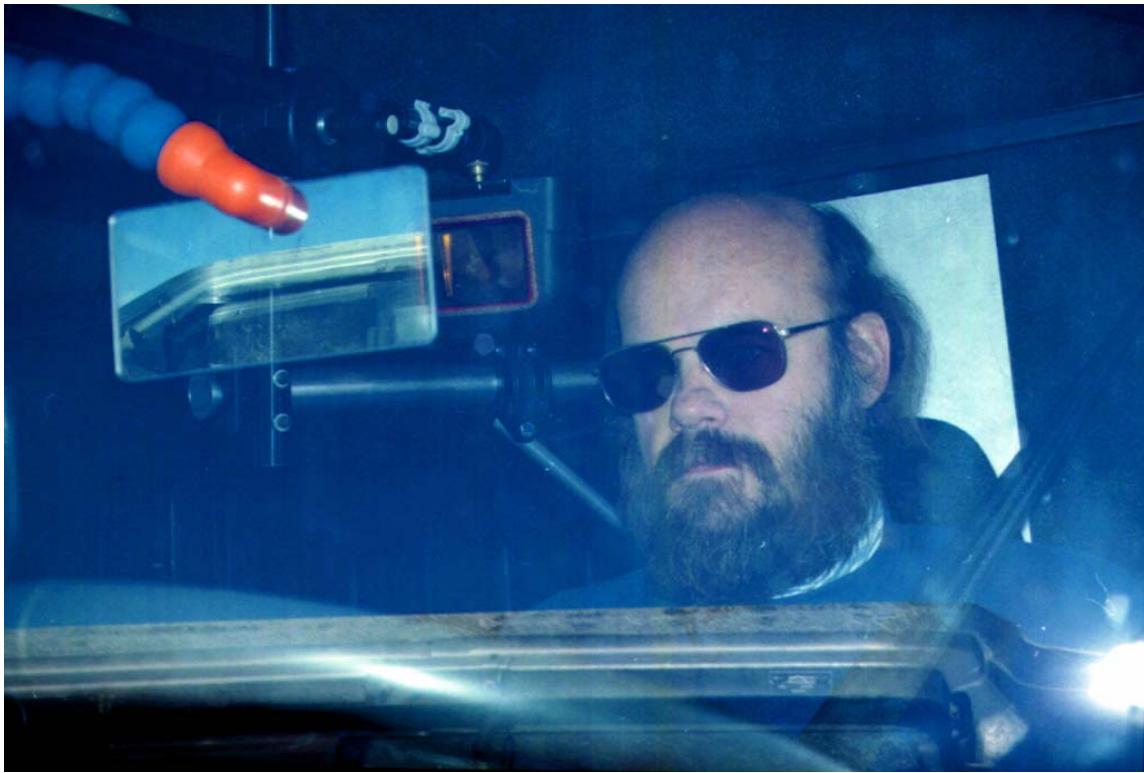
Figure 15. View of the system looking towards the driver through the windshield.

3.2   Computer System

A Windows based notebook computer was used for the entire HUD operations: map data management, DGPS data receive, coordinate transformation, and all of the graphical image reconstruction. Furthermore, the computer system was designed as two separate computer subsystems, one for map data management and another for computer graphic operations. Followings are the key specifications for the notebook computer used for the HUD development.

Items	Specifications
Model	Compaq Presario 1080
CPU	Intel Pentium 133 MHz MMX
Memory (RAM)	16 Mbytes
Graphic	800 X 600 (SVGA) 16bit High color NeoMagic MagicGraph 128ZV

Table 3. Specification of the laptop computer used for HUD development.

Most recent personal computer systems are designed for use with the Microsoft Windows operating systems (Win95/98, NT), and they usually have special device drivers for their hardware circuits including graphic systems. The device drivers are usually first developed for the Windows system. Even though the computer used for the HUD development was not particularly fast, it was possible to develop a HUD which generates real time screen updates by combining the hardware accelerated graphic system and properly optimized HUD graphic software. The graphic display part, its video screen drawing speed and the size of the graphic memory for colors and pixel representation, are the most crucial aspects defining system performance in the HUD system.

The MagicGraph 128ZV system integrated in the notebook computer used for HUD development was developed by NeoMagic. The system has a 128-bit-wide graphic system local bus for accelerator circuits which enable live zoom-video capture, full-motion video, and TV support functions. Newer laptop computer models are using a MagicGraph 256 series that has a 256 bit-wide graphics system bus. In our opinion, any of the commonly used notebooks would be adequate for drawing HUD screens in real time for the simple test drive experiments using the Mn/ROAD testing facilities. Actual

performance for driving situations on real roads needs further analysis (presently

underway in a separate study).

3.3   Truck Test Bed

A Navistar manufactured trailer truck, the International model 9400 series, as shown in

Figure 16, was used as the test bed for the implementation of the head up display system.

Figure 16. Truck test bed.

Figure 17 shows the dimensions of the truck cab. The dimensions are needed to compose

the coordinate transformation matrix [T] which converts road data which are given in

terms of the Minnesota state coordinate frame into the local coordinate frame data which

represents the relative location and orientation with respect to the driver's eyes.
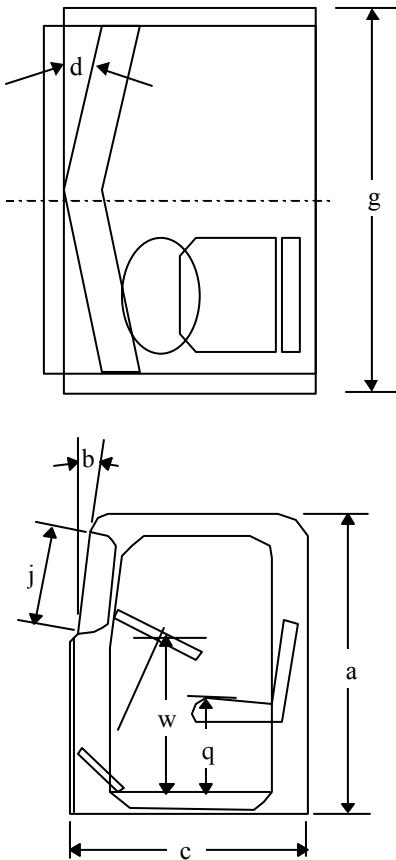
Figure 17. Dimensions of the truck cab.

Dimensions of each part in the cab are provided in the maintenance manual for the truck

and are as described in Table 4.

Items	Dimension	Items	Dimension
a	2.1209 (83.5)	f	0.0762 (3.0)
b	8 °	g	1.9812 (78.0)
c	1.3208 (52.0)	j	0.5080 (20.0)
d	7 ° 30'	k	0.5080 (20.0)
e	1.7780 (70.0)	l	1.3398 (52.75)

Table 4. Cab Dimensions, units:m (in).
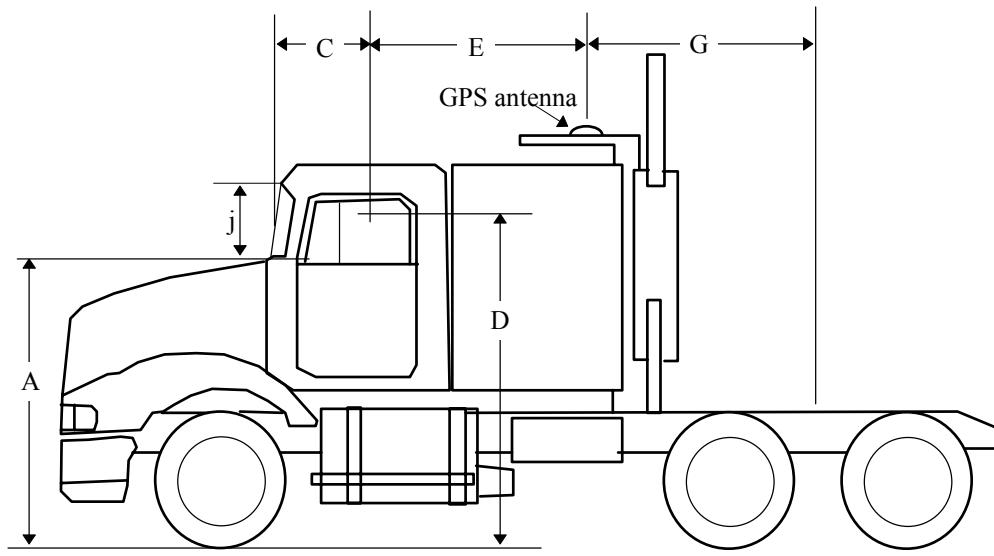
Figure 18. External dimensions of the truck.

Items	Dimension	Comment
A	2.07 (6.8)	Height of the bottom of the front windshield from ground
B	0.8534 (2.8)	Width of the half windshield (driver side)
J	0.5080 (20)	Height of windshield glass
C	0.7014 (2.3)	Distance of the driver's eye from the windshield
D	2.408 (7.9)	Height of driver's eye from ground
E	1.7374 (5.7)	Horizontal distance between GPS antenna and driver's eyes
F	6.0655 (19.9)	Horizontal distance of wheel base
G	2.8346 (9.3)	Horizontal distance between effective rear wheel and GPS antenna

Table 5. External dimensions, units:m (ft).

The driver's normal visual field through the full windshield was measured as well (see Figure 19).
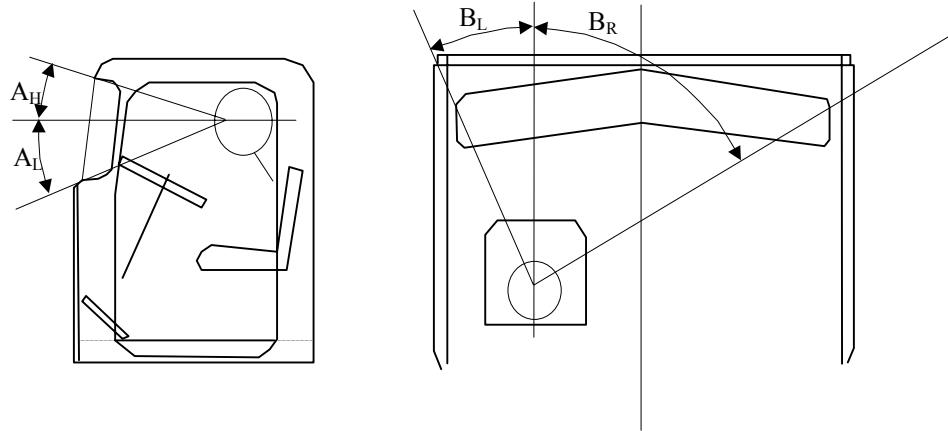
Figure 19. Field of view through the full windshield.

The drivers' height and their normal sight angle vary with their height or seating position. A driver of average height was selected for the design. The optical system for the HUD was fixed for based on this driver's dimension. The parameters for the Figure 19 are as listed in Table 6.

Items		Dimension (degrees)
Vertical View	A_H	12.1
	A_L	25.7
Horizontal View	B_L	31.3
	B_R	61.3

Table 6. Field of view through the full windshield.

The angles specified in Table 6 are calculated numbers using the relative locations and configurations of the truck cab and the driver's head position within the cab.

3.4   Differential GPS

A Novatel RT-20 DGPS was used as the primary position sensing system. In previous experiments [27, 28] (1997), we found that its performance readily met its specifications of 20cm accuracy while operating at a 5 Hz sampling rate. Serial communication routines were coded as a separate thread (same concept as a process or task in a Unix-based or real time operating system) for faster processing of the received GPS data strings.
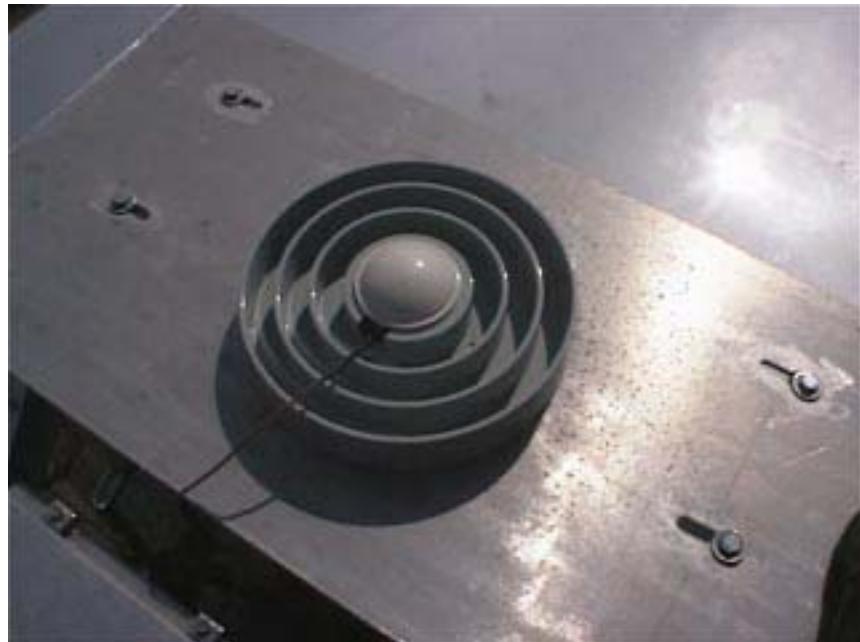
Figure 20. DGPS receiver antenna mounted on the top of the test truck within a choke ring.

The P20A log format was used for 20 cm accuracy and 5 Hz operation. A typical P20A log message and its components are as follows:

*$P20A,910,250783.00,0.000,6,45.25951317,-93.70147699,295.050,-26.380,61,0.994,0.752,1.293,0, 8,2,33,0*27*

53

where, each part of the log string is defined below

- $P20A   Log header

- 910   GPS week number

- 250783.00   GPS seconds into the week

- 0.000   Age of differential correction

- 6   Number of satellites in use (0-12)

- 45.25951317   Latitude of position in current datum, in degrees

- -93.70147699   Longitude of position

- 295.050   Height, in meters with respect to mean sea level

- -26.380   Geoidal separation, in meters

- 61   Datum ID

- 0.994   Standard deviation of latitude solution element, in meters

- 0.752   Standard deviation of longitude solution element, in meters

- 1.293   Standard deviation of height solution element, in meters

- 0   Solution status

- 8   RT20 status

- 33   Idle time of the CPU, integer value. If this value is less than 10, the system performance degrades.

- 0   Differential reference station

- *27   Checksum

The GPS log strings are normal ASCII strings.

3.5   Operating Software

The HUD software was developed using Microsoft Visual C++ under the Windows 95/98 operating system. Because the program was developed as a standard 32-bit application, the HUD software can be run under either Windows NT or 95/98 without any modification. The software was coded using the object oriented programming language C++. For real time screen drawing, sophisticated graphic packages (for example, Open-GL or Tcl) were not used; only basic screen drawing routines (point drawing, line drawing, and polyline) supported by Visual C++ and the operating system were used. This facilitated porting to other operating systems like the QNX real time operating system where graphic libraries are not readily available.

The size of the executable file is about 1.17 Megabytes.

The basic skeleton was prepared by following the standard generating method which is built into the Visual C++ development tool. In detail, the software was developed as a "Single Document Interface (SDI)" style. The SDI means that the software can handle one document at a time which is convenient to the HUD system. The HUD system needs to access an entire computer screen for the single purpose of drawing road boundaries.

To facilitate connection to the previous and future systems, various DGPS input methods were prepared and coded. These included: Direct RS-232 serial input from the DGPS receiver, UDP/IP communication from a separate data collecting computer system, and using simulated GPS values from a driving simulator.

Chapter 4   Computer Graphics

4.1   Head Up Display Screen

Figure 21 shows a typical screen of the HUD system on a curved section of the

Mn/ROAD.
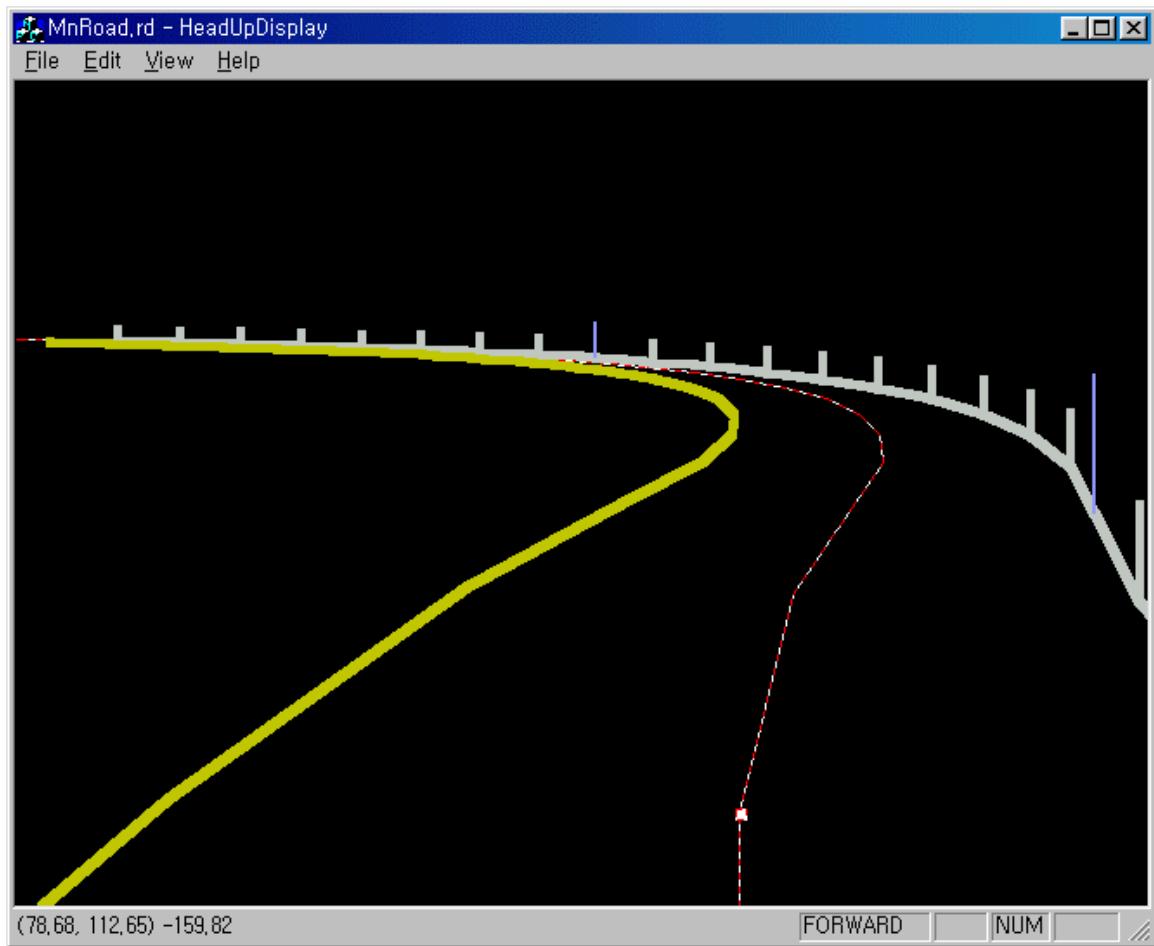
Figure 21. Typical HUD Screen. The image is in color on a standard display and monochrome in the HUD combiner.

The left (yellow) curved line is the left side road boundary. The dotted line with white dots represents the yellow centerline of the two-way land road. The right side curved line with the vertical poles is the right side of the road boundary. The driver is supposed to drive in the lane between the centerline and the right side boundary. The screen in Figure 21 is projected in the forward-looking visual field of the driver with the correct scale so that objects (including the painted line stripes) in the screen are superimposed on the real objects in the outer scene. The black area of the screen in Figure 21 is transparent on the combiner under real operating conditions. Only the bright colored lines appear on the virtual image that is projected onto the combiner; the dark areas are transparent and are thus filled with the image that one sees through the combiner.

The Delco made projector can display only monochrome color. All yellow, red-dotted and white lines were drawn as white for maximum illumination. Line widths of the road boundaries were changed to 5-pixels thick for better perception. The red-dotted centerline was a 1-pixel wide dotted line but it was also changed to a white solid line with the same thickness as the side boundary lines. Thin lines were very difficult to see when the outside environment was bright. A newer HUD design has now overcome this problem.

In Figure 21, the HUD screen is the same as that generated by ordinary windows-based software composed with a title bar, menu, client area, and status bar. This screen was designed for debugging and the HUD screen was displayed as a full desktop window that was used during actual driving experiments. The major working area of the window software where the graphics objects are drawn is called the client area. All of the HUD

graphical information about the road is drawn in the client area. System menus are located on top of the client area. Filling the background with black color, or zero illuminating intensity, to achieve transparency, is done by changing the display setting of the Windows system. By changing the Windows OS level setting, the filling operation of the background with black can be processed faster than doing a solid fill by the HUD software routines. At the bottom, brief status information appears. Current location and heading angle of the vehicle are displayed in the state plane coordinates. The first two numbers in parentheses are the X and Y values of the state plane coordinate, and the next number is the heading angle of the vehicle in degree units which is measured in a counterclockwise angle direction from the north. The heading angle is zero when the vehicle is headed in the true north direction and increases as the vehicle turns counterclockwise as viewed from the top.

The centerline in the graphic screen of Figure 21 is the yellow painted centerline stripe, which demarcates the other lane on the test road but could represent a lane for travel in the opposing direction, as found on most normal roads. In our case, the digital map contains only the centerline data but other representations are possible. The centerline data was mathematically generated using the construction data. The two road boundaries are generated mathematically using the centerline data and the roads width as the HUD software draws the output screen. The mathematical calculation of road edges from the centerline data will be discussed in the "Road Edge Calculation" section.

The "forward" text appearing on the right side of the status line on the bottom means that the HUD software detected that the vehicle is moving in the forward direction on the digital map. In our case, the forward direction of the digital map is the direction in which the digital map data is stored. The digital map data is a 1-dimensional array of points for the clock-wise direction of the Low Volume Road of Mn/ROAD. The bottom status line was used for debugging the HUD software and was made invisible while performing experiments on the road to make the visual field for the HUD wider and clearer. As we expected, the status line annoyed drivers driving the truck. The upper tool bar, where the file, edit and view are located was hidden during actual experiments.

The map of the newly designed system has been improved to incorporate complex shaped road data. In case of the LVR of the Mn/ROAD, a 1-dimensional array of points was good enough to express entire LVR section and process the retrieval tasks. The left and right road boundaries were calculated by mathematically expanding the centerline data. Later, the data structure for the map was changed to multiple sets of 1-dimensional array of points, which represents shape of the actual road boundaries. In this structure, the left and right boundary, and centerline are stored in separate array structure. This scheme requires more memory and computing power to retrieve a local map which is visible to the driver. In the newly designed system, the map handling and retrieval tasks are performed in a separate computer system then transmitted to HUD computer via the local network in the truck.

4.2 Block Diagram of Head Up Display Software

The blockdiagram shown in Figure 22 shows all the software components and internal

data flow throughout the HUD system.

Head Tracking System

Driver's eye data
location (D_x, D_y, D_z)
yaw angle $\Delta\theta$
pitch angle $\Delta\phi$

GPS

Vehicle location
(V_X, V_Y, V_Z)

Moving coordinate frame attached to driver's eye

[T] matrix

Yaw rate gyro

Yaw angle
θ

Tilt sensor

Pitch angle
ϕ

Not implemented yet

Digital road data

Extracted local road data

Road data with respect to moving coordinates

Generate road Shape

Perspective Projection

Clipping

Projected road edges

Figure 22. Block diagram of the Head Up Display System.

The blocks for the digital map, coordinate transformation, and perspective projection are the most crucial. A coordinate transformation matrix [T] is constructed from the location and heading angle of the moving vehicle and the driver's head or eye data. The location data retrieved from the digital map are converted into local coordinate data using the transformation matrix [T], then fed into the perspective projection routines. The perspective projection routines calculate and draw the road shape in the computer's graphic memory, which then appears as a virtual view in the driver's visual field of view.

The digital map block is the road map data management system that maintains the digital map described in the previous section. The digital map is given by the global coordinate frame which is based on the Minnesota South State Coordinate frame. The coordinate frames defined and used for the HUD will be described in the following section.

The coordinate transformation block transforms the coordinate frame of the digital map from the global coordinate frame to the local coordinate frame. The local coordinate frame is a moving coordinate frame that is attached to the driver's head. The coordinate transformation is performed by multiplying a 4x4 homogeneous matrix [T] to the road data points. Because the vehicle is kept moving, the matrix [T] must be updated in real time too. The movement of the driver's eye that is included in the matrix [T] also should be measured and fed into the matrix [T] calculation in real time. However, the heading angle and position of the driver's eyes are assumed to be constants in the experiments; driver always sees straight forward direction at a fixed position. This is a reasonable

assumption for the experiment with a head up type display system where displayed images and the eye (or head) position are positioned at a specific configuration to see the reflected images. If driver's head is located far from the designed position, the driver cannot see the reflected image. Furthermore, the optical system of the HUD was designed to minimize the effect of the viewer's eye location if it is bounded in a designated area. If the driver's head doesn't move far from the designated insensitive eye frame, the images tend to stay at the same position independent of the eye position. Therefore, if the position of the combiner is fixed once the HUD is adjusted and the driver doesn't move the head out of the designated frame, then it can be assumed that the HUD images stay in the same position. When the driver moves his head position significantly, then he would already knows that the HUD image may not be valid.

On the other hand, head-mounted displays (HMD), i.e. helmet-mounted types, in which display units are attached to the helmet or goggles, are very sensitive to head movement. Whenever the driver moves or rotates his head to the left or right, the screen images move as well. Furthermore, it is impossible to make a position-insensitive optical system for the head-mounted display. If the head-mounted display is used for the conformal augmented system, the position and orientation of the head must be measured and used to compensate for head motion in the display computation. The problem however, is that if there is any mismatch or lag between the true head motion and the projected display maps, motion sickness will result.

The heading angle of the vehicle is estimated from the past history of the GPS location data. We attempted to see whether a GPS based estimate of the heading angle would be sufficient. Otherwise, a rate gyro would be needed. An absolute heading angle is needed to compute correct coordinate transform matrix [T]. An error or lag in the heading angle estimation (or measurement) affects the HUD matching accuracy. In addition to the heading angle estimation by successive differentiation of GPS data, a method to measure an absolute heading angle using a magnetometer (digital compass) or an Inertial Measurement Unit (IMU) are being considered for better accuracy and dynamic response on the calculation of the coordinate transformation. Furthermore, other angles such as roll and pitch angles need to be considered when computing the correct coordinate transform matrix [T]. The roll is the angle that the vehicle makes in the vertical plane along the lateral direction of the vehicle. This angle would appear if the vehicle moves along a banked road. The pitch is the angle that the vehicle makes in a vertical plane along the longitudinal direction. The pitch angle appears if the vehicle climbs up or down a hill. These two angles are included in the coordinate transformation matrix but were set as zeros for the experiments on the LVR of Mn/ROAD because the road profile of the testing sections of the LVR are flat. The relative position of the driver's head was also included in the coordinate transformation matrix, but were set as constants. The roll angle was set as zero and the pitch angle was set as – 5 degrees down in to the ground from the horizontal line in order to maximize the effective viewable area of road boundaries.

The result of the coordinate frame transformation is the road boundary data seen from the driver's eyes' perspective. The resultant local coordinate data must be projected onto the

planar surface of virtual screen made by the combiner and projector. Actually, the projector projects the image onto the curved surface of the combiner but the projection screen is the virtual screen located at 43.2 ft (13.17m) in front of the driver.

4.3   Coordinate Frames

There are 3 coordinate frames used to construct the graphics on the head up display system; the global coordinate frame, the local vehicle-attached coordinate frame, and the graphic screen coordinate frame. The global coordinate frame is the coordinate frame used for the road map data (see Figure 23).
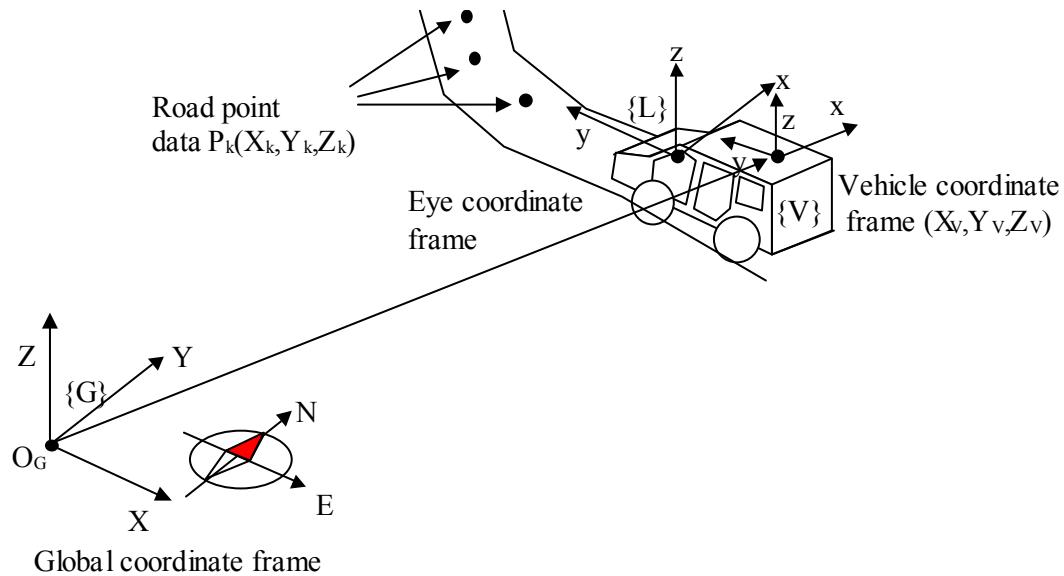
Figure 23. Coordinate frames (global, vehicle, and local coordinate frames).

Global Coordinate Frame

The Minnesota South State Coordinate system explained in the previous chapter was used as the global coordinate frame, {G}. The road point data in the digital road map data and the location of the vehicle (actual location of the origin of the vehicle coordinate frame) are expressed in terms of the global coordinate frame. The capital letters X, Y, and Z were used as names of each axis. The positive Y-axis is the direction to the true North and the East direction is defined as the positive X-axis. The compass was drawn in Figure 23 to show the Y-axis and the true north. The elevation was defined as the Z-axis to the express elevation of the road shape and objects adjacent to or on the road. All of the road points stored in the road map data file are expressed in terms of the global coordinate frame. DGPS system gives latitudinal and longitudinal angle data, then these are converted into the Minnesota State coordinate data and fed into the mathematical calculation routines in the graphic processor.

The location and heading angle of the vehicle coordinate frame (following section) are expressed in terms of the global coordinate frame.

Vehicle-Attached Coordinate Frame

The vehicle-attached intermediate coordinate frame, {V}, was defined and used to express the vehicle configuration data (including the location and orientation of the driver's eye within the cab) relative to the origin of vehicle. The vehicle coordinate frame is attached to the vehicle and moves as the vehicle moves. The origin was defined as the point on the ground under the location of GPS receiver antenna. Please note that the

origin of the vehicle coordinate is drawn at the position of the GPS antenna in Figure 23

for the sake of clarify. Originally the vehicle coordinate frame was considered as attached

to the GPS antenna. However, due to difficulties in measuring the driver's eye location

with respect to the vehicle coordinate frame, it was changed so that the vehicle coordinate

frame is attached on the ground where the elevation, Z-axis, is zero. Everything in the

vehicle was measured from the ground point under the GPS antenna.

The forward moving direction was defined as the positive y-axis. The direction to the

right when the vehicle is moving forward was defined as the positive x-axis. The vertical

upward direction was defined as the positive z axis which is parallel to the global

coordinate frame axis Z. The reason to choose x and y axis in this manner was to make it

easy to convert the local coordinate frame into the graphic screen coordinate frame. In the

graphic coordinate frame, the positive directions are to the right and in the upward

direction as explained in the following section. Conceptually this is also convenient for

the mathematical calculations.

Only the yaw angle, i.e. heading angle, of the vehicle from among the three possible

directional angles; yaw, pitch, and roll angle, was used to draw the graphics screen

display. The yaw angle is the vehicle's heading angle as measured from the true North.

The counterclockwise direction represents the positive yaw angle because the positive z-

axis is pointing upward. The pitch angle results from the changing elevation of the road

along its moving direction, i.e. longitudinal direction. The roll angle comes from the

lateral road profile. The pitch and roll angles were assumed to be zero, i.e. the road is flat

both latitudinal and longitudinal directions. This was a reasonable assumption for driving

on straight sections of the Mn/ROAD where the road profile is relatively flat.

Local Eye Coordinate Frame

The local coordinate frame, {L}, was defined and used to express the road data relative to

the viewer's location and direction. This coordinate system will be called the local

coordinate frame through out this paper. Even though the driver's eye location and

orientation are constant due to the nature of the combiner, all of the global information

needs to be converted into the eye coordinate frame for calculating the perspective

projection. The location of the driver's eye, i.e. the viewing point, is the origin of the local

coordinate frame. The local frame is defined with respect to the vehicle coordinate frame.

The relative location of the driver's eye from the origin of the vehicle coordinate frame

was measured and used in the coordinate transformation matrix [T]. The directional angle

information for the driver's line of sight is very important for constructing the projection

screen. This angle information also needs to be integrated into the coordinate

transformation matrix.
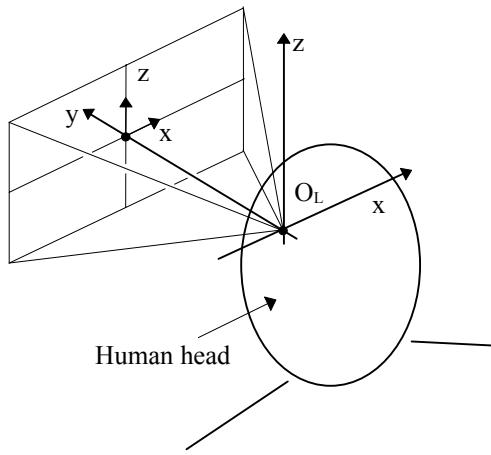
Figure 24. Local eye-coordinate frame.

The current version of the HUD software performs the coordinate transformation using a constant angle value, but the software is programmed to allow for a variable angle data for future use. This feature would be essential if one were to use a head-mounted type of display rather than a HUD.

Projection Screen Coordinate Frame

Ultimately all objects in the outer world should be drawn on a flat two-dimensional video projection screen. The projection screen in this paper is the virtual screen which is perceived by human drivers. The screen coordinate frame has only two axes. It is natural to define the upward and right directions as the positive directions in the vertical 2-dimensional plane. The positive x-axis of the screen was defined to be the same as the positive x-axis of the vehicle coordinate frame for easy coordinate conversion. There are two choices of selecting the remaining two axes with respect to the positive x-axis direction. One possible coordinate frame is to choose the upward direction as the positive y-axis and the forward looking direction as the negative z-axis. The other one is to select

the upward direction as the positive z-axis and forward looking direction as the positive y-axis. The screen coordinate frame was selected to be the latter case. In this coordinate frame, the upward direction is the positive z-axis and the forward-looking direction (or distance to the objects located in the visual sight) is the positive y-axis. The definition of the positive z-axis as the forward-looking direction makes the perspective calculation easier to conceptualize because everything in the visual field of view is expressed in terms of positive values.

Computer Graphics Memory Coordinate Frame

Everything needs to be drawn in the graphic memory of the computer hardware. The computer graphic memory is considered as a two-dimensional arrays of pixel points. In the computer video screen, the left-top corner is the beginning of the video memory. The x-axis increases as a pixel point moves to the right, and the y-axis increases as a pixel point moves to the bottom of the screen. Basically, the positive x-axis (right direction) and z-axis (upward direction) in the projection screen are mapped to the positive x-axis and the negative y-axis in the computer memory space and its origin is shifted to the left-top corner. The pixel locations in the computer screen can only be integer values.

4.4 Road Edge Calculation

The road edges, both the right and the left side boundaries, were not stored in a file but calculated from the center line data which are stored in the digital map. The width of the road is also stored in the digital map file. If the road width is not defined in the road map file, then twelve feet, the standard lane width of a Minnesota State highway, is used. If points along the centerline and the lane width are known, then the road edges can be calculated readily by doing simple 2-dimensional geometric calculations.
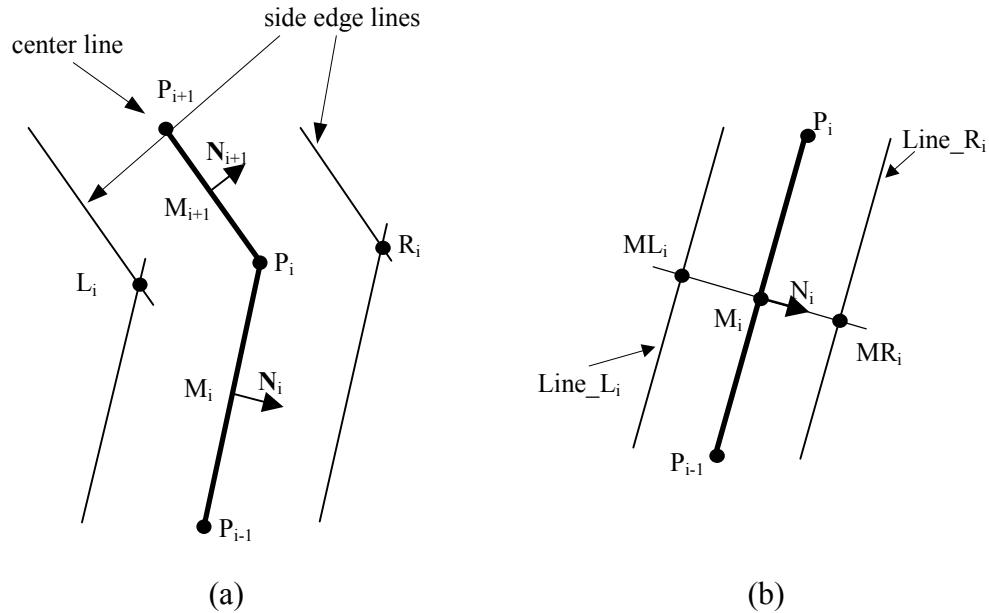
Figure 25. Finding road edge lines. (a) Relationship between 3 consecutive points (b) Finding center M$_i$.

The centerline contains a series of road points, P_i, P_{i+1} where each point P_i contains 2-dimensional (X, Y) location data. The goal of the following calculations is to find R_i and L_i, where R_i is the right road boundary and L_i is the left road boundary. M_i and M_{i+1} represent the center of the line segment $\overline{P_{i-1}P_i}$ and $\overline{P_iP_{i+1}}$ respectively. N_i and N_{i+1} are

71

vectors normal to the line segments $\overline{P_{i-1}P_i}$ and $\overline{P_iP_{i+1}}$ respectively and originate from

each line segment at M_i and M_{i+1}. If the line vector $\overline{P_{i-1}P_i}$ is as follows:

$$\overline{P_{i-1}P_i} = (a,b) \qquad\qquad (1)$$

then,

$$N_i = (b,-a) \qquad\qquad (2)$$

R_i and L_i can be found from following equations. Since M_i is the middle of line segment

$\overline{P_{i-1}P_i}$, where P_i and P_{i+1} are end points for each line segment, then

$$M_i = \frac{1}{2}\left(P_i + P_{i-1}\right) \qquad\qquad (3)$$

Additional variables were defined in order to simplify the calculations. MR_i and ML_i are

the center of the right and left side edge segments. W is the lateral width of each lane.

$Line\_R_i$ and $Line\_L_i$ are the line segments for each side.

$$MR_i = M_i + \frac{W}{|N_i|} N_i \tag{4}$$

$$ML_i = M_i - \frac{W}{|N_i|} N_i \tag{5}$$

Therefore,

$$Line\_R_i = MR_i + s\left(P_i - P_{i-1}\right) = MR_i + s\Delta P_i \tag{6}$$

$$Line\_L_i = ML_i + t\left(P_i - P_{i-1}\right) = ML_i + t\Delta P_i \tag{7}$$

where,

$$\Delta P_i = P_i - P_{i-1} \text{ and}$$

s and t are arbitrary real numbers.

$Line\_R_{i+1}$ and $Line\_L_{i+1}$ can be calculated in a similar manner. They are

$$Line\_R_{i+1} = MR_{i+1} + u\left(P_{i+1} - P_i\right) = MR_{i+1} + u\Delta P_{i+1} \tag{8}$$

$$Line\_L_{i+1} = ML_{i+1} + v\left(P_{i+1} - P_i\right) = ML_{i+1} + v\Delta P_{i+1} \tag{9}$$

where,

$$\Delta P_{i+1} = P_{i+1} - P_i \text{ and}$$

u and v are arbitrary real numbers.

Now, the intersection points of the right and left edge lines can be defined using the line equations (6), (7), (8), and (9). The calculation goal is finding the intersecting point R_i, L_i, R_{i+1}, and L_{i+1} expressed in terms of P_i and P_{i+1}. The equations for the two lines should be equal at the intersection point. Therefore,

$$Line\_R_{i+1} = Line\_R_i \tag{10}$$

$$Line\_L_{i+1} = Line\_L_i \tag{11}$$

and their intersection points are L_i and R_i so,

$$Line\_R_{i+1} = Line\_R_i \equiv R_i \tag{12}$$

$$Line\_L_{i+1} = Line\_L_i \equiv L_i \tag{13}$$

By letting $Line\_R_{i+1}$ equals $Line\_R_i$,

$$MR_i + s\Delta P_i = MR_{i+1} + u\Delta P_{i+1} \tag{14}$$

$$ML_i + t\Delta P_i = ML_{i+1} + v\Delta P_{i+1} \tag{15}$$

Unknown variable s, t, u, and v can be found using the above two equations.

$$s\Delta P_i - u\Delta P_{i+1} = MR_{i+1} - MR_i \equiv \Delta MR_i \qquad (16)$$

If the x and y components of the above equation are separated, each component will be as follows:

$$x \text{ component: } s\Delta P_{i,x} - u\Delta P_{i+1,x} = \Delta MR_{i,x} \qquad (17)$$

$$y \text{ component: } s\Delta P_{i,y} - u\Delta P_{i+1,y} = \Delta MR_{i,y} \qquad (18)$$

These two equations can be expressed by the following matrix equation,

$$\begin{bmatrix} \Delta P_{i,x} & -\Delta P_{i+1,x} \\ \Delta P_{i,y} & -\Delta P_{i+1,y} \end{bmatrix} \begin{bmatrix} s \\ u \end{bmatrix} = \begin{bmatrix} \Delta MR_{i,x} \\ \Delta MR_{i,y} \end{bmatrix} \qquad (19)$$

If the determinant D of the matrix $[M]$ is not zero,

$$[M] = \begin{bmatrix} \Delta P_{i,x} & -\Delta P_{i+1,x} \\ \Delta P_{i,y} & -\Delta P_{i+1,y} \end{bmatrix} \qquad (20)$$

$$D = \det[M] = -\Delta P_{i,x}\Delta P_{i+1,y} + \Delta P_{i,y}\Delta P_{i+1,x}$$

then,

$$\begin{bmatrix} s \\ u \end{bmatrix} = \frac{1}{D} \begin{bmatrix} -\Delta P_{i+1,y} & +\Delta P_{i+1,x} \\ -\Delta P_{i,y} & \Delta P_{i,x} \end{bmatrix} \begin{bmatrix} \Delta MR_{i,x} \\ \Delta MR_{i,y} \end{bmatrix} \tag{21}$$

Therefore, R_i can be determined as follow

$$s = \frac{1}{D} \left(-\Delta P_{i+1,y} \Delta MR_{i,x} + \Delta P_{i+1,x} \Delta MR_{i,y} \right) \tag{22}$$

$$R_i = MR_i + s\Delta P_i$$

and the left intersection point L_i can be calculated in a few steps,

$$t = \frac{1}{D} \left(-\Delta P_{i+1,y} \Delta ML_{i,x} + \Delta P_{i+1,x} \Delta ML_{i,y} \right) \tag{23}$$

$$L_i = ML_i + t\Delta P_i$$

If D is zero, then it means that the two line segments $\overline{P_{i-1}P_i}$ and $\overline{P_iP_{i+1}}$ are parallel to each other as shown in Figure 26. In this case,

$$R_i = P_i + \frac{W}{|N_i|} N_i \tag{24}$$

$$L_i = P_i - \frac{W}{|N_i|} N_i \tag{25}$$
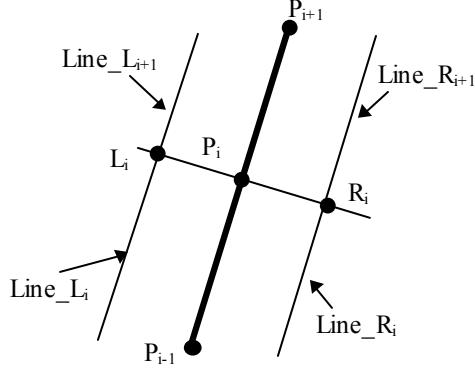
Figure 26. The case when 2 lines are parallel to each other, i.e. the determinent of [*M*] is zero.

The right and left sides of the road edges were calculated only once, right after the road data was loaded into memory, in order to increase the drawing speed.

4.5   Coordinate Transformation

Road data points including the left and right edges, which are expressed with respect to the global coordinate frame {G} as P_k, shown in Figure 27, are converted into the local coordinate frame {L} which is attached to the moving vehicle coordinate frame {V}. Its origin (O_V) and direction (θ_V) are changing continually as the vehicle moves. The origin (O_L) of the local coordinate frame {L}, i.e. driver's eye location, and its orientation (θ_E) change as driver moves his head and eyeballs. Even though driver's orientation (θ_E) is assumed as constant in the current version of the HUD system, all of the potential effects were considered in the coordinate transformation equations for future extension of the HUD software. All road data that are given in terms of the global coordinate frame {G}

need to be converted into the eye coordinate frame {L} ultimately. Then they are

projected into the video screen using a perspective transformation.

A homogeneous transformation matrix [T] was defined and used to convert the global

coordinate data into local coordinate data throughout the HUD software. We will now
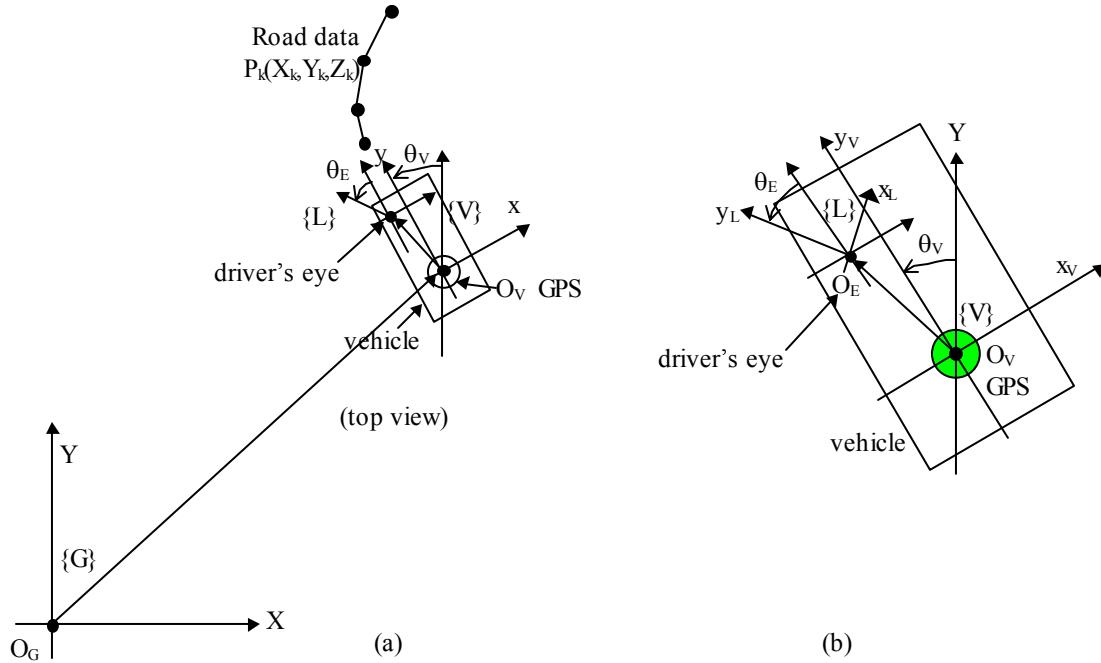
develop the matrix [T].

**Figure 27. Coordinate frames used to determine the transformation matrix [T].
(a) Overall view, (b) Blowup of vehicle.**

The parameters in Figure 27 are as follows,

- P_k is the k-th road point

- O_G is the origin of the global coordinate frame,

- O_V is the origin of the vehicle coordinate frame with respect to the global coordinate frame.

- O_E is the origin of the local eye-attached coordinate frame.

Any point in 3-dimensional space can be expressed in terms of either a global coordinate frame or a local coordinate frame. Because everything seen by the driver is defined with respect to his or her location and viewing direction, i.e. relative geometrical configuration between the viewer and the environment, all of the viewable environment should be expressed in terms of a local coordinate frame. Then, any objects or line segments can be projected onto a flat surface or video screen by means of the perspective projection. The mathematical calculation of the coordinate transformation is performed by constructing a homogenous transformation matrix and applying the matrix to the position vectors [29].

The coordinate transformation matrix [T] was defined as a result of the multiplication of a number of matrices described in the following paragraphs.

To change the global coordinate data to the local coordinate data, the translation and rotation of the frame should be considered together.
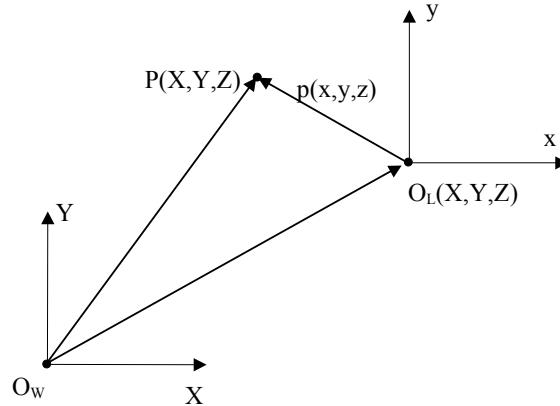
Figure 28. Translation of the coordinate frame.

The translation of the coordinate frame transforms point data using the following matrix

equation

$$
\begin{aligned}
x &= X - O_L.X \\
y &= Y - O_L.Y \\
z &= Z - O_L.Z
\end{aligned}
\tag{26}
$$

or

$$
\begin{bmatrix} x \\ y \\ z \\ 1 \end{bmatrix} =
\begin{bmatrix}
1 & 0 & 0 & -O_L.X \\
0 & 1 & 0 & -O_L.Y \\
0 & 0 & 1 & -O_L.Z \\
0 & 0 & 0 & 1
\end{bmatrix}
\begin{bmatrix} X \\ Y \\ Z \\ 1 \end{bmatrix}
\qquad \text{or} \qquad
{}^L p = {}^L_G\left[T_{trans}\right]{}^G P
\tag{27}
$$

where,

$$
{}^L p = \begin{bmatrix} x \\ y \\ z \\ 1 \end{bmatrix}, \quad
{}^G P = \begin{bmatrix} X \\ Y \\ Z \\ 1 \end{bmatrix}, \text{ and }
{}^L_G\left[T_{tran}\right] =
\begin{bmatrix}
1 & 0 & 0 & -O_L.X \\
0 & 1 & 0 & -O_L.Y \\
0 & 0 & 1 & -O_L.Z \\
0 & 0 & 0 & 1
\end{bmatrix}
\tag{28}
$$

80

The rotation of the coordinate frame about the Z-axis can be expressed by the following matrix equation;
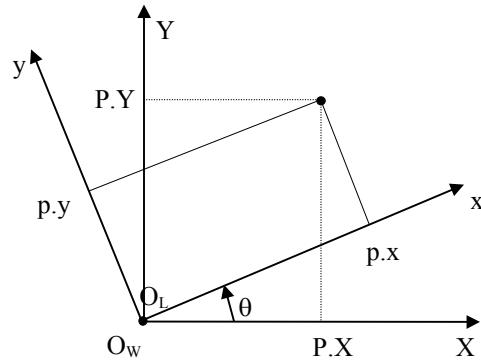
Figure 29. Rotation of the coordinate frame (P: world coordinates, p: local coordinates).

$$
\begin{aligned}
x &= X\cos\theta + Y\sin\theta \\
y &= -X\sin\theta + Y\cos\theta \\
z &= Z
\end{aligned}
\tag{29}
$$

or

$$
\begin{bmatrix} x \\ y \\ z \\ 1 \end{bmatrix} = \begin{bmatrix} \cos\theta & \sin\theta & 0 & 0 \\ -\sin\theta & \cos\theta & 0 & 0 \\ 0 & 0 & 1 & 0 \\ 0 & 0 & 0 & 1 \end{bmatrix} \begin{bmatrix} X \\ Y \\ Z \\ 1 \end{bmatrix}
\tag{30}
$$

This equation can be written using the following matrix equation,

$$
{}^{L}p = {}^{L}_{G}\left[T_{rot}\right]{}^{G}P
\tag{31}
$$

where,

$$\begin{bmatrix} L \\ G \end{bmatrix} [T_{rot}] = \begin{bmatrix} \cos\theta & \sin\theta & 0 & 0 \\ -\sin\theta & \cos\theta & 0 & 0 \\ 0 & 0 & 1 & 0 \\ 0 & 0 & 0 & 1 \end{bmatrix} \tag{32}$$

If we think about rotation and translation at the same time, then these two matrices can be combined by the following equations,

$$^{L}p = {}_{G}^{L}[T]\,{}^{G}P \tag{33}$$

where,

$${}_{G}^{L}[T] = {}_{G}^{L}[T_{rot}]\,{}_{G}^{L}[T_{tran}]$$

$$= \begin{bmatrix} \cos\theta & \sin\theta & 0 & 0 \\ -\sin\theta & \cos\theta & 0 & 0 \\ 0 & 0 & 1 & 0 \\ 0 & 0 & 0 & 1 \end{bmatrix} \begin{bmatrix} 1 & 0 & 0 & -O_{L,X} \\ 0 & 1 & 0 & -O_{L,Y} \\ 0 & 0 & 1 & -O_{L,Z} \\ 0 & 0 & 0 & 1 \end{bmatrix} \tag{34}$$

$$= \begin{bmatrix} \cos\theta & \sin\theta & 0 & -O_{L,X}\cos\theta - O_{L,Y}\sin\theta \\ -\sin\theta & \cos\theta & 0 & +O_{L,X}\sin\theta - O_{L,Y}\cos\theta \\ 0 & 0 & 1 & -O_{L,Z} \\ 0 & 0 & 0 & 1 \end{bmatrix}$$

This relationship can be expanded through the {G}, {V}, and {L} coordinate frames. The coordinate transform matrix [T] was defined as follows assuming that only heading angles θ_E and θ_V are considered as rotational angle data;

$$^{L}p = {}_{V}^{L}[T]\,{}_{G}^{V}[T]\,{}^{G}P = [T]\,{}^{G}P \tag{35}$$

where,

$$[T] = \begin{bmatrix} c_E & s_E & 0 & -O_{L,X}c_E - O_{L,Y}s_E \\ -s_E & c_E & 0 & +O_{L,X}s_E - O_{L,Y}c_E \\ 0 & 0 & 1 & -O_{L,Z} \\ 0 & 0 & 0 & 1 \end{bmatrix} \begin{bmatrix} c_V & s_V & 0 & -O_{V,X}c_V - O_{V,Y}s_V \\ -s_V & c_V & 0 & +O_{V,X}s_V - O_{V,Y}c_V \\ 0 & 0 & 1 & -O_{V,Z} \\ 0 & 0 & 0 & 1 \end{bmatrix} \quad (36)$$

and,

$$c_E = \cos\theta_E, \ s_E = \sin\theta_E, \ c_V = \cos\theta_V, \text{ and } s_V = \sin\theta_V \quad (37)$$

The resultant matrix [T] is then as follows:

$$[T] = \begin{bmatrix} T_{11} & T_{12} & T_{13} & T_{14} \\ T_{21} & T_{22} & T_{23} & T_{24} \\ T_{31} & T_{32} & T_{33} & T_{34} \\ T_{41} & T_{42} & T_{43} & T_{44} \end{bmatrix} \quad (38)$$

where,

$$T_{11} = c_E c_V - s_E s_V = \cos(\theta_E + \theta_V) \quad (39)$$

$$T_{12} = c_E s_V + s_E c_V = \sin(\theta_E + \theta_V) \quad (40)$$

$$T_{13} = 0 \quad (41)$$

$$T_{14} = c_E\left(-O_{V,X}c_V - O_{V,Y}s_V\right) + s_E\left(O_{V,X}s_V - O_{V,Y}c_V\right) + \left(-O_{L,X}c_E - O_{L,Y}s_E\right) \quad (42)$$

$$= -c_{E+V}\left(O_{V,X} + O_{L,X}c_V - O_{L,Y}s_V\right) - s_{E+V}\left(O_{V,Y} + O_{L,X}s_V + O_{L,Y}c_V\right)$$

$$T_{21} = -s_E c_V - c_E s_V = -\sin(\theta_E + \theta_V) \quad (43)$$

$$T_{22} = -s_E s_V + c_E c_V = \cos(\theta_E + \theta_V) \quad (44)$$

$$T_{23} = 0 \tag{44}$$

$$T_{24} = s_E\left(O_{V,X}c_V + O_{V,Y}s_V\right) + c_E\left(O_{V,X}s_V - O_{V,Y}c_V\right) + \left(O_{L,X}s_E - O_{L,Y}c_E\right) \tag{45}$$

$$= s_{E+V}\left(O_{V,X} + O_{L,X}c_V - O_{L,Y}s_V\right) - c_{E+V}\left(O_{V,Y} + O_{L,X}s_V + O_{L,Y}c_V\right)$$

$$T_{31} = 0 \tag{46}$$

$$T_{32} = 0 \tag{47}$$

$$T_{33} = 1 \tag{48}$$

$$T_{34} = -O_{L,Y} - O_{L,Z} \tag{49}$$

$$T_{41} = 0 \tag{50}$$

$$T_{42} = 0 \tag{51}$$

$$T_{43} = 0 \tag{52}$$

$$T_{44} = 1 \tag{53}$$

where,

$$c_{E+V} = \cos\left(\theta_E + \theta_V\right), \text{ and } s_{E+V} = \sin\left(\theta_E + \theta_V\right) \tag{54}$$

By multiplying the road points P by the $[T]$ matrix, we will have local coordinate data p. The resultant local coordinate value p is then fed into the perspective projection routine to calculate the projected points on the head up display screen. The calculations for the perspective projection will be discussed later in this chapter.

4.6   Perspective Projection

After the coordinate transformation, all the road data are expressed with respect to the driver's viewing location and orientation. These local coordinate data should be projected onto a flat screen, i.e., the virtual screen of head up display.

Projecting the scene onto the display screen was done using simple geometrical mathematics and computer graphics theory. Physically the display screen is the reflective mirror or the virtual focused image plane. The display screen is the plane, which is located at s_y position, parallel to the z-x plane.
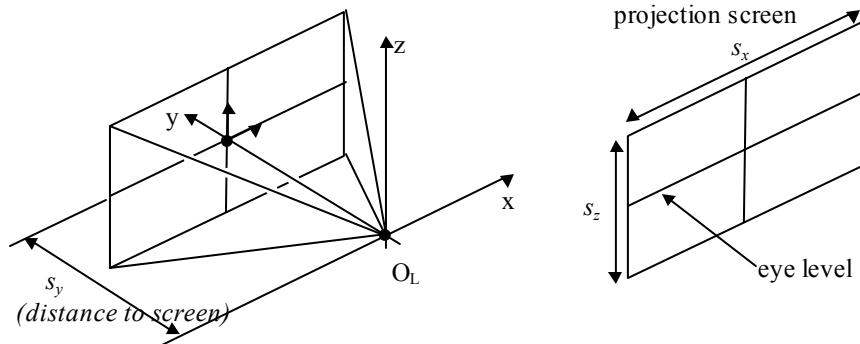
Figure 30. Projection screen in the perspective projection.

Where, s_x, s_z are the horizontal and vertical dimensions of the display screen. When the object is projected onto the screen, it should be projected with the correct perspective projection so that the projected images match with the outer scene. It is crucial that the head up display system match the drawn road shapes exactly when the actual road is in front of the driver.
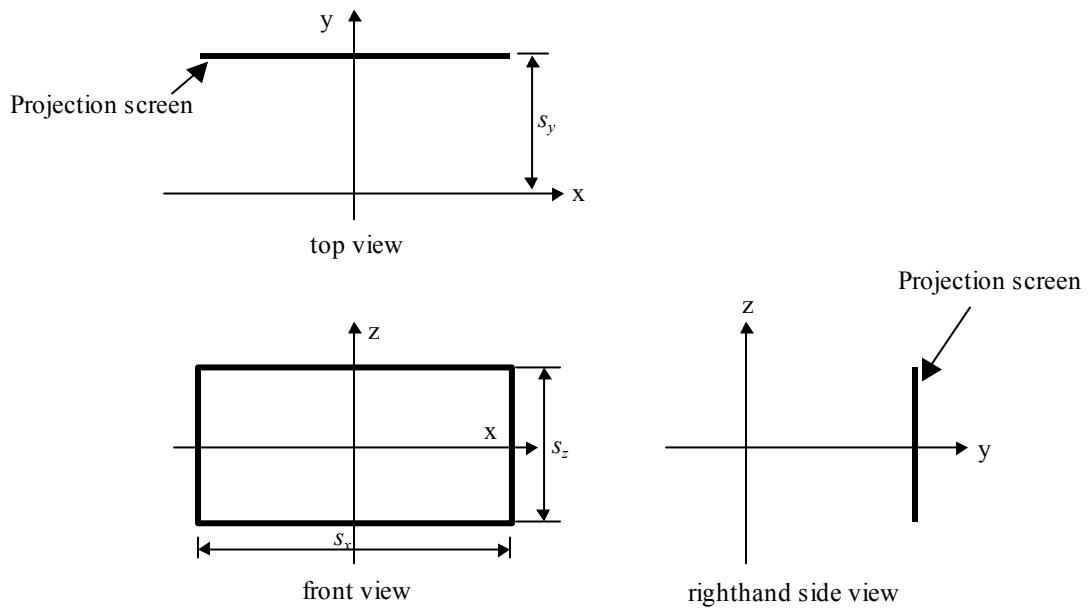
Figure 31. Geometric diagram of the projection screen.

The perspective projection makes closer objects appear larger and further objects appear smaller.
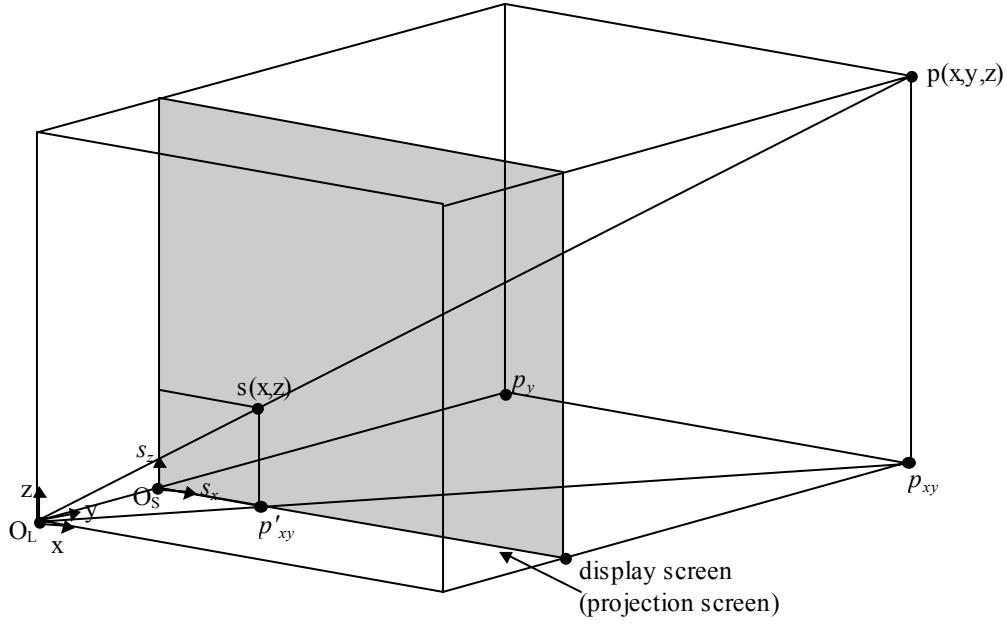
Figure 32. Geometry of perspective projection.

The prospective projection can be calculated from the triangle similarity. From the figure

we can find the location of the point s(x,z) for the known data p(x,y,z).
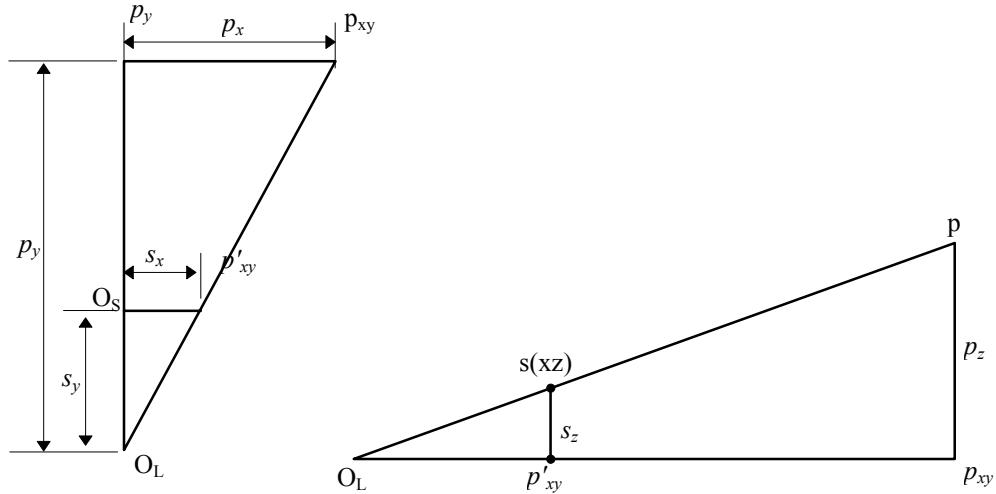
Figure 33. Similarity of triangle.

The values of the s_x and s_z can be found by similarity of triangles.

$$p_y : s_y = p_x : s_x \tag{55}$$

so,

$$s_x = p_x \frac{s_y}{p_y} \tag{56}$$

$$s_z = p_z \frac{s_y}{p_y} \tag{57}$$

As expected, s_x and s_z are small when the value p_y is big, i.e. when the object is located far away. This is the nature of perspective projection.

After calculating the projected road point on the display screen by the prospective projection, the points were connected using straight lines to build up the road shapes. The line-connected road shape provides a better visual cue of the road geometry than plotting just a series of dots.

## 4.7 Clipping: Finding The Visible Part of Road

The road points that have passed behind the driver's moving position don't need to be drawn. Furthermore, because the projection screen has limited size, only road points and objects that fall within the visible field of view need to be drawn on the projection screen. Finding and then not drawing these points outside the field of view are important in order to reduce the computation load of the HUD system and enhance the display refresh speed.
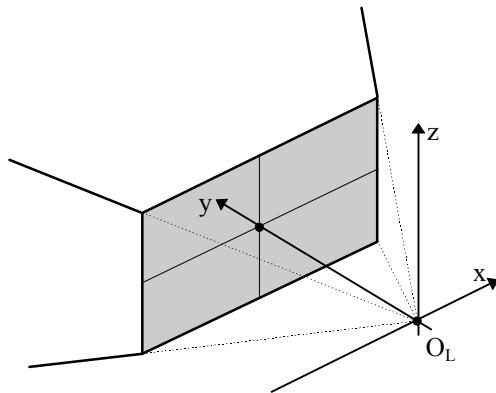
Figure 34. Visible region.

The visible limit is defined by the following Figures 30 and 31. The visible three

dimensional volume is defined as a rectangular cone cut at the display screen. Every

object in this visible region needs to be displayed on the projection screen. Objects in the

small rectangular cone defined by O_L and the display screen, a three dimensional volume

space between the viewer's eye and the displaying screen, will be displayed in an

enlarged size. If the object in this region is too close to the viewer then it results in an out

of limit error or a divide by zero error during the calculation. The purpose of the HUD is

to draw the road upcoming and adjacent objects. However, usually there are no objects

located in the "enlarging space." Figure 35 and the following equations of lines were

used for checking whether an object is in the visible space or not.
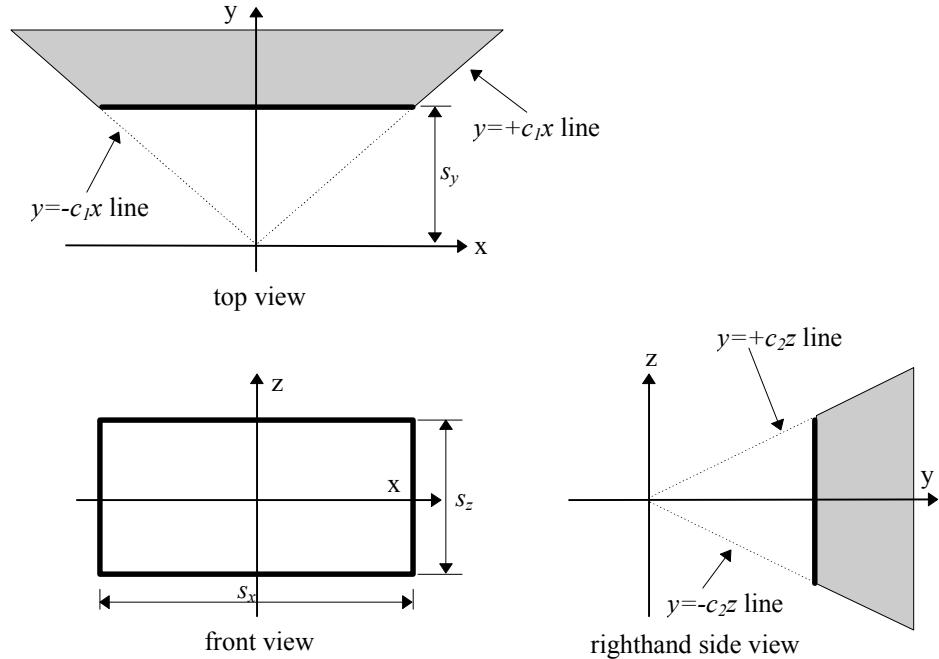
Figure 35. Visible region (detail 3D view).

If the position of a point in the local coordinate frame is defined as *p(x, y, z)* then this point is visible to the viewer only if

- the point p is in front of the $y = +c_1x$ plane. (marked as dark in the top view diagram of Figure 35)

- the point p is in front of the $y = -c_1x$ plane.

- the point p is in front of the $y = +c_2z$ plane. (dark region in the right hand side view diagram of Figure 35)

- the point p is in front of the $y = -c_2z$ plane.

- the point p is in front of the display screen.

Equations in the diagram of Figure 35, e.g. $y = +c_1 x$, are not line-equations but equations of planes in 3 dimensional space. The above conditions can be expressed by the following equations mathematically, which describe what we mean by "in front of"

$$p_y > +c_1 p_x \qquad (58)$$

$$p_y > -c_1 p_x \qquad (59)$$

$$p_y > +c_2 p_z \qquad (60)$$

$$p_y > -c_2 p_z \qquad (61)$$

and

$$p_y > s_y \qquad (62)$$

Only those points that satisfy all of the five conditions are in the visible region and are then drawn on the projection screen.

In some cases, there could be a line segment of the road whose one end is in the visible region and the other is out of the visible region. In this case, the visible portion of the line segment should be calculated and drawn on the screen. Figure 36 shows one of many possible situations. The upper drawing of the Figure 36 is a top view, which is a projection of the xy plane. We will describe how to locate point p so that only the contained segment is drawn.
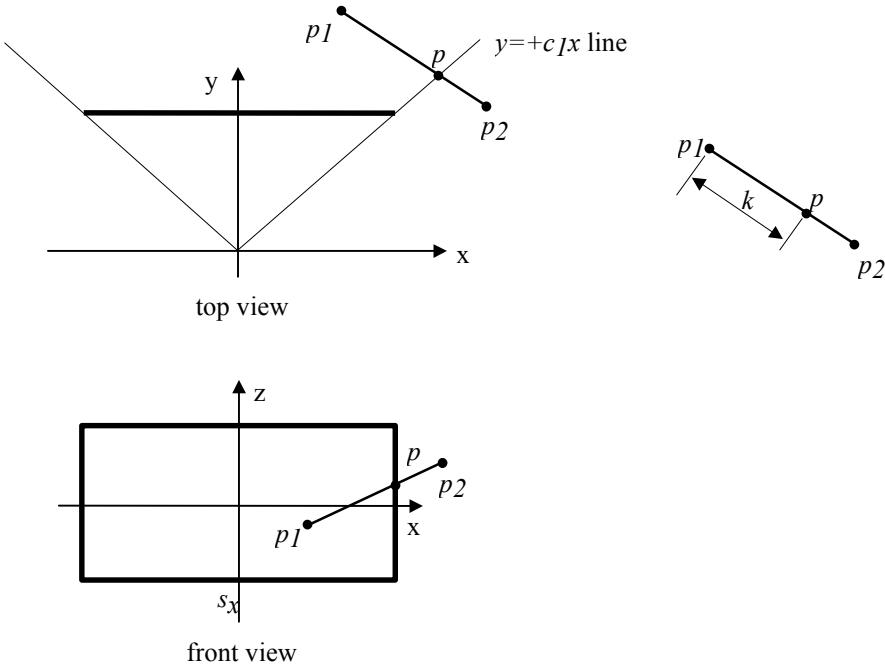
Figure 36. Out of sight.

The range of the ratio value k marked as the distance between point p and p_1 is from 0.0 to 1.0. The position of point p can be written as,

$$p = p_1 + k\left(p_2 - p_1\right) = p_1 + k\Delta p \qquad (63)$$

where,

    k is an arbitrary real number, $0 \le k \le 1$ and

    $\Delta p = p_2 - p_1$

The x and y components of the above equation can be written as follows:

$$p_x = p_{1,x} + k\Delta p_x \tag{64}$$

$$p_y = p_{1,y} + k\Delta p_y \tag{65}$$

The x and y components of point p also should satisfy the line equation $y = +c_1 x$ in order to intersect with the line. Therefore,

$$p_y = p_{1,y} + k\Delta p_y = c_1\left(p_{1,x} + k\Delta p_x\right) = c_1 p_{1,x} + kc_1 \Delta p_x \tag{66}$$

$$k\left(\Delta p_y - c_1 \Delta p_x\right) = c_1 p_{1,x} - p_{1,y} \tag{67}$$

then,

$$k = \frac{c_1 p_{1,x} - p_{1,y}}{\Delta p_y - c_1 \Delta p_x} \tag{68}$$

Applying the value k to the above equation, p_x, p_y and p_z can be determined as follows,

$$p_x = p_{1,x} + \Delta p_x \frac{c_1 p_{1,x} - p_{1,y}}{\Delta p_y - c_1 \Delta p_x} \tag{69}$$

$$p_y = p_{1,y} + \Delta p_y \frac{c_1 p_{1,x} - p_{1,y}}{\Delta p_y - c_1 \Delta p_x} \tag{70}$$

$$p_z = p_{1,z} + \Delta p_z \frac{c_1 p_{1,x} - p_{1,y}}{\Delta p_y - c_1 \Delta p_x} \tag{71}$$

Using these p_x, p_y, and p_z, the projected values s_x and s_z can be calculated by a perspective projection in the same manner as the other parameters.

4.8   Lateral Position Indicator

A horizontal bar and cursor were also included in the HUD system. This graphical indicator was designed to give the driver a measure of the lateral distance from the centerline of the driving lane. The lateral distances are calculated from the GPS data and measured from the centerline. The lateral position data sensed by 3M's magnetic tape system was also displayed in the HUD system.

The distance is calculated by finding the closest distance between the location of the vehicle (its vehicle coordinate origin, a ground spot under the GPS antenna) and the centerline of the digital map. The location of the vehicle is measured from the GPS data, i.e. it is the origin of the vehicle-attached moving coordinate. Road data are stored as a series of location data in the digital map. Line segments were defined as a series of line segments connecting adjacent road points. The lateral distance indicator is displayed at the bottom of the client area overlaid on the perspective projection. If needed, the lateral position indicator can be turned on and off.

Calculation of the lateral distance is composed of two parts; finding the lateral distance offset, and determining on which side the vehicle is located with respect to the

centerline. The distance was calculated using geometrical mathematics and vector

calculation, but the resultant value is a scalar value. It doesn't indicate the configuration

of the road segments and vehicle location. The road segment given by the digital map

represents the centerline. If the distance is 0 (zero), then it means that the vehicle is

moving along the centerline. The driver needs to know on which side of the lane he/she is

driving as well as how far the vehicle is located from the center line.

Calculating Lateral Distance

A distance between a line segment and a point can be calculated from a series of

mathematical calculations. The HUD software keeps track of the closest road points from

the most recent vehicle locations from among all the points of road data. Whenever the

HUD system tries to calculate the lateral distance of the vehicle, it extracts the number of

the line segments before and after the recent closest road point. A line segment is

expressed by two endpoints mathematically. Figure 37 shows the configuration of a line

segment $\overline{P_1P_2}$ and a point Q.
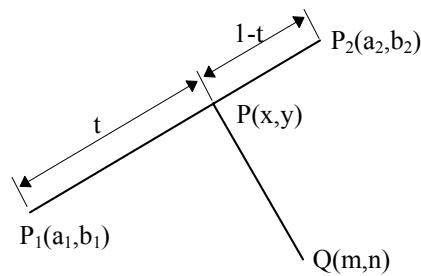
Figure 37. Geometrical configuration of a line segment and a point.

The point P is the closest point to the point Q from the line $\overline{P_1 P_2}$. It is mathematically

known that the line segment $\overline{PQ}$ and $\overline{P_1 P_2}$ are perpendicular to each other when the

distance is closest. Because the lateral distance is a horizontal distance, 2-dimensional

vectors were considered for the mathematical calculations. The vector representation of

the equation of the point on the line segment $\overline{P_1 P_2}$ is as follows,

$$P = (1-t)P_1 + tP_2 \tag{72}$$

or,

$$x = (1-t)a_1 + ta_2 \text{ and} \tag{73}$$

$$y = (1-t)b_1 + tb_2$$

where,

$$0 \le t \le 1$$

When t=0, the point P becomes P_1, and when t=1 the point P becomes P_2. All of the

possible points P are located between P_1 and P_2. Because the equation is linear, the

trajectory of the point P is linear and will form a straight-line segment. The distance

between P and Q is defined by the following equation.

$$d = |P - Q| \tag{74}$$

$$= \sqrt{(x-m)^2 + (y-n)^2}$$

The closest location can be found by finding a solution for the following differential

equation.

$$M(t) = (x-m)^2 + (y-n)^2 \tag{75}$$

$$\frac{M(t)}{dt} = 0 \tag{76}$$

The derivative of $M(t)$ will be as follows,

$$\frac{M(t)}{dt} = \frac{d}{dt}\left[(x-m)^2 + (y-n)^2\right] \tag{77}$$

$$= 2(x-m)\frac{dx}{dt} + 2(y-m)\frac{dy}{dt}$$

$$= 2(x-m)(a_2 - a_1) + 2(y-m)(b_2 - b_1)$$

$$= 2\big(((1-t)a_1 + ta_2) - m\big)(a_2 - a_1) + 2\big(((1-t)b_1 + tb_2) - m\big)(b_2 - b_1)$$

By, letting $\frac{M(t)}{dt} = 0$, the solution t can be found as follows,

$$t = \frac{(a_2 - a_1)(m - a_1) + (b_2 - b_1)(n - b_1)}{(a_2 - a_1)^2 + (b_2 - b_1)^2} \tag{78}$$

Now, we can determine the location of the point P using the value t calculated as above. The resultant t should be in the range of [0, 1] if the point P is in the line segment $\overline{P_1 P_2}$. The HUD software checks value t first before the HUD software calculates actual distances between the line segment and the vehicle location. If the value t is out of the range [0,1] then, further calculation is not performed anymore, and the closest point is selected as one of the end points and the closest distance is chosen as a distance from the endpoint to the vehicle location. Since there was no expression for the sign of the

97

distance, it will always be a positive scalar value. Because the road data of the digital map represents the centerline, if the resultant distance value is 0, then it means that the vehicle is located on the centerline. Usually a vehicle moves along the center of the lane, so the origin of the moving coordinate frame where the GPS antenna is located moves along the center of the driving lane. Therefore the distance value should be half of the usual lane width. The road width of typical roads in Minnesota is 12 feet (3.66m) wide. The lateral distance indicator shows a full 12 feet of travel and whether the location of the vehicle is in the range. If the lateral distance is more than 12 feet, i.e. in case that the vehicle departs outside the right lane boundary, the lateral distance indicator changes its color to red in order to provide an alert. Departing the lane from the left boundary, or in other words, crossing the centerline will be detected by performing further calculations described in the following section. As mentioned above, because the distance is just a scalar value and it is always positive, it is impossible to identify whether the vehicle is located on the right side or left side from the distance value alone. Identification of whether the vehicle is left or right was performed using the method described in the following section.

Determining On Which side The Vehicle Is Located

The location of the vehicle with respective to the line segment was found using the following vector calculation. The calculation should be performed with information given as to the moving direction of the vehicle. The definition for "which side of the road" depends on the moving direction. The same location can be thought of a left side or right

side of the line segment. Figure 38 shows a line segment of the road data and a location of the vehicle.
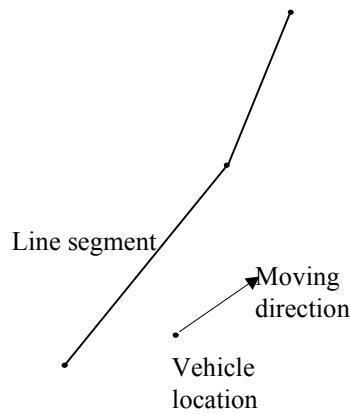
Figure 38. Determining location of the vehicle with respect to the line segment.

The situation displayed in Figure 38 is when the vehicle is moving along the right side of the centerline. The location of the vehicle with respect to the centerline was identified by the following calculations. Figure 39 shows the two vectors that are used for the calculation.
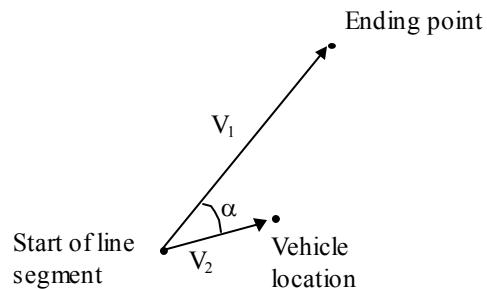

Figure 39. Vectors for finding the vehicle location with respect to the centerline.

The location of the vehicle with respect to the line segment was determined by finding the angle between the two vectors. The angle between the vectors can be found either using the dot product or the cross product. The dot product gives only the absolute value of the angle, i.e. the magnitude of the angle, but the cross product gives its size as well as magnitude. Actually, the most important information needed to determine vehicle location is not the value itself but its sign. The HUD software calculates the cross product to determine the vehicle location with respect to the line segment.

$$v_1 \times v_2 = \begin{vmatrix} i & j & k \\ v_{1,x} & v_{1,y} & 0 \\ v_{2,x} & v_{2,y} & 0 \end{vmatrix} \qquad\qquad (79)$$

$$= 0i + 0j + (v_{1,x}v_{2,y} - v_{1,y}v_{2,x})k$$

where the vector v_1 is a vector starting from the beginning of the line segment and ends at the next road point. The beginning point depends on the moving direction of the vehicle. The v_2 is a vector that starts from the beginning of the line segment and ends at the vehicle's current location. Because the two v_1 and v_2 vectors are on the x-y plane surface, the cross product should have +z direction or -z direction. If the sign is positive then the angle α is positive, i.e. the vehicle is located on the right side of the line segment, otherwise it is on the left side.

If the HUD software detects that the vehicle is moving along the left side of the center line, which is a very dangerous situation, then it changes the indicator color to red.

100

4.9   Map Data Query Area

Only the needed part of the entire map data is extracted and used for the screen drawing. Combined with the clipping of the invisible area, an efficient query can also reduce a significant amount of computation time by reducing the total amount of data needed. An efficient query area operation also reduces the communication time between the HUD and the geo-spatial database system, when the HUD needs to operate together with a separate database system.

Figure 40 shows the concept of the query area used for the HUD development. It is a top view of a vehicle at given a moment. All of the coordinate data in Figure 40 are global coordinate data which is based on the Minnesota South State coordinate frame. The X and Y coordinates describe the location of the vehicle and θ is the heading of the vehicle. The φ is the sight angle visible through the combiner. Actually, the φ should be a little bit larger than the real field of view through the combiner. n is the nearest visible limit which defines the closest point of the road data that we want to display on the HUD. f is the far visible limit, data beyond the f distance will not be drawn nor will it be extracted from the digital map.
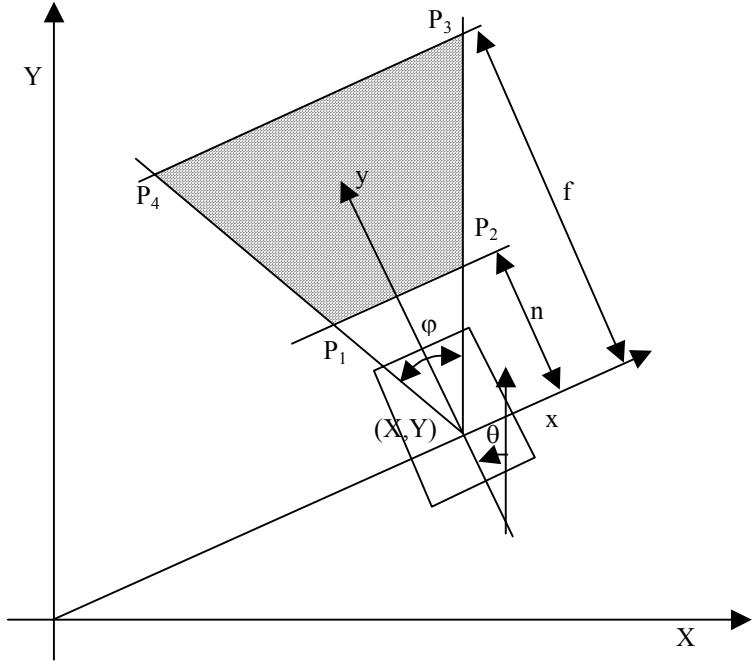
Figure 40. Query area to retrieve required map information from the entire map database.

The four points P_1, P_2, P_3, and P_4 define the resultant query area. Everything in the trapezoidal shape will be extracted and transmitted to the HUD from the geo-spatial managing system. The equations for the four points are as follows. The lower case letter p_1, p_2, p_3, p_4 are the same as P_1, P_2, P_3, and P_4 but expressed in terms of the local coordinate frame which is attached to the moving vehicle. Please note that this is not the same as the vehicle coordinate frame discussed in the previous sections. The local coordinate frame used in this section is a specifically defined one needed in order to calculate only the query area.

$$p_1 = \left(-\frac{n}{c}, n \right) \tag{80}$$

$$p_2 = \left(\frac{n}{c}, n\right) \tag{81}$$

$$p_3 = \left(\frac{f}{c}, f\right) \tag{82}$$

$$p_4 = \left(-\frac{f}{c}, f\right) \tag{83}$$

where, c is the slope of the left visible limit line which can be calculated as follow:

$$c = \tan\left(\frac{\pi}{2} - \frac{\varphi}{2}\right) = \frac{1}{\tan\left(\frac{\varphi}{2}\right)} \tag{84}$$

The global coordinate frame data of p_1, p_2, p_3, p_4 can be found by multiplying the coordinate frame transform matrix [T] that is defined as follows:

$$[T] = \begin{bmatrix} \cos\theta & -\sin\theta & X \\ \sin\theta & \cos\theta & Y \\ 0 & 0 & 1 \end{bmatrix} \tag{85}$$

The resultant point values of the four corners are as follows:

$$P_1 = \begin{pmatrix} -\dfrac{n}{c}\cos\theta - n\sin\theta + X \\ -\dfrac{n}{c}\sin\theta + n\cos\theta + Y \end{pmatrix} \tag{86}$$

$$P_2 = \begin{pmatrix} \dfrac{n}{c}\cos\theta - n\sin\theta + X \\ \dfrac{n}{c}\sin\theta + n\cos\theta + Y \end{pmatrix} \tag{87}$$

$$P_3 = \begin{pmatrix} \dfrac{f}{c}\cos\theta - f\sin\theta + X \\ \dfrac{f}{c}\sin\theta + f\cos\theta + Y \end{pmatrix} \tag{88}$$

$$P_4 = \begin{pmatrix} -\dfrac{f}{c}\cos\theta - f\sin\theta + X \\ -\dfrac{f}{c}\sin\theta + f\cos\theta + Y \end{pmatrix} \tag{89}$$

The following set of variables were used for the HUD experiments and prototype design discussed here.

    n = 10 m (30 ft)

    f = 300 m (1000 ft)

    c = 4.0427 (φ = 27.78 degrees)

Chapter 5 Driving Simulator

5.1 Driving Simulator

A simple driving simulator was also developed as a part of the HUD system. The simulator was used to demonstrate the concept of the head up display to the public and to perform laboratory tests and debugging during the early development period. The current version of the HUD system can be run in either the simulation mode or in an actual operational mode.

The simulator receives the user's steering and acceleration inputs through the joystick steering wheel and pedals, and feeds the input signals into a kinematics model of the simulated vehicle. The kinematics model is run as a separate thread (same concept as a process in Unix or a task in a real time operating system). The model generates the vehicle's position and orientation at each time step as a result of user inputs. The calculated new position and orientation of the simulated vehicle are fed into the HUD system. The same HUD system that is used for the real operation works with the input information from the simulated model, and finally the perspective projected road shapes appear on the graphic screen. Human subjects feel as if they are controlling the virtual vehicle by sensing its status through the visual feedback that appears on the computer screen.

5.2 Kinematics Model

A simple kinematics model for the vehicle was developed and used for the laboratory

simulator. There are many variations in the mathematical models of vehicles from the

simplest kinematics model to the most sophisticated dynamic model [30, 31].

The forward moving velocity was assumed as a 1st order system, i.e. the speed profile

increases as an exponential curve when a unit step input of acceleration is applied.

Consequently, the speed will increase rapidly during the beginning part of the

acceleration, then it converges to an asymptote value that is the final equilibrium speed

for the acceleration pedal input. In other words, the amount of speed increment at any

instantaneous moment is proportional to the difference between the current and the final

equilibrium speed for the acceleration pedal input. The equation for the speed of a 1st

order system can be written by the following equation.

$$v(t) = K_1\left(1 - e^{-K_2 t}\right) \qquad (89)$$

Where, K_1 and K_2 are constants depending on the system parameters. Velocities of the

system are,

$$v(0) = K_1\left(1 - e^0\right) = K_1(1 - 1) = 0 \qquad (90)$$

$$v(\infty) = K_1\left(1 - e^{-\infty}\right) = K_1 \qquad (91)$$

and acceleration values are,

$$a(0) = \left.\frac{dv(t)}{dt}\right|_{t=0} = \left.K_1K_2e^{-K_2t}\right|_{t=0} = K_1K_2 \qquad (92)$$

$$a(\infty) = \left.\frac{dv(t)}{dt}\right|_{t=\infty} = \left.K_1K_2e^{-K_2t}\right|_{t=\infty} = \frac{K_1K_2}{\infty} = 0 \qquad (93)$$

Figure 41 shows a typical velocity profile when K_1 is 1.0 and K_2 is 0.75
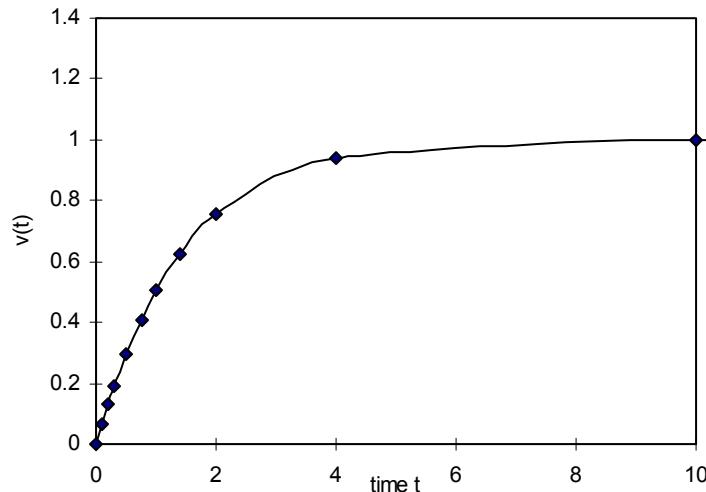
Figure 41. Velocity profile of the 1st order system

The constant K_1 is the final equilibrium velocity at a given acceleration input that is the

resultant input value from the driver's action of pushing the acceleration pedal. The

equilibrium velocity was assumed to be linearly dependent on the acceleration pedal

input. The constant K_2 determines the speed response for the input value. The bigger the

value of K_2 the faster the speed response for the acceleration pedal movement. The value

107

K_2 was chosen so that the human operator feels a speed response similar to that of driving a truck.

In order to reduce the calculation time of exponential terms, the following incremental form for the velocity equation was derived and used for the simulator. The exponential function takes considerable more computation time than simple multiplication and divisions.

$$v(t + \Delta t) = v(t) + v'(t)\Delta t \qquad (94)$$

Therefore, the amount of the speed increment is

$$\Delta v(t) = v(t + \Delta t) - v(t) \qquad (95)$$

$$= v'(t)\Delta t$$

$$= K_1 K_2 e^{-K_2 t} \Delta t$$

$$= K_2 \Delta t \left(K_1 e^{-K_2 t} - K_1 + K_1 \right)$$

$$= K_2 \Delta t \left(K_1 - v(t) \right)$$

$$= K_2 \Delta t \left(v_\infty - v(t) \right)$$

where, v_∞ is the final equilibrium speed for the current acceleration pedal input value. Under real operating conditions, the final speed is changed constantly as the operator pushes the acceleration pedal. When the HUD is working with the simulator, the

simulator was set to sample input values and updated its status every 30 ms, so that the HUD screen was updated at 30 times a second.

The longitudinal displacement was calculated by integrating the forward moving velocity and instantaneous heading angle of the vehicle. The lateral displacement at each time stamp was calculated using a bicycle model with the following assumptions. It was assumed that there is no time delay in the steering system. The kinematics model is valid if the following conditions are satisfied,

- Vehicle is moving on a flat surface,
- Steering angle is small,
- Vehicle is moving slowly,
- There is no slippage between the tires and the road surface.

In the usual driving situation, it is reasonable to assume that the actual angle of the steering wheels, not the rotation of the steering column, is small. It is also a reasonable assumption that there is no slip between the tires and the road surface in most driving situations. The exception will be when the vehicle is accelerating or decelerating on a slippery surface or is turning at sharp corners. During most typical highway driving situations even if the speeds are high, the change of the steering angle will be quite small, therefore the kinematics model can be used with little error. Addressing "how real is the simulator" was not the major goal of the simulator development. The simple simulator was good enough to debug the HUD operation, which was its main purpose.

Figure 42 shows a typical situation for a bicycle model vehicle that has only two wheels, the front and rear wheels. The uppercase letter X and Y are the axes of the global coordinate frame and the other variables are defined as follows:

θ: heading angle of the vehicle with respect to the global coordinate frame.

ϕ: steering angle

L: wheel base

v_f: (measured) velocity of the front wheel

v_r: rear wheel velocity

R_f: radius of rotation of the front wheel

R_r: radius of rotation of the rear wheel

w: rotational angular velocity

The bicycle vehicle model follows a circular path when the steering wheel is turned by an angle as shown in Figure 42. The real vehicle has four wheels but in the bicycle model each wheel is considered as attached at the center of each axle. Only the front wheel is able to be steered and affects the heading angle. Figure 42 shows when the steering angle and the vehicle speed are positive values. The steering angle was defined as positive when it is turned in the counterclockwise direction. The local coordinate frame, written as lowercase x and y, is attached to the center of the rear wheel to make it easier to develop kinematics equations for the vehicle motion. The forward moving direction (heading

direction) is the y axis and the right side direction of the vehicle is represented by the x

axis.
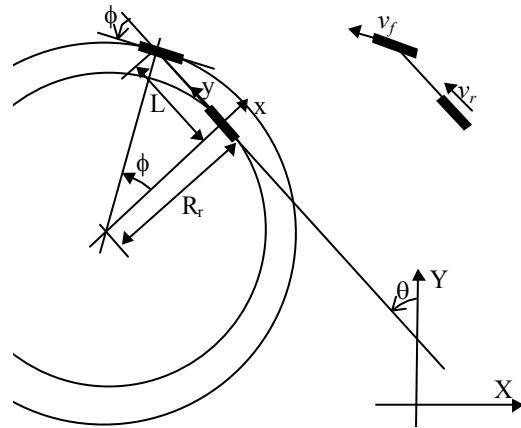
Figure 42. The bicycle kinematics model.

To make the calculation simple, we assumed that the vehicle speed is measured from the

front wheel, which is v_f. From the triangle that consists of the center of the rotational

movement, the center of the rear wheel and the front wheel,

$$\tan \phi = \frac{L}{R_r} \tag{96}$$

therefore,

$$R_r = \frac{L}{\tan \phi} \tag{97}$$

Because the rotational angular speed of the front wheel and rear wheels are as follows,

$$R_f w = v_f$$
$$R_f w = v_r \qquad \qquad (98)$$

the angular speed w is

$$w = \frac{v_f}{R_f} \qquad \qquad (99)$$

then,

$$v_r = R_r \frac{v_f}{R_f} = v_f \frac{R_r}{R_f} = v_f \cos\phi \qquad \qquad (100)$$

v_r is the forwarding moving velocity of the rear wheel. Because the heading angle of the vehicle is θ, the speed of vehicle at the instantaneous time and location can be expressed as follows,

$$v_x = -v_r \sin\theta = -v_f \cos\phi \sin\theta \qquad \qquad (101)$$

$$v_y = v_r \cos\theta = v_f \cos\phi \cos\theta \qquad \qquad (102)$$

The vehicle heading angle changes if the vehicle moves forward even when the steering wheel is fixed to a non-zero angle. So, the changing rate of heading angle is related to the steering angle. The changing rate of the heading angle is written as $\dot{\theta}$ and Figure 43 shows its relationship to the vehicle parameters.

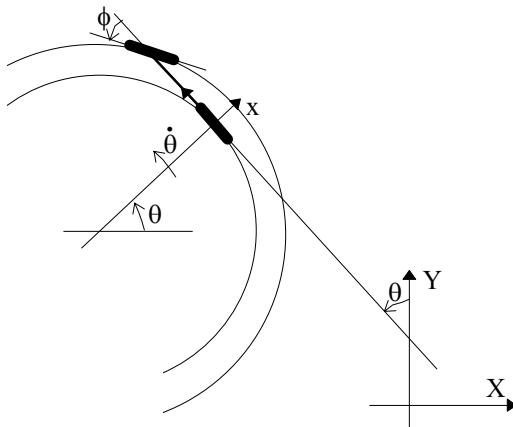**Figure 43. The changing rate of the heading angle with respect to the steering angle.**

Now,

$$R_r \dot{\theta} = v_r \tag{103}$$

$$\dot{\theta} = \frac{v_r}{R_r} = \frac{v_f \cos \phi}{R_r} \tag{104}$$

Because R_r can be expressed by the following equation,

$$R_r = \frac{L}{\tan \phi} \tag{105}$$

$\dot{\theta}$ can be expressed as follows

$$\dot{\theta} = \frac{v_f \cos \phi}{R_r} \tag{106}$$

113

$$= \frac{\frac{v_f \cos\phi}{L}}{\tan\phi}$$

$$= \frac{v_f \cos\phi\tan\phi}{L}$$

$$= \frac{v_f}{L}\sin\phi$$

If v_f is given or determined by some speed measuring device, then the speed and changing rate of heading angle can be calculated by the following equations,

$$v_x = -v_f \cos\phi\sin\theta \qquad\qquad (107)$$

$$v_y = v_f \cos\phi\cos\theta \qquad\qquad (108)$$

$$\dot\theta = \frac{v_f}{L}\sin\phi \qquad\qquad (109)$$

5.3 Joystick Interface

A game oriented joystick device, Formula T-2, was purchased and used as an input device for the simulator. The joystick device shown in Figure 44 was designed for car driving games by ThrustMaster Company [32]. This device has all of the major components needed to drive a simulated car: steering wheel, gear lever, acceleration pedal, and brake pedal. The steering wheel also has a return spring system in it so that the

steering wheel returns to the straight forward (or center) position when it is released. The input signals for the steering wheel, acceleration pedal, and brake pedal are analog signals which vary linearly by pushing or rotating the individual units. The output of the sensors are variable resistances and fed into the joystick I/O card of an IBM PC compatible computer then converted into voltage signals, then finally converted into linearly changing digital numbers. The output values of the joystick movement sensors are 16 bit integer values.

Figure 44. Formula T2 game device used for lab experiments.

Because the internal wiring of this game device is a little bit different than the standard circuitry of PC compatible joystick devices as shown in Figure 45, the standard device driver in Windows 95 or NT for game devices neither detects nor works with this game device. The system was designed to work only with their special interface card. The connection was modified as described in the circuit diagram of Figure 46 to make it work with the standard device driver of the Windows operating system.
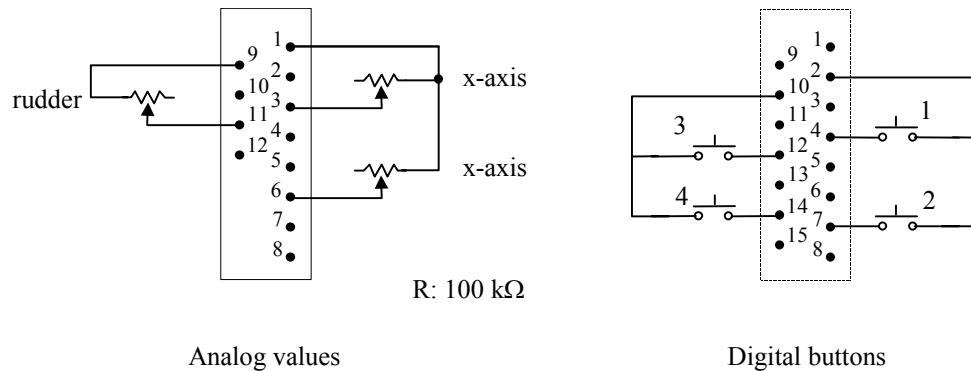
Figure 45. Standard circuit diagram for the game device for 2 axis type with 1 rudder input and 4 button inputs.

The joystick port of a standard PC can receive four separate analog inputs and for digital inputs. Analog inputs read resistance value between COM (common) terminal and its input terminal. The typical range of the potentiometer is zero to 100 kΩ. Zero resistance yields 0 (0x0000 in hexadecimal) value and over 100kΩ gives the full range value of two byte integers 65535 (0xFFFF in hexadecimal).

116

Figure 46. Modified connector for the game port.

The accelerating and decelerating pedal output were fed into the X-axis and Y-axis

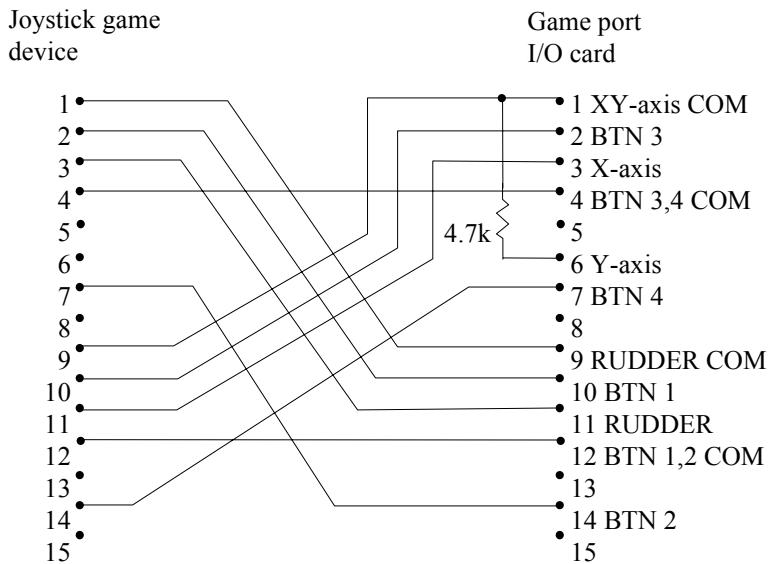movement of a standard joystick. The accelerator pedal's potentiometer was connected to

X-axis. The brake was connected to the Y-axis. The third axis, the steering input, was

connected to the rudder input.

Chapter 6   Experimental Setup

6.1   Yaw Angle Estimation

The yaw angle, or the heading angle, of the vehicle was estimated by linear successive difference of two GPS samples. Figure 47 shows the concept of the linear successive difference method. It was assumed that the linear estimation is valid on a straight path. If the sampling rate of GPS data is fast enough so that the movement of the vehicle between the GPS sample data can be safely assumed as linear motion, then the linear successive difference method will yield a reasonable estimated heading angle.
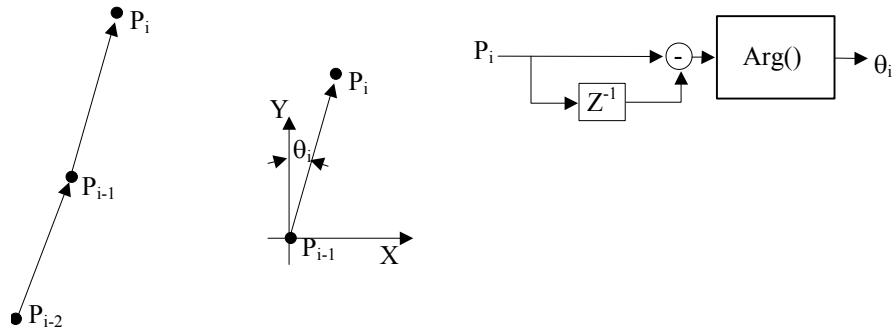
Figure 47. Yaw angle estimation for linear motion.

In Figure 47, the vehicle is moving from P_{i-1} to P_i. The X and Y axes represent the global coordinate frame. In linear successive estimation, the vehicle's heading angle is the angle of the vector starting from the point P_{i-1}, the previous GPS point, to the end point P_i, the current GPS point. θ_i is the yaw angle of the vehicle at current location P_i.

$$\theta_i = Arg\left(P_i - P_{i-1}\right) \tag{110}$$

$$= Arg(\Delta P_i)$$

where, ΔP_i is $P_i - P_{i-1}$. The yaw angle of the vehicle was defined as an angle from the true north which is the Y axis of the global coordinate frame. When the vehicle is moving toward the true north, its heading angle is zero and the heading angle increases as its angle rotates in the counterclockwise direction. The yaw angle should be calculated as follows,

$$\theta_i = \tan^{-1}\left(\frac{\Delta P_{i,X}}{-\Delta P_{i,Y}}\right) \tag{111}$$

$$= -\tan^{-1}\left(\frac{\Delta P_{i,X}}{\Delta P_{i,Y}}\right)$$

6.2   Characteristics of the DGPS

As mentioned in the previous section, a Novatel RT-20 DGPS was used for this research.

Naturally DGPS has a small amount of random error in both the longitudinal and latitudinal directions. Figure 48 shows a sample data collection at a point on the LVR of

the Mn/ROAD. A total of 1370 continuous samples were collected while the vehicle was stopped. The standard deviations of the sample data were 0.009322351m in x direction and 0.010722545 in y direction. The ellipse drawn in Figure 48 is the three-sigma range for the DGPS samples. The long axis of the ellipse is 32.167634 mm and short axis is 27.967052 mm. The three-sigma radius defines a circular area where 99.99 % of samples are contained.

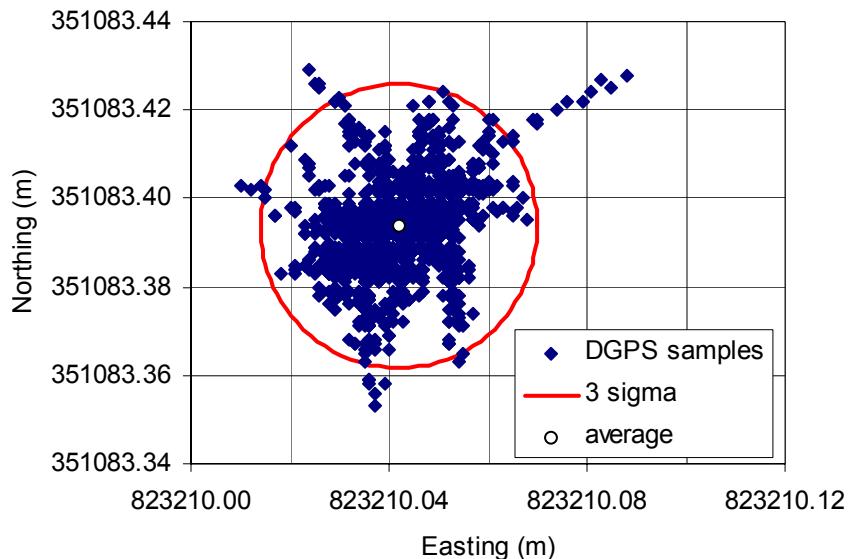**Figure 48. Sample data from a stationary DGPS receiver (Novatel RT20).**

Please note that the standard deviation for the above samples does not represent accuracy but repeatability. The repeatability indicates how consistent the sample data are even though all of them may have offset error. The average offset error is called accuracy. The Novatel claims that the error boundary of the GPS data comes from the RT-20 receiver is

20 centimeters. In previous experiments [27, 28], we found that its performance readily

meets its specifications of 20 cm accuracy while operating at a 5 Hz sampling rate.

6.3   Look-back Distance for Heading Angle Estimation

The heading angle of the vehicle was estimated using the successive difference method

between the current position and the past position of the vehicle. Currently, there is no

rate gyro or magneto sensor being used to estimate heading angle in the current HUD

system. Integration a rate gyro as a primary input for the heading angle measurement is
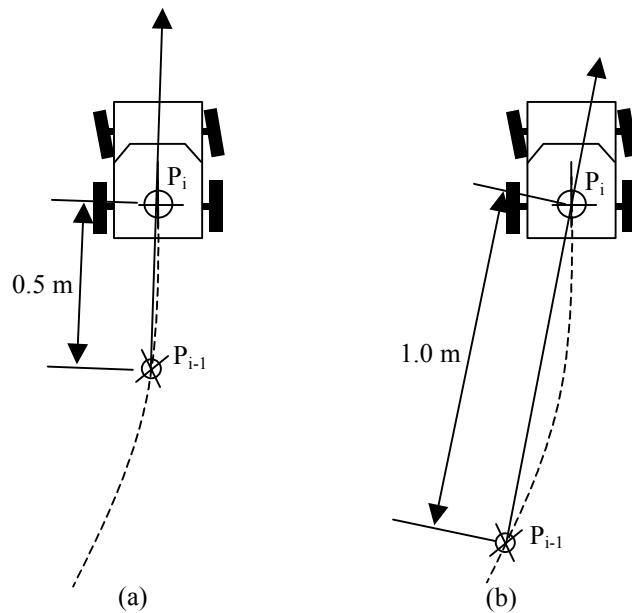
being studied at present.

Figure 49. Concept of the Look-back Distance.
(a) When look-back distance = 0.5m, (b) When look-back distance = 1.0m

We did not consider the gyro in the work presented here for two reasons: (1) we wished to focus on the display algorithms and its accuracy, and (2) we wished to investigate how well the HUD would work with a minimal set of sensors.

Any noise component in the GPS values will affect the estimated heading angle. The concept of look-back distance, as shown in Figure 49, was defined to filter out the random noise component in the GPS data. By increasing the look-back distance, noise in the leading angle estimate was attenuated. Three different look-back distance values were studied: 0.5m, 1.0m, and 1.5m.

P_i and P_{i-1} points are the current and the past location of the vehicle which were discussed in the previous section on "Yaw Angle Estimation."

6.4 Error Definition

The objective of the conformal HUD is to construct and project road characteristics onto the display screen (or combiner) that exactly matches with the real road characteristics. Figure 50 shows typical driving situation with the HUD system. The gray rectangular lens in the screen is the combiner on which the projected computer screen is seen by the driver's eye while the vehicle is moving. In Figure 50, the HUD is projecting the accentuated lines.

Figure 50. Typical driving situation with the HUD combiner.

To quantify how well this is done, the "visual sight angle" (*vsa*) was used to describe the mismatch error. The visual sight angle is defined by the ratio of the actual lateral error associated with the lane projection and distance to the eye point as shown below:

$$vsa = \frac{\text{lateral error at distance } x}{\text{distance } x} \qquad (112)$$

The visual sight angle normalizes error along the depth of the visual field and captures the error that is perceived by the driver. All our experimental results are described in terms of this visual sighting angle based error. To avoid the scaling problem of a camera

lens, reference marks with unit length were put on the HUD screen and the visual error was measured by comparing with the reference marks (see Figure 50).

6.5   Error Analysis

Live video images were captured while a driver was driving the test truck on a road. Position data coming from DPGS was also simultaneously stored. A Canon Optura digital video camcorder was used to record the projected HUD screens during actual driving situations. The camcorder was mounted at the driver's right eye position using custom mounting brackets. The optical image stabilizer in the camcorder was enabled while taking video images. The digitally stored images were transferred to a PC, then processed and analyzed. To synchronize the beginning of the video image stream, a special mark was put on the video screen by the HUD software when recording was started.

Sampling for error analysis was done at two-second intervals along the centerline. A special grid mark was drawn to synchronize these two-second intervals as shown in Figure 51. In Figure 51, the yellow lines (which may not be apparent in a gray scale image reproduction) are the computer generated ones. The three segments along the centerline are reference marks to measure mismatch error. Each horizontal line segment is 0.5m long, and the gap between two line segments is also 0.5m. The height of the

vertical mark is also 0.5m. To provide visual context, the 0.5m length is almost the same width as a standard IBM PC 101-key keyboard.

Errors associated with the projected lane boundaries are computed by comparing the distance the projected lines are displaced from the actual lane boundary. The lateral displacement between the projected lane boundary and the actual lane boundary at the three marks is computed by comparing with the length of the reference mark that is 0.5m. This lateral displacement is then normalized by dividing by the distance to the camera, which yields a value for the normalized visual sighting angle.

The error was measured at three different 'look-ahead' distances: 60m (196.8ft), 90m (295.3ft), and 120m (393.7ft) as measured from the driver's eye. The topmost horizontal grid mark, i.e. the furthest one in Figure 51, is 120m ahead. The enlarged picture is the central white rectangular area.
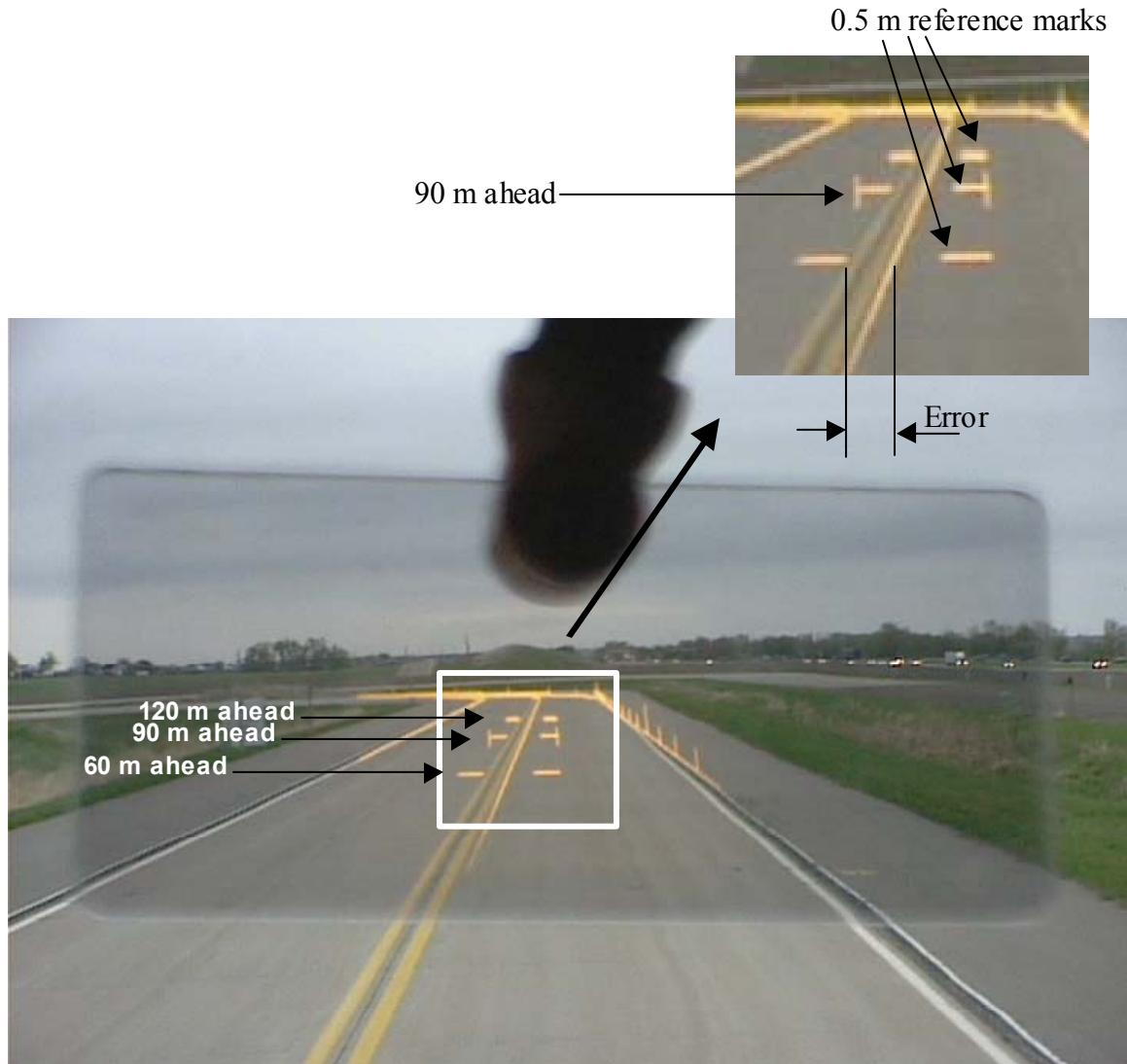
Figure 51. Reference marks for error analysis (blown up from the central portion of the Figure 50).

6.6   Vehicle Trajectory for the Test Drive

The experiment used to evaluate the HUD was intentionally selected to test the outer limits of the system, including a changing heading angle. The truck was driven along an oscillatory trajectory down the LVR as shown in Figure 52. The truck was first driven along the normal driving lane that is the right side of the centerline. Then the truck was intentionally driven onto the left lane, that is the apposite traffic lane, was kept there for a while, then returned to the normal driving lane.

Figure 52 shows one of the vehicle trajectories collected during the experiments. Figure 52 is the enlarged view of the rectangular area of the entire LVR of the Mn/ROAD in Figure 53. The enlarged road shown in Figure 52 is the more southerly of the two straight roads in the rectangular area of Figure 53. Each dot in Figure 52 represents a DGPS sample point that was collected while the vehicle was moving. The three straight lines in Figure 52 are map data used for the experiment. One is the left road boundary (lower line than the dotted DGPS samples), the centerline, and the right road boundary (higher than the dotted DGPS samples). The vehicle was driven from the right-bottom corner, i.e. southeast corner, of the map in Figure 52 to the left-top corner, i.e. northwest.

Figure 54 is the vehicle position on the road shown with the distance of the vehicle along the longitudinal direction. Please note that the lateral axis, X-axis, is enlarged at a greater scale than the longitudinal axis, Y-axis in the figure. The X-axis represents the lateral

position of the vehicle with respect to the centerline. The minus value means that the

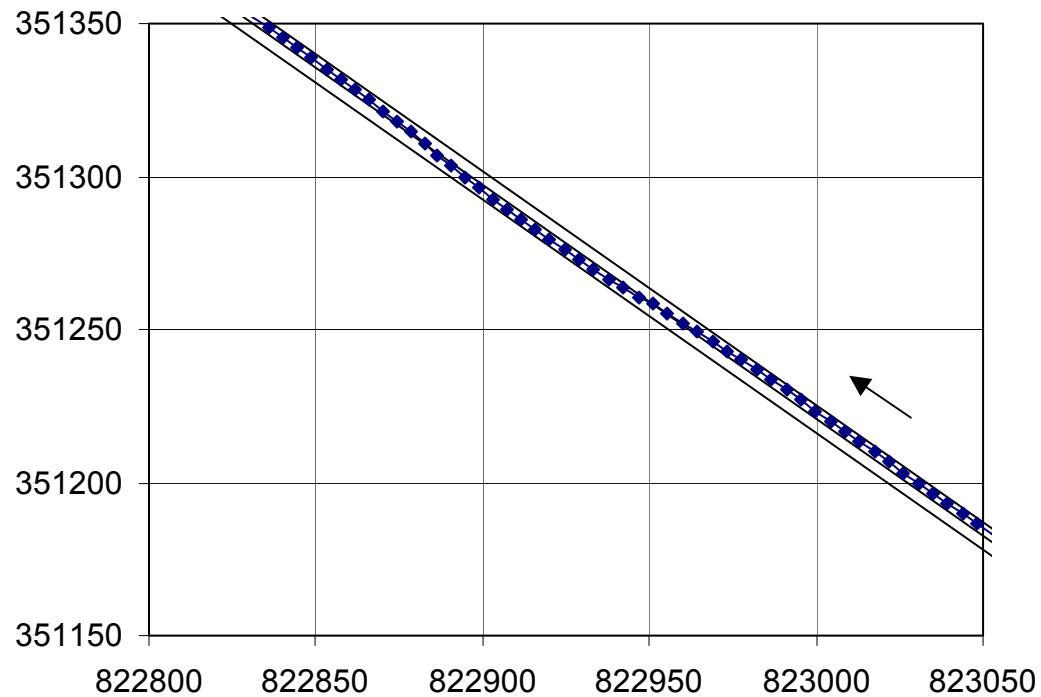vehicle is to the left side of the centerline.

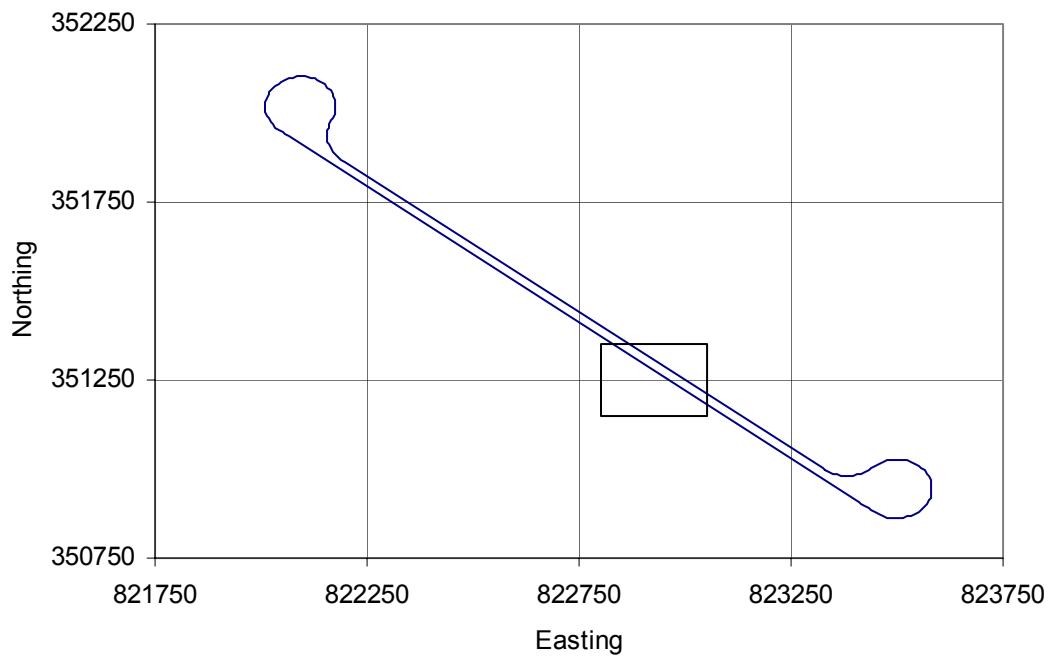**Figure 52. Vehicle trajectory for the test drive**

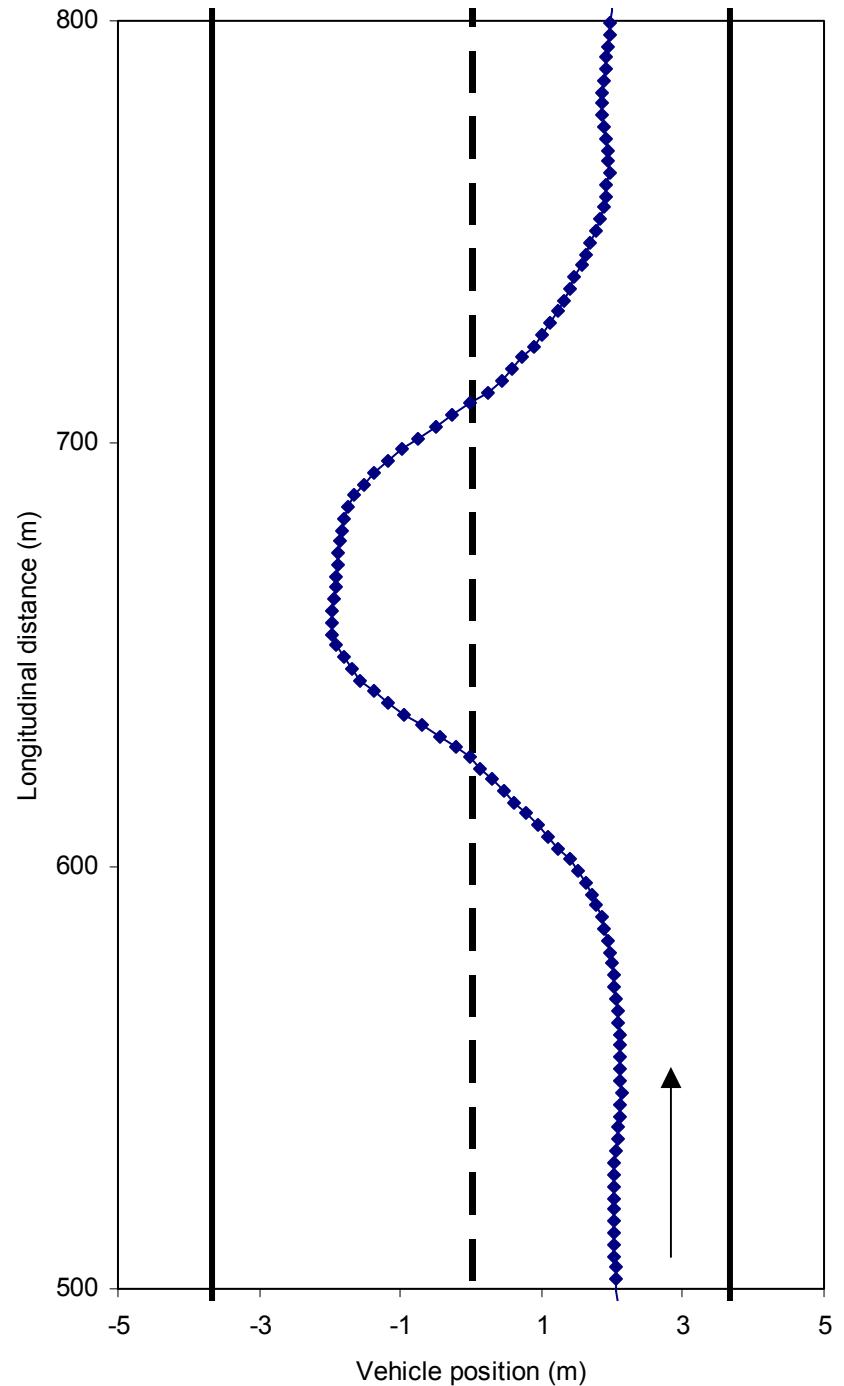**Figure 53. The test section in Mn/ROAD**

Figure 54. Vehicle position along with the driving lane. Note: the scale factor for the vehicle lateral position axis, i.e. X-axis, is greater than the scale factor for the vehicle distance along the longitudinal direction, i.e. Y-axis.

Chapter 7　Experimental Results

7.1　Aspect Ratio of the HUD Optical System

The optical magnification ratio of both the vertical and horizontal directions was measured using computer vision software and a digital camera. It was found that the horizontal and vertical magnification ratio was different and resulted in an elliptical image projected on the virtual screen. The difference in the magnification ratios comes from various sources combined together: video image generating circuits in the computer system, scan converter which converts the VGA signal into NTSC video signal, display circuit in the projector, and finally the curvature and projection angle of the combiner.

The ratio of the horizontal vs. the vertical size is called the aspect ratio (i.e. width : height). Before measuring the aspect ratio of the optical system in the HUD, the aspect ratio of the digital camera and digital image acquisition system was measured. To do this procedure, a perfect circular image needed to be captured by the camera and image acquisition system. A soft white light bulb was used as a perfect circular image shape (see Figure 55).

<center>(a)   (b)</center>
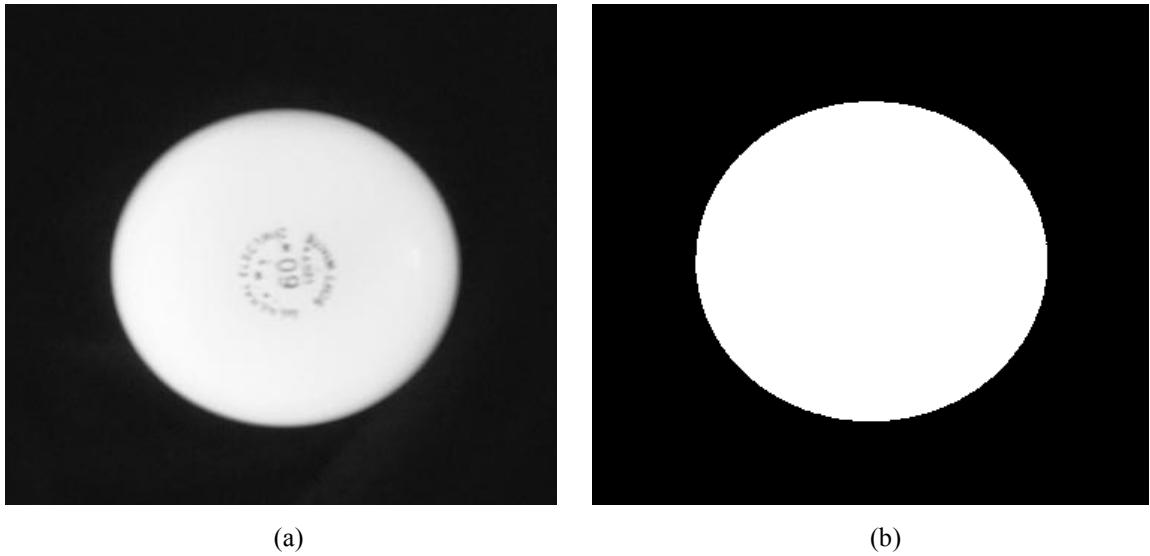
Figure 55. Light bulb used for calibration of the video camera and the digital image acquisition system. (a) Grayscale image of a soft white light bulb, (b) Binary image of the image (a)

The ratio of the width and height of the circle should be equal if the camera has square pixels and the circuits in the acquisition system are designed to capture square pixels. The aspect ratio of a perfect circle should be 1:1 if everything is perfectly square. However, the actual average value of the measured ratios was 1.0990:1, which means that the width is 1.0990 times wider than the actual width when a perfect circle (or sphere) is captured using the digital camera. The actual width of the object captured in the camera should be calculated by dividing by 1.0990.

To measure the aspect ratio of the optical system of the HUD, a perfect circle was generated in the computer memory space, (a) in Figure 56. The graphic image stored in the memory was transmitted to the HUD projector via a scan converter.

<center>134</center>
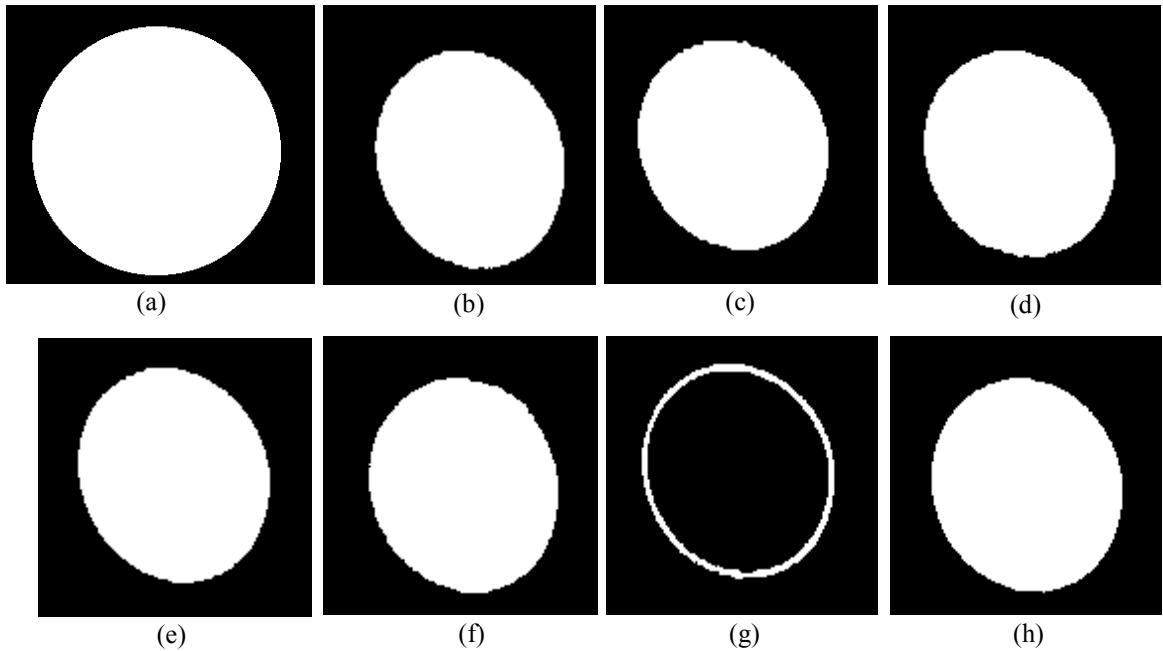
Figure 56. Calibration image for the optical system of the HUD. (a) A perfect circle image stored in the computer graphic memory, (b,c,d,e,f,g,h) Images of the circle projected on the virtual screen of the HUD system and captured by digital camera.

The driver sees the reflected virtual screen composed by the combiner, and the aspect ratio of an object in the virtual screen should be measured and used to calibrate the HUD optical system. Images from (b) to (h) in Figure 56 are calibration marks used to measure the aspect ratio of the HUD optical system.

As you can see in Figure 56, a circle drawn in the computer graphic system is seen as an ellipse. Actually, the circle is stretched in the vertical direction. The tilted ellipse image was due to the tilting angle of the camera with respect to the combiner. As found in the previous section, everything captured by the digital camera is seen as stretched to the horizontal direction with the ratio of 1.0990:1. The vertically long ellipse shows that the

135

vertically stretching effect of the HUD optical system is much greater than the horizontal

stretching effect of the camera. The following table shows the aspect ratio of the ellipses.

No	Image Figure 56	Aspect ratio (in the digital image space)	Aspect ratio (in the real world)
1	(b)	93.8 : 109.4	85.329 : 109.4 (0.7797:1)
2	(c)	95.0 : 105.8	86.452 : 105.8 (0.8173:1)
3	(d)	95.5 : 104.2	86.906 : 104.2 (0.8337:1)
4	(e)	94.8 : 108.3	86.280 : 108.3 (0.7968:1)
5	(f)	94.6 : 108.1	86.079 : 108.1 (0.7966:1)
6	(g)	131.2: 149.5	119.391 : 149.5 (0.7989:1)
7	(h)	95.9 : 107.4	87.245 : 107.4 (0.8126:1)

Table 7. Aspect ratio of the optical system of the HUD.

In Table 7, the "aspect ratio (in the digital image space)" is the calculated resultant values

for the digital images of the ellipses in Figure 56. The "aspect ratio (in the real world)" is

what we perceive when we see through the combiner. Because the digital camera

stretches any object it captures in the horizontal direction with a ratio of 1.0990, the

width of the ellipses in the digital space should be divided by 1.0990. The aspect ratio

values in real world are the divided ones. The average of the ratio in the real world is

0.8051:1, which means that the horizontal component of anything in the graphic system

of the HUD should be divided by 0.8051 or multiplied by 1.2421 (=1/0.8051). The

scaling of horizontal direction should be applied to the computation results of the

perspective projection routines before the actual screen drawing occurs.

7.2 Calibration of The HUD Optical Subsystem

The following parameters are needed to construct the coordinate transformation matrix [T] and project the local coordinate points into the virtual screen in a perspective projection manner.

- Driver's head position with respect to the origin of the vehicle coordinate frame.
- Distance to the virtual screen.
- Dimension of the virtual screen.
- Driver's viewing angle.

The driver's eye position and viewing angle are needed to compose the transformation matrix [T], and distance and dimension of the virtual screen are need for perspective projection. All of these values were kept as constants once they were calibrated. Then the driver was asked to look through the combiner and aim the image in the virtual screen to the real object in real scene. If the display was a HMD type, the the driver's head position and viewing angle would change continuously and would need to be measured in real time in order to perform the needed calculation. However, the HUD type doesn't need to incorporated dynamically changing calibration values, and therefore it is much simpler to calibrate and use.

Driver's Head Position

The origin of the vehicle-attached coordinate frame {V} is located at the GPS antenna

position and the origin of the local eye coordinate frame {L} is located at the driver's

right eye. The origins of both coordinate frames must be known in order to complete the

coordinate transformation matrix [T]. The position of the vehicle-attached coordinate

frame {V} comes from the GPS data. The relative position of the origin of the local eye

coordinate frame {L} from the origin of the vehicle-attached coordinate frame {V} was

carefully measured and used through out the experiments.
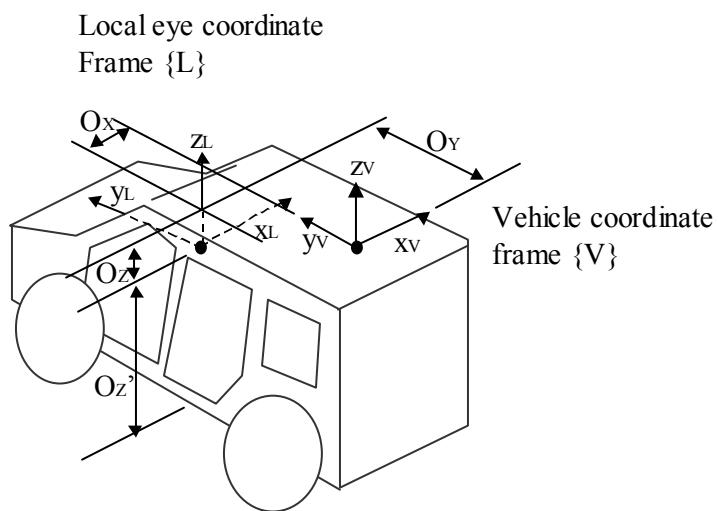
Figure 57. Driver's head position

O_Y is the distance from the origin of the vehicle-attached coordinate frame measured

along the longitudinal direction, that is the y-axis of the vehicle coordinate frame. O_X is

the distance along the latitudinal direction, that is the x-axis of the vehicle coordinate

frame. Because the driver's seat is always on the left side of the vehicle, O_X is always a

negative number. When the HUD is installed on the passenger side (right side), only the

sign of O_X needs to be changed. O_Z is the height of the driver's eye, which is always lower than the GPS antenna.

O_X	-1.9 ft (-0.6 m)
O_Y	5.6 ft (1.73 m)
O_Z'	7.8 ft (2.4 m)

Table 8. Driver's head position.

However, the actual vehicle-attached coordinate was put on the ground level direct under the GPS antenna, the z component of the local eye coordinate system is not O_Z but the O_Z' shown as in Figure 57.

Distance to the Virtual Screen

The distance and size of the projection screen should be measured accurately in order to draw the perspective projection correctly. Every point in the 3D world is projected onto points in the 2D screen, and the location of the point in 2D screen is a function of the distance to the objects as well as its location in 3D space. Further objects appear smaller in size and closer objects appear as bigger in size. Figure 32 shows an object at a certain point in the 3D world and its projected point in the 2D screen in a perspective manner. The projected point on the 2D screen is calculated from the triangle similarity shown in Figure 33. The ratio of the distance to the projection screen and the distance to an object acts as the scaling ratio. There is one more scaling factor when the projected point is drawn in the graphic memory space of the computer. This is the ratio of pixels per inch (or meter). The pixels (or dots) per inch is called DPI. The pixel is an element dot that

139

composes the entire graphic screen. This constant scaling factor was applied at the same value through out the entire 2D-projection screen. The screen resolution (that represents how many dots are in the graphic screen) of the computer used for the experiment was 800 pixels horizontally by 600 pixels vertically. Our newer computer system recently integrated into the new HUD design has 1024 by 768 pixels resolution. The difference in screen resolution gives a measure of how detailed the screen is. The ratio of 800 pixels vs. the measured dimension in the horizontal direction defines the scaling factor.

It was difficult to measure the actual size of and the distance to the virtual screen. The virtual screen appears to float in the air in the driver's visual field and there is no direct way to measure to the distance to the screen. However, an indirect method was used.

The distance to the virtual screen was measured using a camera that has an auto-focusing feature. A Nikon manufactured N-6006 model SLR (single lens reflex) camera with a 35-70 zoom lens was used for the measurement. Measurement of the distance was performed as follows:

- First, camera was firmly fixed on the ground and set to manual focusing mode. The camera continuously measured objects in the field of view and indicated whether the objects are out of focus or not. A dot appears if the object is focused and a left or right directional arrowhead appears on the indicator of the camera if it is out of focus.
- We turned on the HUD optical system and focused on an object in the virtual screen. The camera was fixed firmly on the ground during the entire process.

- Once the camera was focused, the HUD optical system was removed from the front of the camera. The camera was kept turned on.

- A real object was put in front of the camera used to measure the focal distance set above. The camera only indicates whether the object is in focus or not, so the object was moved back and forth from the camera until it indicated that the object was in focus. Then the distance to the object from the camera was measured using a ruler.

- These sequences were repeated 10 times and averaged.

The distance from the eye to the virtual screen was measured as 43.2 ft (13.17 m). The camera is focussing accuracy was within a range of ±10 cm from the focused distance. Although the accuracy of the focusing mechanism of the camera was not perfect, it seems to yield an accurate enough value for use in the HUD application.

Dimension of the Virtual Screen

The width and height of the virtual screen was measured by placing a white board at the focused distance, 43.2 ft, and drawing a rectangle which fits exactly with the outer extent of the virtual screen. Ten measurements were performed then averaged. The width of the virtual screen was determined to be 4.9 ft (1.52 m) and the height was 3.8 ft (1.15 m).

Distance to the virtual screen	43.2 ft (13.17 m)
Width	4.9 ft (1.52 m)
Height	3.8 ft (1.15 m)

Table 9. Dimension of the virtual screen.

Following further verification, it was found that the distance to the virtual screen doesn't affect the perspective projection significantly if the ratio between the distance and size of the virtual screen is maintained as a constant.

Driver's Viewing Angle

Once, the relative location of the driver's eye, distance and dimension of the virtual screen are determined, only the orientations of the drive's viewing sight are needed for calculating the perspective projection. Among the possible three angles, roll, pitch, and yaw angle, only the pitch angle was used for the coordinate transformation. The yaw and roll angles were set to zero for the all experiments. Please note that the driver's yaw angle is not the yaw angle of the vehicle. The driver's yaw angle is the sight angle of the driver with respect to the vehicle coordinate frame. The zero yaw angle means that driver is assumed to look straightforward the vehicle's moving direction. The pitch angle was set as −5.0 degrees, which indicates that the driver is looking down 5.0 degrees from the horizontal line. This −5.0 degrees was arbitrarily selected to get project a wider area of the road through the combiner. The visible area through the combiner was very limited when the pitch angle was set to zero. When the pitch angle was set to zero, half of the upper screen was filled with sky at where no interesting objects are located. Since we put constant angle values to the sight angles, the optical system of the HUD should be adjusted or aligned so that they compose the assumed angle with respect to the driver, vehicle, and outer scene.

Two square-shaped calibration marks were painted on the LVR of Mn/ROAD as shown in Figure 58. The size of each mark was 12 feet by 12 feet. Locations of the center of the two calibration marks were measured using the same DGPS that was used for the experiments. The calibration marks were included in the digital map as a special object so that they appear in the projected virtual screen whenever the driver is driving toward the marks. If the marks are located in the visible region shown in Figure 34 in Chapter 4, then the marks will appear in the HUD virtual screen with the correct perspective.

Figure 58. Calibration mark seen through the combiner

The final step of the calibration was the aiming or adjusting of the combiner and projector so that the center of the calibration mark image in the virtual screen matches to the center of the real calibration mark visible through the combiner. Figure 58 shows one of the calibration marks painted on the LVR of the Mn/ROAD. The central darker area is the combiner, and the white square shape with cross in it is the calibration mark.

The calibration for finding the scaling factors and dimension of the virtual screen need to be done only one time after the assembly of the HUD system. The aiming step was performed whenever a new experiment was started.

7.3 Effect of the Look-back Distance

To measure the effect that the heading angle estimation error has on the accuracy of the projection of lane boundaries onto the HUD, a series of experiments were performed. In these experiments, the test truck was driven as shown in Figure 59. After full acceleration, the vehicle was driven to the left of the centerline, and then driven back into the normal driving lane.

The effect of look back distance for estimating the vehicle heading angle was measured at 10mph (Figure 59). In the graph, errors for three different points (60m, 90m, and 120m ahead) are drawn. Data was computed at 2-second intervals. At the beginning of the data (0 to approximately 10 seconds), the level of *vsa* may be attributed to vibration due to vehicle acceleration.

144

The broken interval between 40 to 45 seconds is when the lane boundaries are not displayed on the combiner. This is due to the size (4"x6") of the combiner. The lane boundaries fall outside the field of view. (This has been corrected with the subsequent development of a new, larger combiner and brighter projector.) It can be seen that the errors at all three distances match quite well.
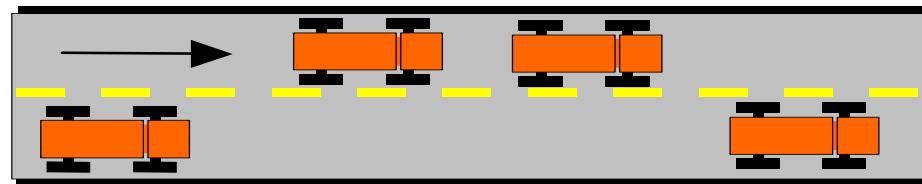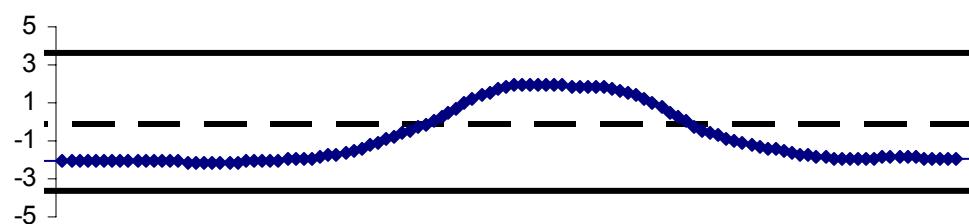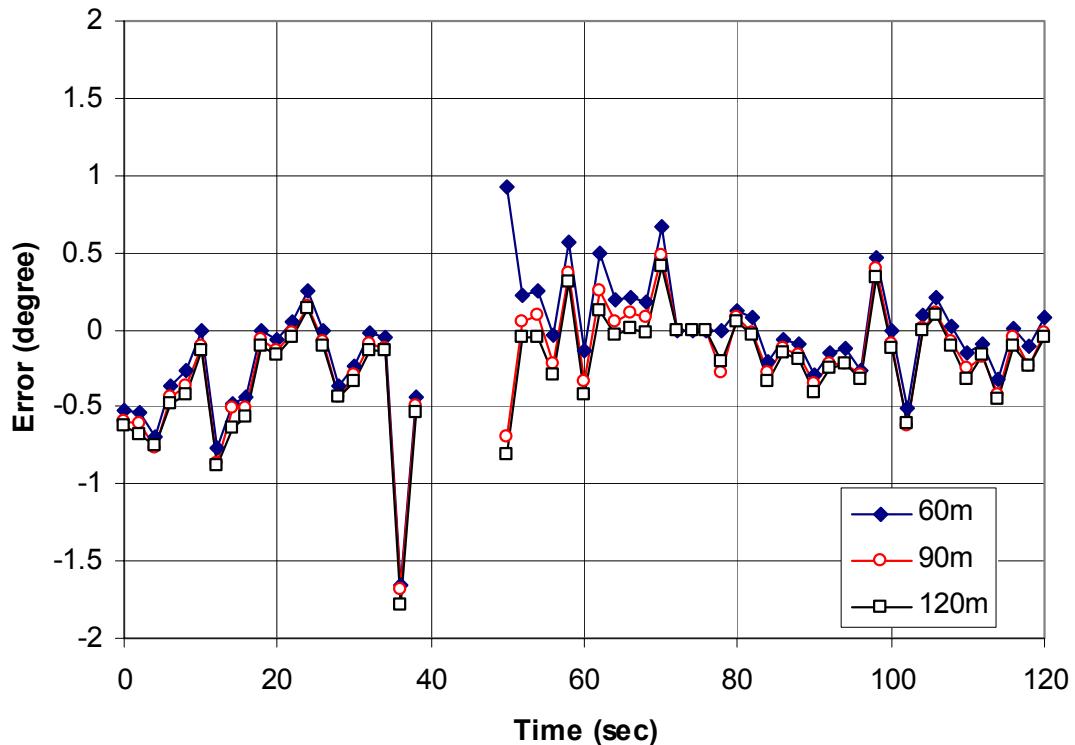
Figure 59. Error in terms of *vsa* for various look-ahead distances for heading angle estimate based on look-back distance 0.5m, at 10 mph. Lower image indicates the vehicle motion during the experiment.

Figure 60 displays the mismatch error or *vsa* at the 60 m ahead distance for look-back distances of 0.5 m and 1.0 m while the vehicle is moving at 10mph for the same maneuver shown in Figure 59.

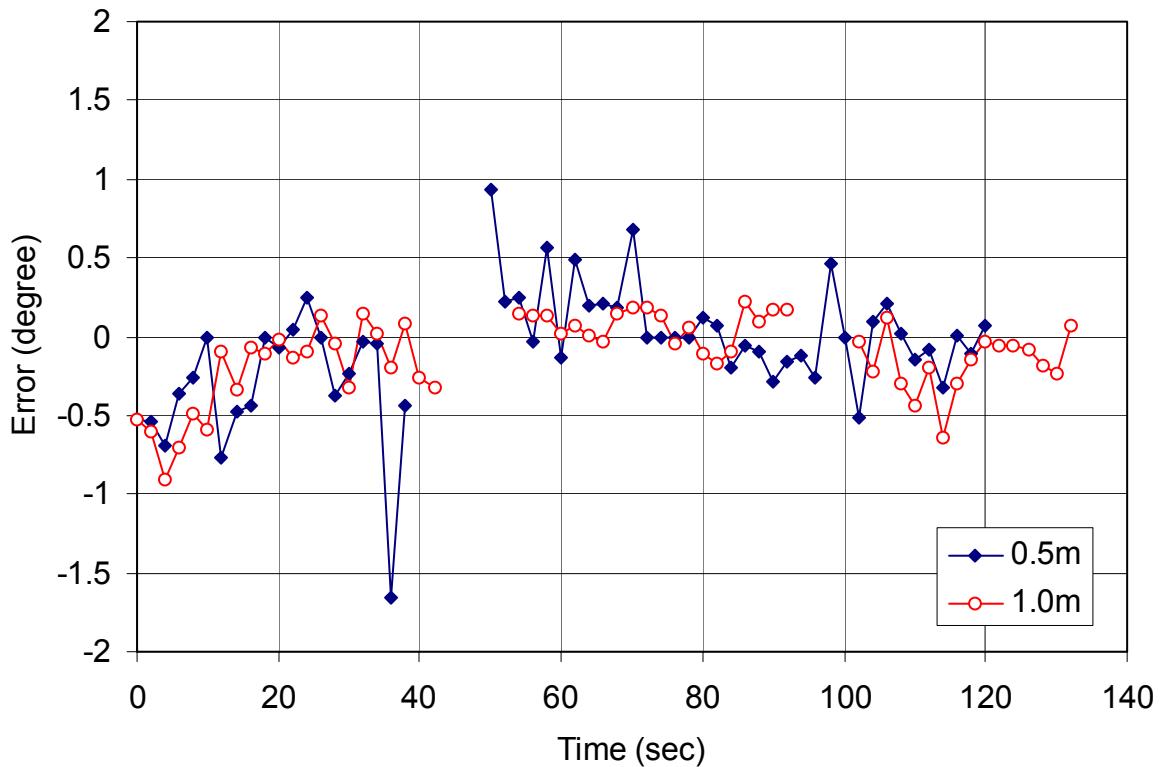**Figure 60. Effect on error or *vsa* of look-back distances 0.5m and 1.0m at 10mph.**

Longer look-back distances result in a smoother *vsa* trajectory, but result in a longer time constant. To the driver, this results in a more stable image, albeit at a price of greater error when transients occur. Given a trade-off, the more stable image is desired because it is less likely to annoy or lead to driver motion sickness.

Note again, that in all the experiments the vehicle was intentionally driven from one lane to the next and back again during each test run. This was done to examine the limitations of the system and was used to design a subsequent second generation HUD. As a result of the side to side motion, the data following a lane change for all the error graphs was dominated by transient effects. The length of the test track limited the maximum test speeds to 30mph. When the vehicle traveled faster (i.e. at 30mph), the effects for varying look-back distances do not change appreciably, as is shown in **Figure 61**. The transient effects (still below 1 degree maximum error or *vsa*) disappear in the last few seconds for all the experiments. The results for those driving segments which were not affected by intentional side to side weaving motion indicated that the system could indeed achieve an average error of approximately 0.25 degrees (equivalent to 0.5m at 120m).
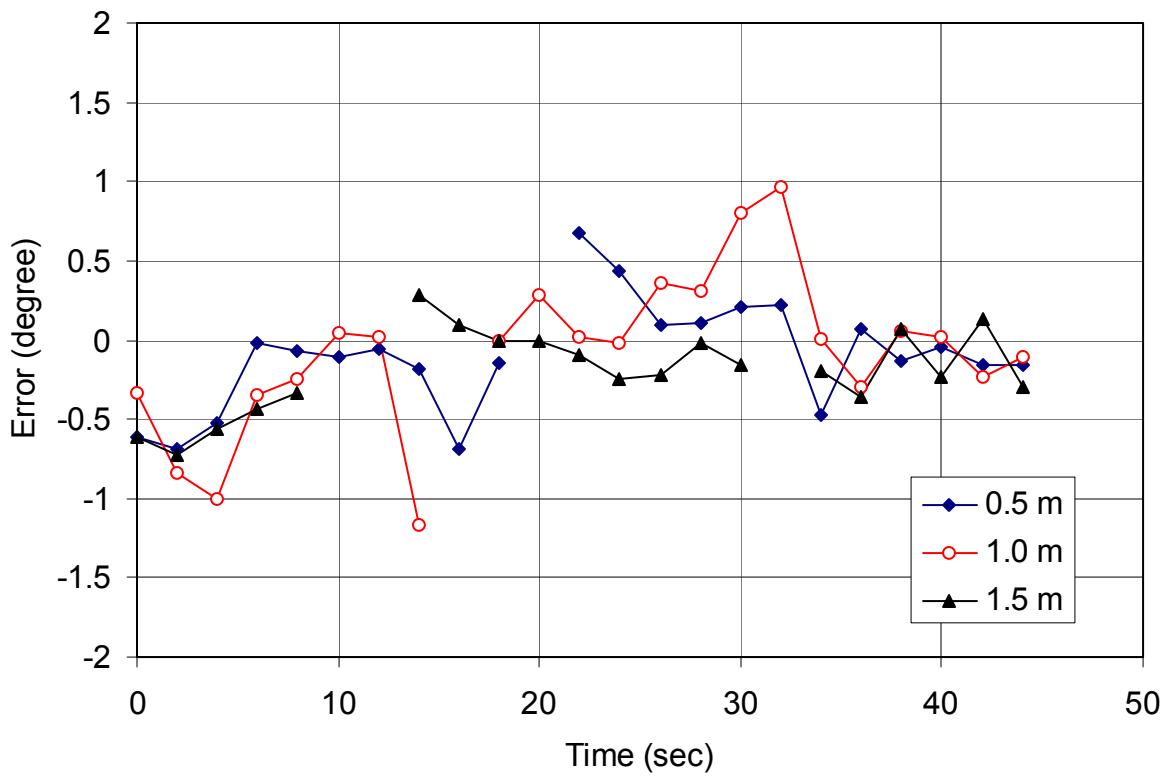
Figure 61. Effect on error or *vsa* of look-back distances 0.5m, 1.0m, 1.5m at 30mph.

7.4   Effects on Different Look-ahead Distance Points

The mismatch errors or *vsa* measured at the different look-ahead distances (i.e., 60m, 90m, and 120m) can be found in **Figure 62**. The look-ahead distance does not affect any of the heading angle estimation. The term "look-ahead" was used just to compare error amounts at some distances ahead of the moving vehicle.

The important errors to analyze are those during the no transient condition (i.e. during steady state driving from 18 to 26 seconds and 38 seconds on). The system was calibrated at the 60m distance; thus we would expect that the largest error would occur at the

furthest point, i.e. at 120. Although we expected that there would be an error offset between the three look-ahead distances, we assumed that they would be constant for all speeds. However, we found that error offsets were larger (by about 0.1 degree) at higher speeds than at slower speeds. This appears to be the result of the vehicle motion from the time that the GPS position is acquired until the display image is rendered (i.e. the time delay or latency). To minimize the separation of the errors at different distances ahead of the vehicle, time delay from the GPS sensing to the actual screen update should be minimized as much as possible.

Errors also arise because of mounting errors associated with the projector. As is seen in Figure 51, the road centerline did not exactly match the centerline drawn in the HUD image. The closer reference mark was shifted to the right side but the farther mark was shifted to the left side. As the vehicle speed increases, this mounting error resulted in the shifted patterns of errors at different locations.
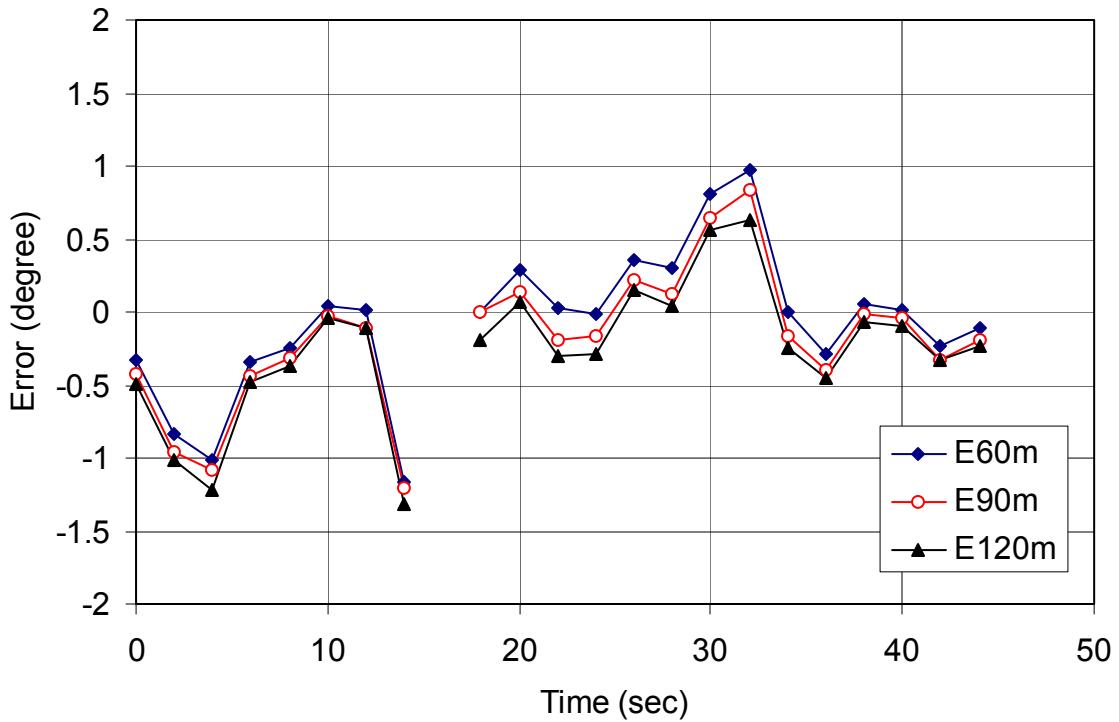
Figure 62. Effect on error or *vsa* at different forward-looking distances at 30 mph.

Estimate based on look-back distance 1.0 m.

7.5 Time Required to Draw HUD Screen

Figure 63 depicts the total time measured for all the computation associated with coordinate transformation from the DGPS signals in the global coordinate system to the perspective projection in the eye coordinate system, including clipping the results outside the field of view, and including the HUD screen drawing time for a typical driving situation. The time to refresh each screen is measured from the moment that the DGPS data is received. The screen refresh time (which includes the computation time listed above) was typically less than 16ms in most cases. The segment from 100 to 300

sampling points is for the case when the vehicle is moving in a straight line. Centerline
and both side line segments were drawn in the field of view.
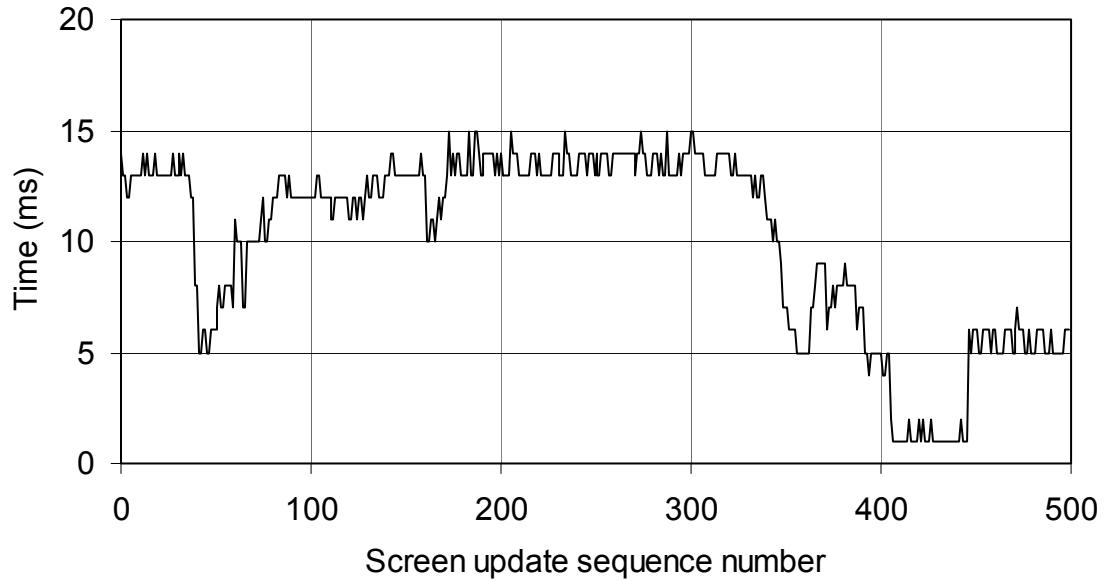
Figure 63. Time required for screen refresh.

Drawing was limited to 1000 ft ahead in the heading direction of the vehicle. A reduction
in the screen refresh times occurred at the beginning and end of the graph when there was
little or nothing to draw, i.e. everything was out of the visual field of the combiner.
During the segment from 50 to 100 sample points, the vehicle moved to the left and then
to the right within the driving lane. Then vehicle changed lanes completely during the
segment between 350 to 450 points.

Chapter 8   Conclusions

A conformal HUD to assist drivers by presenting augmented visual information was developed and successfully tested under real driving conditions. The system has now been in operation for some time and has been demonstrated to hundreds of individuals in Minnesota, Indiana (Navistar International, Fort Wayne), and in Ohio (Demo 99 sponsored by ITS America at the TRC in Liberty).

Nevertheless, some error is unavoidable in every system. In this system, image projection error (less than 0.5 degrees for normal driving condition on a straight path) arise from DGPS positioning error, error in the digital map data, drawing latency, system vibration, and from the calibration errors of the system. The visual sight angle was defined to analyze mismatch error between the real road lane marking and the computer generated ones projected on the combiner. Effects on the look-back distance were studied and summarized. Generally, longer look-back distance cases resulted in smooth, i.e. less noisy, heading angle estimation but poor responses for periods of heading angle change. When the vehicle is moving at slow speeds, longer look-back distances resulted in better responses than for shorter look-back cases. However, as the vehicle speed increases, it was found that their differences become negligible. One interesting fact that was determined during the experiments is that the mismatch errors at three different distances ahead of the vehicle becomes separated as the vehicle speed is increased. It was assumed

that this separation effect comes from the time delay between the actual vehicle position and the position at which the HUD screen was displayed.

In order to reduce the errors due to transient effects which appeared during lane changes, we plan to integrate a yaw rate gyro, to improve the heading angle estimate, with a faster and more accurate DGPS receiver. Just how much error can be tolerated by a driver remains an open research question.

A larger and brighter video image projection system has now been installed. Information about obstacle location on the road (based on the radar data) has recently also been incorporated into the HUD screen as a means to assist drivers with collision avoidance. This work is at an early stage, and will be reported on in the future. Clearly, we need to also determine the minimal field of view necessary for safe vehicle guidance.

Finally, more study is needed to determine how much information should or can be presented to the driver so that the driver can drive comfortably and efficiently in low visibility situations.

References

1. Hills, B.L., "Vision, visibility, and perception in driving," <u>Perception</u>, Vol. 9, pp. 183-216.

2. Boff, K.R., Lincoln, J.E., <u>Engineering Data Compendium</u>, Human Perception and Performance Volume 1, Chap 1.2, Optics of the Eye, Harry G. Armstrong Aerospace Medical Research Laboratory, 1988.

3. Gibson, J.J., College, S., and Crooks, L.E., "A Theoretical Field-Analysis of Automobile-Driving," <u>Journal of Psychology</u>, Vol. LI, No. 3, 1938, pp. 453-471.

4. Wohl, J.G., "Man-Machine Steering Dynamics," <u>Human Factors</u>, Vol. 3, 1961, pp. 222-228.

5. Senders, J.W., "The Attentional Demand of Automobile Driving," <u>Report No. 1482</u>, Bolt, Beranek and Newman, Inc., 1967.

6. Rockwell, T.H., Ernst, Ronald, R.L., and Rulon, M.J., "Visual Requriements in Night Driving," <u>National Cooperative Highway Research Program Report 99</u>, Highway Research Board, 1970.

7. ---, <u>Minnesota Driver's Manual</u>, Department of Public Safety, State of Minnesota, 1996.

8. ---, <u>Minnesota Commercial Driver's Manual</u>, Department of Public Safety, State of Minnesota, 1997.

9. Modjahedzadeh A. and Hess R.A., "A Model of Driver Steering Control Behavior for Use in Assessing Vehicle Handling Qualities," <u>Journal of Dynamic Systems, Measurement, and Control</u>, Vol. 115, 1993, pp.456-464

10. Tripmate, DeLorme Inc., <u>http://www.delorme.com</u>, Two DeLorme Drive, P.O. Box 298, Yarmouth, ME 04096.

11. CoPilot, TravRoute Software, <u>http://www.travroute.com</u>, 1000 Herrontown Road, Princeton, NJ 08540.

12. SkyMap, Etak, Inc., <u>http://www.etak.com</u>, 1605 Adams Dr., Menlo Park, CA 94025-1486.

13. CARiN, Philips, <u>http://www.carin.com</u>, Rembrandt Tower Amstelplein 1, 1096 HA, Amsterdam, Netherlands.

14. Lowe J.R. and Ornelas J.R., "Applications of Head-Up Displays in Commercial Transport Aircraft," <u>Journal of Guidance, Control, and Dynamics</u>, Vol. 6, 1983, pp. 77-83.

15. Grunwald, A.J., Merhav, S.J., "Vehicular Control by Visual Field Cues-Analytical Model and Experimental Validation," <u>IEEE Trans. on Systems, Man, and Cybernetics</u>, Vol. SMC-6, No. 12, 1976, pp. 835-845.

16. Grunwald, A.J., Robertson, J.B., and Hatfield, J. J., "Experimental Evaluation of a Perspective Tunnel Display for Three-Dimensional Helicopter Approaches," <u>Journal of Guidance, Control, and Dynamics</u>, Vol. 4, 1981, pp. 623-631.

17. Negrin M., Grunwald, A.J., and Rosen, A., "Superimposed Perspective Visual Cues for Helicopter Hovering Above a Moving Ship Deck," <u>Journal of Guidance, Control, and Dynamics</u>, Vol. 14, 1991, pp. 652-660.

18. Hess, R.A. and Gorder P.J., "Design and Evaluation of a Cockpit Display for Hovering Flight," <u>Journal of Guidance</u>, Vol. 13, No. 3, 1990, pp. 450-457.

19. Weihrauch, M., Meloeny, C.C., and Geosch, T.C., "The First Head Up Display Introduced by General Motors," <u>SAE #890288</u>, 1989.

20. Beyerlin, D.G., "New Uses and Image Sources for Head-Up Displays of the Future," <u>SAE #950960</u>, 1995.

21. McCosh, D., "Second Sight," <u>Popular Science</u>, 1998, Oct..

22. Sojouner, R.J., and Antin, J.F., "The Effects of a Simulated Head-Up Display Speedometer on Perceptual Task Performance," <u>Human Factors</u>, 1990, 32(3), pp. 329-339.

23. Steinfeld, A. and Green, P., "Driver Response to Navigation Information on Full-Windshield Head-Up Displays," <u>Int. Journal of Vehicle Design</u>, Vol. 19, No. 2, 1998.

24. Office of Land Management, <u>http://rocky.dot.state.mn.us</u>, 395 John Ireland Boulevard, St. Paul, MN 55155

25. Map projections, <u>http://www.forestry.umt.edu/courses/FOR503/part4.htm</u>, Hans Zuuring, University of Montana.

26. Snyder J.P., and Voxland P.M., <u>An Album of Map Projections</u>, U.S. Geological Survey Professional Paper 1453, Department of the Interior, 1989.

27. Bajikar, S., Gorjestani, A., Simpkins, P., and Donath, M., "Evaluation of In-Vehicle GPS-Based Lane Position Sensing for Preventing Road Departure," <u>Proceedings of the IEEE Conference on Intelligent Transportation Systems</u>, ITSC '97, Boston, MA, 1997.

28. Morellas, V., Morris, T., Alexander, L. and Donath, M., "Preview Based Control of a Tractor Trailer Using DGPS for Preventing Road Departure Accidents," <u>Proceedings of the IEEE Conference on Intelligent Transportation Systems</u>, ITSC '97, Boston, MA, 1997.

29. Craig, J. J., <u>Introduction to Robotics</u>, 2nd ed., Addison-Wesley Publishing, 1989

30. Wong, J. Y., <u>Theory of Ground Vehicles</u>, 2nd ed., Wiley-Interscience Publications, 1993.

31. Paromtchik I. E. and Laugier C., "Autonomous parallel parking of a nonholonomic vehicle," <u>Proceedings of the 1996 IEEE Intelligent Vehicles Symposium</u>, 1996, pp. 30.

32. ThrustMaster Inc., <u>http://www.thrustmaster.com</u>, 7175 NW Evergreen Parkway, Bldg 400, Hillsboro, OR 97124.